DIAL/MSU Saltcake Dissolution: Fiscal Year 2000 Status Report

R. K. Toghiani and J. S. Lindner
Diagnostic Instrumentation and Analysis Laboratory
Mississippi State University
205 Research Blvd.
Starkville, MS, 39759

The authors gratefully acknowledge funding by the United State Department of Energy under the DIAL Cooperative Agreement No. DE-FC26-98FT40395. Additional funding provided from Oak Ridge National Laboratory through Lockheed Martin Energy Research Corporation Subcontract No. 4500004991.

Executive Summary

Continued studies aimed at assessment of the Environmental Simulation Program (ESP) for Hanford site operations are reported. Validating the model is being accomplished through a comparison of results to core sample analyses performed at the site, evaluation of model predictions against the results from other thermodynamic codes, and obtaining additional data needed to improve the quality of database entries for specific double salts and other prevalent systems. These tasks were selected as the most appropriate means for establishing the current limitations of the model and remedying any shortcomings prior to widespread application. Previous work has focused on the use of specific databases that have been identified from comparisons to saltcake dissolution experiments, assessment of the fundamental data contained in the ESP databases, additional solid-liquid equilibria data for natrophosphate ($Na_7F(PO_4)_2 \cdot 19H_2O$), development of a method for performing charge reconciliation, and application of the model to specific remediation projects (tank 241-SY-101).

ESP model predictions were compared to companion saltcake dissolution experiments for samples from tanks 241-TX-113 and 241-S-102. Both of these saltcakes contained very low amounts of water and this initially led to convergence difficulties. The charge reconciliation method developed previously was augmented to allow modeling of these systems based on nitrate dissolution. Site studies indicated that the TX-113 saltcake had the largest concentration of sulfate of any saltcake examined thus far providing a direct probe of ESP performance under these conditions. Results indicated that the ESP PUBLIC database was not capable of describing the experimental sulfate concentrations and a second database (Na2snacl) was obtained from OLI Systems, Inc., that provided for improved representation of the sulfate concentration profile as a function of diluent added. Agreement between experimental measurements and model predictions was also observed for nitrate, nitrite, and chloride anions using both the PUBLIC database alone as well as the PUBLIC database in tandem with the Na2snacl database and the Trona database. Mixed results were observed for fluoride with agreement between the model and experimental data observed at 25°C but with ESP predicting dissolution to occur at lower levels of diluent addition at 50° C. The model predictions were also somewhat different for phosphate and this is believed to arise from the inaccurate data currently contained in the databases for the natrophosphate and Na_3FSO_4 double salts.

Similar trends in the solubility behavior of the various anions were observed in comparing the model predictions with the experimental results for the saltcake from S-102. Dissolution profiles for nitrate, sulfate, chloride, and nitrite concentrations all agreed well with the experimental data. A discrepancy was observed with phosphate and, again, it is believed that this can be traced to the quality of the fundamental data called by the code. For both saltcakes the revised method for generation of the molecular stream appears to be one means of performing simulations with low water content samples.

ESP model predictions were also compared to Hanford laboratory experiments designed to evaluate the re-precipitation of solids when batches of supernate, from, for example, a staged retrieval process, were mixed. For selected saltcake compositions, laboratory

studies indicated that solids formation occurs when clear supernates obtained from different staged contacts are recombined in a cumulative receiver. ESP predicted that the nitrate and carbonate containing solids would dissolve first followed by solids that contain fluoride, phosphate, and sulfate. Sodium oxalate was expected to require the largest amount of diluent. These results are in accord with the experimental results for all of the saltcakes examined. The only difference observed between the model predictions and the experimental results was an overestimation of the liquid phase ionic concentrations (more complete dissolution) predicted by ESP. This difference is thought to reflect the fact that the ESP calculations are at equilibrium (infinite time) and the experimental measurements were for a specific period. Upon combination of the supernate fractions, the newly formed solids tended to be the double salts Na_3FSO_4 and natrophosphate. The results indicate that some care will be required during retrieval in order to prevent unwanted solids formation in receiving tanks.

Further comparisons of the predictions of the ESP model with other models are also given. Results on the solubility behavior of $NaNO_3$ are compared against lattice model calculations and literature data for three different temperatures over a wide range of ionic strengths. The ESP predictions were found to be within 1% for ionic strengths of from 0 to 6 at 25°C. Above the ionic strength of 6, both models showed a slight underestimation of from 1 to 3.5% in the vapor pressure exerted over the aqueous solution as compared to the data from the International Critical Tables. Calculations performed at 100 and 125°C indicated agreement to within 1% below an ionic strength of 6; somewhat higher deviations were observed at the highest ionic strengths (>20) investigated. ESP results ranged from ~3 to 8% below the literature values at 100°C and from ~3 to 10% below the data at 125°C with the larger deviations being observed at the highest ionic strengths. Taken together, the results indicate that at the conditions typical of Hanford operations, the ESP model will accurately account for the behavior of $NaNO_3$.

The ESP model was also compared to predictions from the SOLGASMIX code for the Na-NO_3-SO_4-OH and Na-F-SO_4-OH systems. The double salts, $Na_3NO_3SO_4 \cdot 2H_2O$ and Na_3FSO_4, will form under certain conditions and both of these species have been observed in Hanford wastes. Evaluation of the model predictions for the both the nitrate containing system and the fluoride containing system indicated that an additional ESP database that correctly accounts for the solid phase partitioning of sodium sulfate (Na_2SO_4 anhydrous or $Na_2SO_4 \cdot 10H_2O$) was required. ESP databases do not contain data for the $Na_3NO_3SO_4 \cdot 2H_2O$ double salt, however, the limited conditions in which this molecule has been observed to form indicate that the solubility envelope is primarily comprised of the simple salts. ESP and SOLGASMIX predictions are in agreement with the available experimental data.

Model comparisons for the Na-F-SO_4-OH system were carried out at 25 and 50°C in water, 1m, and 3m OH. Comparison with the available experimental data in water at 25°C indicated that ESP underestimates the liquid phase ionic concentrations. Good agreement was observed between the predictions of the two models in 1m and 3m OH. Measured solubilities at 25°C indicated excellent agreement with the reported literature data in water, higher ionic phase concentrations in 1m OH and slightly increased

concentrations in 3m OH as compared to the model predictions. Additional data at 50°C is being obtained. Reasons for the discrepancy of the ESP predictions in water are not known at this time, however, the availability of the experimental data will allow upgrading of the database called by ESP.

Contents

Executive Summary ii

List of Figures vii

List of Tables x

I. ESP Simulation of Saltcake Dissolution 1

A. Saltcake Compositions 1
B. Data Pre-Processing for Low-Water Content Saltcakes 2
C. Simulation of Saltcake Dissolution Experiments 4
1. Thermodynamic Database Selection 5
2. Comparison of Model Calculations with Experimental Results For Nitrate, Carbonate, and Sulfate for TX-113 Saltcake 7
3. Comparison of Model Calculations with Experimental Results For Phosphate and Fluoride Anions for TX-113 Saltcake 12
4. Comparison of Model Calculations with Experimental Results For Nitrite, Chloride and Oxalate Anions for TX-113 Saltcake 16
5. Summary/Conclusions for TX-113 Saltcake Dissolution Modeling 20
6. Comparison of Model Calculations with Experimental Results For Nitrate, TIC, and Sulfate for S-102 Saltcake 20
7. Comparison of Model Calculations with Experimental Results For Phosphate, Nitrite, Chloride, and Oxalate for S-102 Saltcake 23
8. Summary/Conclusions for S-102 Saltcake Dissolution Modeling 25
9. Overall Summary for Saltcake Dissolution Modeling 26

II. ESP Simulation of Feed Stability Studies 27

A. Data Post-Processing of Simulation Output 28
B. Discussion of Results 28
1. Anion Dissolution Behavior – Model Predictions 28
2. *Formation of Solids in Cumulative Supernate Receiver* 30
C. Summary of Feed Stability Studies 37

III. ESP Comparison Studies 39

A. Calculations for Sodium Nitrate 39
B. Comparative Calculations for Sodium Double Salts 42
1. Sodium-Nitrate-Sulfate-Hydroxide System 42
2. Sodium-Fluoride-Sulfate-Hydroxide System 45

II. Experimental Studies of Double Salt Systems 48

References 52

Appendices 53

Appendix A. Tabulated Results – ESP Model Calculations for TX-113 and S-102 Saltcakes 53

Appendix B. Comparative Plots – Dissolution Studies for Saltcake S-102 at 50° C 66

Appendix C. Input Molecular Streams for Feed Stability Studies 71

Appendix D. Summary Tables for Feed Stability Studies 73

Appendix E. Comparative Calculations for Sodium Nitrate Tabulations of Data 84

Appendix F. Experimental Data for Na-F-SO4-OH System at 25° C 88

List of Figures

Figure 1.	Prior (FY99) Comparison of Predicted and Experimental Nitrate Anion Concentrations for Tank S-102 [4].	3
Figure 2.	Comparison of ESP Prediction and Experimental Data for Sulfate Anion from Series Dissolution Tests on TX-113 Saltcake - 25° C.	6
Figure 3.	Comparison of ESP Prediction and Experimental Data for Sulfate Anion - Series Dissolution Tests on TX-113 Saltcake – 25° C - Incorporation of Na2snacl Database.	6
Figure 4.	ESP Predictions and Experimental Nitrate Concentrations for TX-113 Saltcake at 25° C.	8
Figure 5.	ESP Predictions and Experimental Nitrate Concentrations for TX-113 Saltcake at 50° C.	9
Figure 6.	ESP Predictions and Experimental TIC Concentrations for TX-113 Saltcake at 25° C.	9
Figure 7.	ESP Predictions and Experimental TIC Concentrations for TX-113 Saltcake at 50° C.	11
Figure 8.	ESP Predictions and Experimental Sulfate Concentrations for TX-113 Saltcake at 50° C	13
Figure 9.	ESP Predictions and Experimental Fluoride Concentrations for TX-113 Saltcake at 25° C	14
Figure 10.	ESP Predictions and Experimental Fluoride Concentrations for TX-113 Saltcake at 50° C.	14
Figure 11.	ESP Predictions and Experimental Phosphate Concentrations for TX-113 Saltcake at 25° C	15
Figure 12.	ESP Predictions and Experimental Phosphate Concentrations for TX-113 Saltcake at 50° C	16
Figure 13.	ESP Predictions and Experimental Nitrite Concentrations for TX-113 Saltcake at 25° C	17
Figure 14.	ESP Predictions and Experimental Nitrite Concentrations for TX-113 Saltcake at 50° C	17
Figure 15.	ESP Model Predictions and Experimental Chloride Concentrations for TX-113 Saltcake at 25° C	18
Figure 16.	ESP Predictions and Experimental Chloride Concentrations for TX-113 Saltcake at 50° C.	18
Figure 17.	ESP Model Predictions and Experimental Oxalate Concentrations for TX-113 Saltcake at 25° C	19
Figure 18.	ESP Predictions and Experimental Oxalate Concentrations for TX-113 Saltcake at 50° C	19
Figure 19.	Comparison of Experimental Nitrate Concentrations with Model Predictions for S-102 Saltcake at 25° C.	21

List of Figures (continued)

Figure 20. Comparison of Experimental TIC Concentrations with Model Predictions for S-102 Saltcake at 25° C. 22
Figure 21. Comparison of Experimental Sulfate Concentrations with Model Predictions for S-102 Saltcake at 25° C. 22
Figure 22. Comparison of Experimental Phosphate Concentrations with Model Predictions for S-102 Saltcake at 25° C. 23
Figure 23. Comparison of Experimental Nitrite Concentrations with Model Predictions for S-102 Saltcake at 25° C. 24
Figure 24. Comparison of Experimental Chloride Concentrations with Model Predictions for S-102 Saltcake at 25° C. 24
Figure 25. Comparison of Experimental Oxalate Concentrations with Model Predictions for S-102 Saltcake at 25° C. 25
Figure 26. Dissolution Profiles for TX-113 Saltcake – ESP Predictions for Feed Stability Experiment of Herting [3]. 29
Figure 27. Dissolution Profiles for BY-102 Saltcake 31
Figure 28. Dissolution Profiles for BY-106 Saltcake 31
Figure 29. Dissolution Profiles for A-101 Saltcake 32
Figure 30. Solids Speciation – Cumulative Receiver Tank – BY-102 Saltcake 34
Figure 31. Solids Speciation – Cumulative Receiver Tank – A-101 Saltcake 34
Figure 32. Solids Speciation – Cumulative Receiver Tank – TX-113 Saltcake 35
Figure 33. Solids Speciation – Cumulative Receiver Tank – BY-106 Saltcake 36
Figure 34. Solids Speciation – Cumulative Receiver Tank – S-102 Saltcake 36
Figure 35. Comparison of ESP Predictions with Lattice Model Results and Literature Data at 25° C. 40
Figure 36. Comparison of ESP Predictions with Lattice Model Results and Literature Data at 100° C. 40
Figure 37. Comparison of ESP Predictions with Lattice Model Results and Literature Data at 125° C. 41
Figure 38. Solubility Envelope for Sodium-Nitrate-Sulfate System at 25° C. Comparison of Model Predictions with Literature Data. 44
Figure 39. Solubility Envelope for Sodium-Nitrate-Sulfate-Hydroxide System at 25° C. Comparison of Model Calculations. 44
Figure 40. Predicted Solubility Envelopes in the Sodium-Nitrate-Sulfate-Hydroxide System at 50° C. 46
Figure 41. Solubility in the Sodium-Fluoride-Sulfate-Hydroxide System at 25° C. 46
Figure 42. Solubility in the Sodium-Fluoride-Sulfate-Hydroxide System at 50° C. 47

List of Figures (continued)

Figure 43.	Experimental Solubilities and Model Predictions for the Na-F-SO4-OH System at 25° C in Water.	49
Figure 44.	PLM Image of the Na_3FSO_4 Double Salt.	50
Figure 45.	Comparison of the Experimentally Determined Solubilities with the Model Predictions for 1m Hydroxide at 25°C.	51
Figure 46.	Experimental Measurements and Model Predictions in 3m Hydroxide at 25°C.	51

List of Tables

Table 1.	Major Constituents in Saltcakes Examined (Weight % of Sample)[a].	1
Table 2.	Molecular Streams for TX-113 and S-102 Saltcakes Generated Using Revised Strategy for Pre-Processing of Low-Water Content Saltcakes.	4
Table 3.	Comparison of Solid Phase Speciation – Inclusion of $Na_6(SO_4)_2CO_3$ as Potential Solid Species.	12
Table 4.	Solids Present in Cumulative Supernate	38

I. ESP Simulation of Saltcake Dissolution

A. Saltcake Compositions

The saltcake chosen for examination during FY00 was from tank TX-113. This saltcake contains significant amounts of a number of anions and was chosen to examine the predicative capabilities of ESP when a variety of species are expected to be present in the solid phase. The saltcake composition, determined from total sequential dissolution experiments conducted by Herting [3], is shown in Table 1 along with the compositions of the four saltcakes examined during FY98 and FY99 [1,2]. The compositions of the saltcakes studied in prior years are included for comparison.

Table 1. Major Constituents in Saltcakes Examined (Weight % of Sample)[a]

	Tank				
	TX-113	**BY-102**	**BY-106**	**A-101**	**S-102**
H_2O	12.90	26.51	14.7	31.2	(5.0)
Al^{+3}	0.30	1.65	1.58	2.39	0.67
Ca^{+2}	0.02	0.043	0.013	0.008	
Cr^{+3}	0.04	0.199	0.113	0.17	0.12
Fe^{+3}	0.02	0.053	0.019	0.014	(0.03)
K^{+}	0.03	0.10	0.243	0.31	0.07
Mn^{+2}		0.024			
Na^{+}	29.1	27.75	24.98	21.20	23.0
Ni^{+2}		0.026	0.006		
P	1.17	0.998	0.078	0.14	0.18
Si	0.04	0.072	0.017	0.027	0.03
S	5.30	2.03	0.447	0.8	0.13
U	0.14	0.064	0.019	0.034	<0.01
TIC [b]	14.4	20.6	7.15	9.04	2.95
$C_2O_4^{-2}$	0.12	1.99	1.26	1.35	0.17
Cl^{-1}	0.06	0.11	0.16	0.41	0.16
F^{-1}	0.27	1.17	0.62	0.069	<0.02
NO_2^{-1}	0.25	1.85	2.71	7.43	2.04
NO_3^{-1}	18.2	10.92	40.54	12.6	53.7
OH^{-1}	0.30	1.09	1.14	2.1	0.42
PO_4^{-3}	1.35	(0.6)	0.34	0.44	0.56
SO_4^{-2}	16.0	5.12	1.16	2.41	0.38
TOC		0.63	0.48	0.56	0.17

a Data from references [1,2,3]; ( ) represents questionable result
b Total Inorganic Carbon (TIC) reported as CO_3^{2-}
c estimated result

As evidenced by the data in Table 1, the TX-113 saltcake contains the largest weight percentages (of any of the saltcakes examined thus far) of sodium, carbonate, phosphate, and sulfate, with the sulfate weight % being significantly higher than in other saltcakes. Examination of a saltcake such as this provides the means to probe the predictive capabilities of ESP with respect to certain species. In this case, the predominance of sulfate in the original saltcake provides the mechanism through which deficiencies in ESP's representation of the various sulfate-containing solid species can be identified. The saltcake from tank BY-102, which contained significantly more carbonate than others examined during earlier work, allowed deficiencies in ESP, with respect to sodium carbonate monohydrate and sodium carbonate decahydrate speciation under high ionic strength conditions, to be identified [4].

B. Data Pre-Processing for Low-Water Content Saltcakes

In the FY99 status report [4], a recommended method for data pre-processing was detailed. This approach combined charge reconciliation by proration coupled with an iterative scheme to adjust the estimated input density to Water Analyzer to provide a weight % water in the equilibrated stream equivalent to that measured experimentally by Herting. This approach was successful in generating ESP molecular streams that had the appropriate loading of the various anions and cations for three of the saltcakes examined during earlier work (BY-102, BY-106, and A-101). These saltcakes all contained a significant amount of water. For the remaining saltcake, S-102, it was not possible to adjust the estimated input density low enough to provide the experimentally determined weight % water without encountering convergence problems within the Water Analyzer component of ESP. The saltcake from S-102 was reported by Herting to be extremely dry (no readily identifiable liquid phase at 0% dilution). The saltcake from TX-113 was similar in its physical constitution (very dry, no identifiable liquid phase). Strategies for ESP simulation of saltcakes with low water content are important so that the ESP simulation package can be routinely applied during operations planning at the Hanford site.

In order to avoid data pre-processing problems with TX-113 input data similar to those encountered during FY99 with the S-102 saltcake, sufficient water was added to the original saltcake composition prior to data input to the Water Analyzer. For a basis of 100 kg of saltcake with the composition given in Table 1, 20 kg of water were added to the mixture and ppm (mg/kg) values were calculated. Concentrations were then computed using an arbitrary density value. Addition of water in this manner does not alter the adjustment of cations and anions during charge reconciliation. However, it does impact the molalities for the various species into which the cations and anions are partitioned by the Water Analyzer component. The impact of water addition is mitigated during the iterative step in the recommended method for data pre-processing.

In this iterative step, the estimated input density (input as an entry in Water Analyzer) is adjusted to achieve the experimentally measured % water by weight. For treatment of low water content saltcakes, this is the step in the recommended procedure that gave rise to convergence difficulties. Rather than trying to match the experimentally determined % water by weight of the original saltcake by adjusting the input density, the estimated input density was adjusted using the concentration of nitrate anion in the solution at a dilution of 300% by

weight. For all of the saltcakes examined during FY98 and FY99, sodium nitrate, if present in the original saltcake, was completely dissolved at this level of diluent addition. Nitrate was also a significant component in all of the saltcakes examined and concentrations realized for nitrate anion were well above the limits of detection by ion chromatography.

A basis of 1200 kg of TX-113 saltcake was used as input to the ESP program. This represented the 1000 kg of original saltcake equilibrated with diluent at a 20% addition level (200 kg diluent). Thus, to achieve a level of 300% diluent addition, 2800 kg of water were added to the 1200 kg of saltcake using the MIX block available in ESP. The equilibrated output stream was examined to make sure that all the nitrate was partitioned into the liquid phase and the nitrate concentration was computed. This calculated concentration was then compared to the experimentally measured nitrate concentration reported by Herting for a dilution level of 300%. The estimated input density to Water Analyzer was adjusted in an iterative manner until the calculated nitrate concentration was approximately equivalent to the experimentally measured nitrate concentration at a dilution level of 300%.

In the FY99 status report [4], ESP predictions of the series dissolution test performed by Herting for S-102 were reported. These predictions used the molecular stream generated using the recommended reconciliation and density tuning approach [4]. A systematic deviation between experimentally measured nitrate concentration and that predicted by ESP was evident in the comparison plot, reproduced as Figure 1.

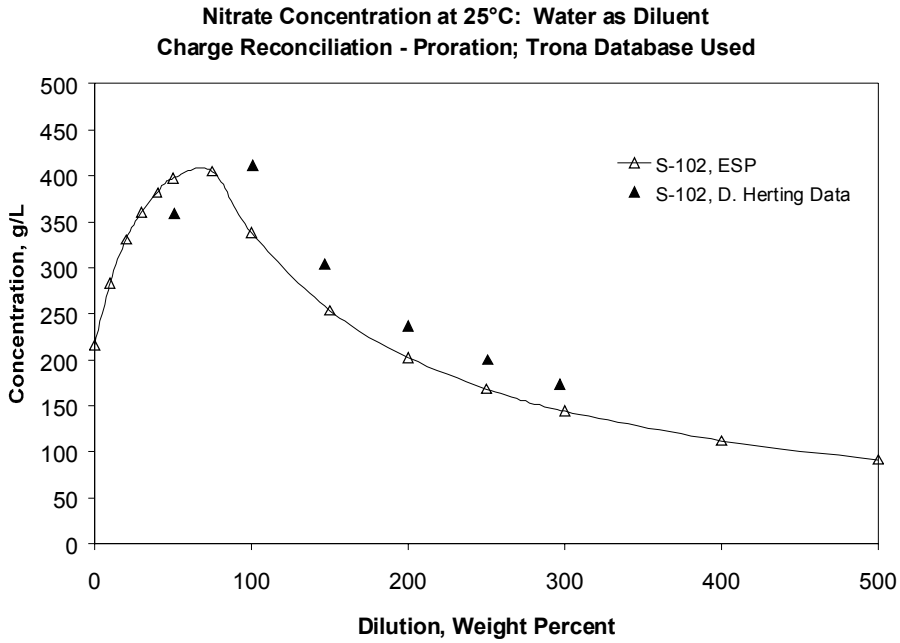

Figure 1. Prior (FY99) Comparison of Predicted and Experimental Nitrate Anion Concentrations for Tank S-102 (Reproduced from [4]).

For the range of dilutions where the nitrate is predicted to be completely dissolved, the predicted concentrations are all lower than the experimentally measured values reflecting the

fact that the input molecular stream generated for S-102 contained more water (~16%) than the original saltcake (experimentally reported value ~5%). In an effort to correct this systematic error in prediction, the strategy employed for charge reconciliation and density tuning for TX-113 saltcake was also applied to S-102 saltcake.

The molecular streams generated for both TX-113 saltcake (including the 20% dilution water) and S-102 saltcake (including 30% dilution water) are listed in Table 2. These molecular streams were used as input to the ESP simulation program for the series dissolution modeling predictions.

Table 2. Molecular Streams for TX-113 and S-102 Saltcakes Generated Using Revised Strategy for Pre-Processing of Low-Water Content Saltcakes (units are molality)

Species	TX-113[a]	S-102[b]
H_2O	55.5087	55.5087
$Al(OH)_3$	0.521157	3.05693
$Ca(OH)_2$	0.021929	
$Cr(OH)_3$	0.033805	0.290647
$Fe(OH)_3$	0.023605	
H_2CO_3	7.10591	
HCl	0.145991	0.526999
H_6F_6	0.073169	
HNO_2	0.244337	5.0344
HNO_3	13.3315	98.2247
KOH	0.033717	0.216171
$Na_6(SO_4)_2CO_3$	3.75134	
$Na_7F(PO_4)_2.19H_2O$	0.85356	
NaOH	29.9097	111.969
$H_2C_2O_4$	0.019647	0.620668
NaPHOH		0.620668
$Na_3H(SO_4)_2$		0.189093
$Na_2CO_3NaHCO_3.2H_2O$		2.78316

[a] incorporates 20 kg water per 100 kg original TX-113 saltcake
[b] incorporates 30 kg water per 100 kg original S-102 saltcake

C. Simulation of Saltcake Dissolution Experiments

The ESP process model for this experiment consisted of three unit operations: a MIX block, a HEATER block, and a SEPARATE block. In the MIX block, the molecular stream describing the overall saltcake composition for a particular tank and including the water of dilution (added during the molecular stream generation described earlier for low-water content saltcakes) is combined with the required amount of diluent to achieve the desired level of dilution. For TX-113, a basis of 1200 kg of saltcake (1000 kg saltcake plus the 200 kg dilution water) is input as one stream. Additional diluent water is added through a second

stream. Equilibration of the 1200 kg saltcake stream provides the predictions used to determine solid/liquid phase partitioning at a 20 % level of dilution. To achieve a 50% level of dilution, the 1200 kg of saltcake would be combined with 300 kg of additional diluent water (50 % dilution by weight of the original saltcake). Equilibration in the MIX block is achieved at 1 atm and 25° C. The equilibrated stream from the MIX block is passed to a HEATER block, where the temperature of the outlet stream leaving the HEATER block is adjusted to the laboratory equilibration temperature (either 25° C or 50° C). The effluent from the HEATER block is then passed to a SEPARATE block where the stream is partitioned into the relevant (solid and liquid) phases.

Preliminary ESP simulations were conducted using version 6.3 along with the PUBLIC database and the Trona (TV60TRON) database. The Trona database was incorporated as a result of FY99 work that indicated that the PUBLIC database was incapable of properly representing the behavior of sodium carbonate species (monohydrate and decahydrate) under high ionic strength conditions. Incorporation of the Trona database was found to significantly improve the predictions for carbonate and nitrate anions in the liquid phase as well as sodium carbonate monohydrate in the solid phase. The Trona database is available from OLI Systems, Inc., at no charge.

Series dissolution experiments were simulated over the range of xx% to 500 % by weight addition of water (xx indicating the % water which had to be added to the original saltcake in order to generate a molecular stream in the Water Analyzer component; e.g., for TX-113, the range examined was 20% to 500%; for S-102, the range examined was 30% to 500%). As detailed in the FY99 report, the anion concentrations reported herein as ESP predictions were obtained by summing weighted contributions from all aqueous species containing a particular anion [4].

1. Thermodynamic Database Selection

Initial simulations for the TX-113 saltcake, conducted using the PUBLIC database and the Trona database, indicated the need for improved thermodynamic data for the sulfate species; in particular, sodium sulfate anhydrous, sodium sulfate decahydrate, and the sodium fluoride sulfate double salt. In Figure 2, predictions for sulfate anion are shown along with the experimental measurements from the series dissolution tests of Herting for TX-113 saltcake [3]. The calculated ionic strength at a dilution level of 50% is ~ 24.4. The sulfate concentration predictions exhibit behavior typical of a species that is entirely found in the supernate, while the experimental data exhibit behavior typical of a species undergoing dissolution as diluent is added. This behavior is very similar to that exhibited by the carbonate anion in preliminary simulations for the BY-102 saltcake [4]. The preliminary simulations with BY-102 saltcake led to the decision to incorporate the Trona database in order to adequately describe the carbonate behavior under the high ionic strength conditions present in the Hanford saltcake waste. Discussions with OLI personnel identified a similar database for anhydrous sodium sulfate (Na_2SO_4) and sodium sulfate decahydrate ($Na_2SO_4.10H_2O$). This database, Na2snacl, developed by OLI personnel to address the

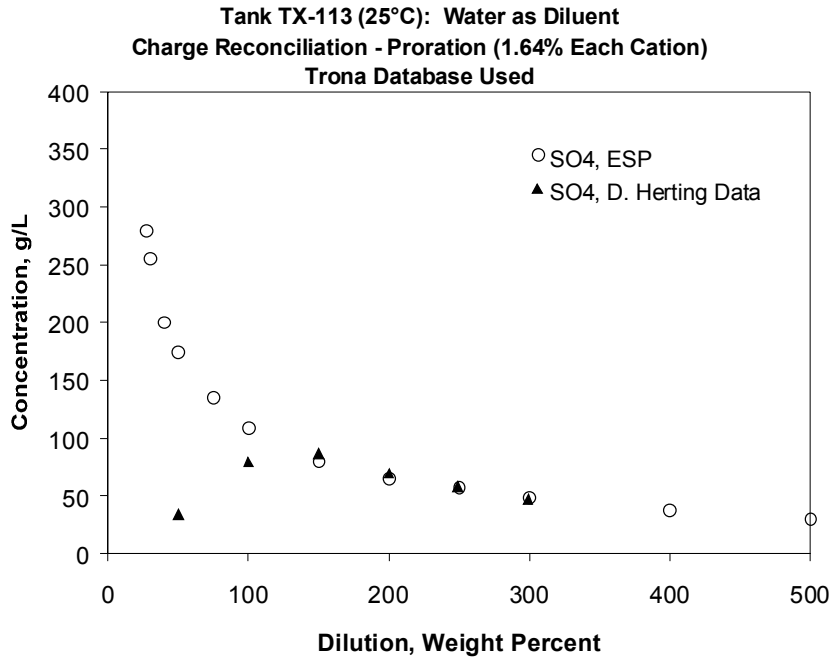

Figure 2. **Comparison of ESP Prediction and Experimental Data for Sulfate Anion from Series Dissolution Tests on TX-113 Saltcake - 25° C**

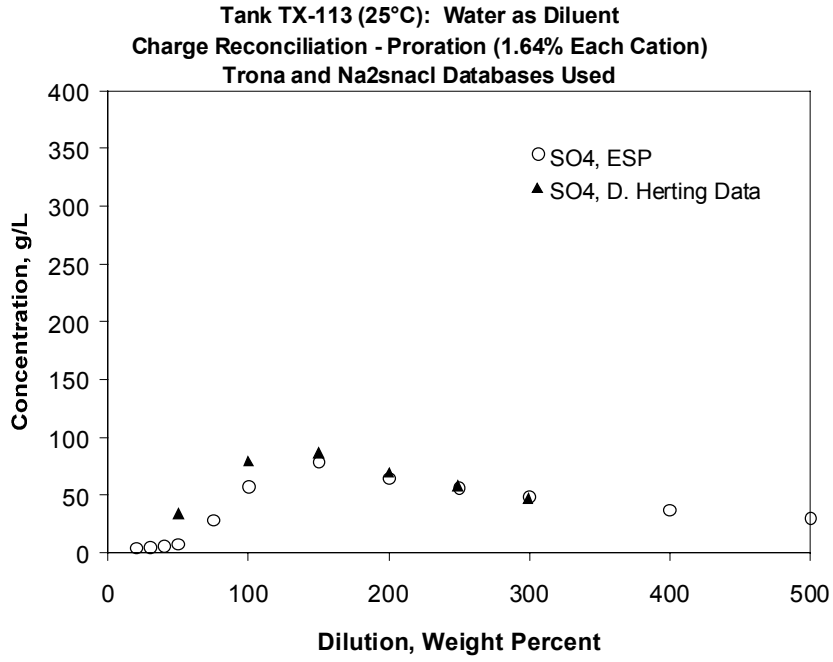

Figure 3. **Comparison of ESP Prediction and Experimental Data for Sulfate Anion - Series Dissolution Tests on TX-113 Saltcake - 25° C - Incorporation of Na2snacl Database**

behavior of the sodium sulfate system under high ionic strength conditions and is available from them at no charge. Incorporation of this database with the Public and Trona databases significantly improved the predictive capabilities of ESP with respect to sulfate anion in the TX-113 saltcake. Figure 3 provides a comparison of the sulfate anion experimental data and the predicted values obtained when the PUBLIC, Trona, and Na2snacl databases are used. The incorporation of the sulfate database significantly improved ESP predictions. The high percentage of sulfate in the original TX-113 saltcake was important in identifying the need for this specialized database. All ESP simulations discussed in this status report were carried out using Version 6.3 of ESP and the combination of three databases: PUBLIC, Trona, and Na2snacl.

2. Comparison of Model Calculations with Experimental Results For Nitrate, Carbonate, and Sulfate for TX-113 Saltcake

The TX-113 saltcake contains significantly more sulfate by weight than the other saltcakes examined through Herting's dissolution studies. Nitrate, sulfate and carbonate account for approximately 50% by weight of the saltcake, with sodium accounting for another 30 % by weight. Although the weight % of phosphate in this saltcake is low compared to the weight % of other components in the saltcake, the level of phosphate in TX-113 saltcake is also approximately six times greater than phosphate levels in the saltcakes examined earlier (Table 1). The level of carbonate in the TX-113 saltcake is comparable to that present in the saltcake from tank BY-102. The combination of these various anions in greater amounts provides a means to validate ESP when the saltcake is relatively free of liquid and contains significant amounts of certain anions that have been identified with formation of various double salts. By contrast, saltcake from tank S-102 was also relatively free of water, but contained very low levels of species implicated in double salt formation (combined fluoride, phosphate, and sulfate weight % of ~ 1.1). Herting identified the nitrate-sulfate double salt ($NaNO_3.Na_2SO_4.2H_2O$) as the major component in the solid phase of TX-113 saltcake [3]. As ESP does not have thermodynamic data available for this species, its presence as a solid cannot be predicted by the ESP code. However, comparison of ESP predictions for the sodium-nitrate-sulfate system as a function of ionic strength and of temperature with SOLGASMIX predictions and literature data indicate that the lack of thermodynamic data for the double salt within ESP does not significantly impact the prediction of the solubility envelope [5].

Figure 4 provides a comparison of the nitrate concentration experimentally determined by Herting with the ESP predictions at various levels of diluent addition at 25° C. Nitrate, accounting for 20-weight % of the original saltcake, is predicted to partition into the solid phase up to 30% diluent addition. Above this level of diluent addition, the nitrate concentration exhibits behavior indicative of a dilution process and is entirely found in the liquid phase. At a 50% diluent addition, the ESP prediction for the nitrate concentration is approximately 250 g/L, while the experimental data point is approximately 20% higher, 300 g/L. This may, in part, be due to the incomplete thermodynamic data for the sodium-nitrate-sulfate system as contained in ESP. Since the sodium-sulfate-nitrate double salt includes 2 moles of hydration water per mole of nitrate, the failure of ESP to predict this double salt could lead to the lower nitrate concentrations obtained by ESP. At the lowest level of diluent

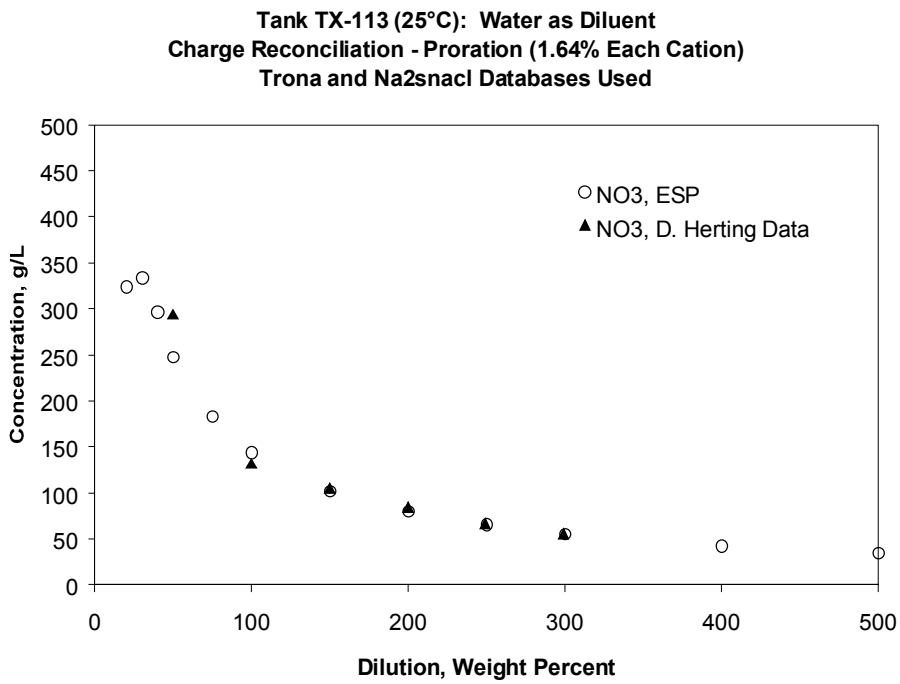

Figure 4. ESP Predictions and Experimental Nitrate Concentrations for TX-113 Saltcake at 25° C

addition (20%), the solid phase is predicted to contain approximately 213 grams of anhydrous sodium sulfate (~ 1.5 gmol) and approximately 103 grams of sodium nitrate (~1.2 gmol). If the entire nitrate was present as the double salt, this would require ~ 2.4 gmol of water (waters of hydration). As a result, concentrations in the supernate would increase by approximately 10%. The discrepancies between predictions and experimental data in the low dilution region are most likely due to the absence of thermodynamic data for the sodium-sulfate-nitrate double salt as well as deficiencies in the thermodynamic data for the other double salts, sodium-fluoride-sulfate and sodium-fluoride-phosphate. These deficiencies have previously been identified as the major contributor to differences between ESP predictions and experimental data from the dissolution tests in this region of low diluent addition (0 to 100%). Figure 5 provides the same comparison between ESP predictions and experimental data at 50° C. Again, no noticeable discrepancies are present except in the region of low diluent addition. SOLGASMIX predictions for the sodium-sulfate-nitrate double salt undertaken by Weber [5] indicate that at this temperature, the double salt is not predicted to form. Thus, the discrepancies between the ESP predictions for nitrate concentrations and the experimental measurements of Herting for TX-113 saltcake in the region of low diluent addition are attributed to deficiencies in ESP's ability to represent the behavior of other double salts of interest, including the sodium-carbonate-sulfate double salt at this higher temperature.

Experimental and predicted TIC concentrations at 25° C are shown in Figure 6 for the TX-113 saltcake. Although the model results for dilution levels of greater than 100% agree quite well with the experimental data, ESP overestimates the concentration of TIC in solution at

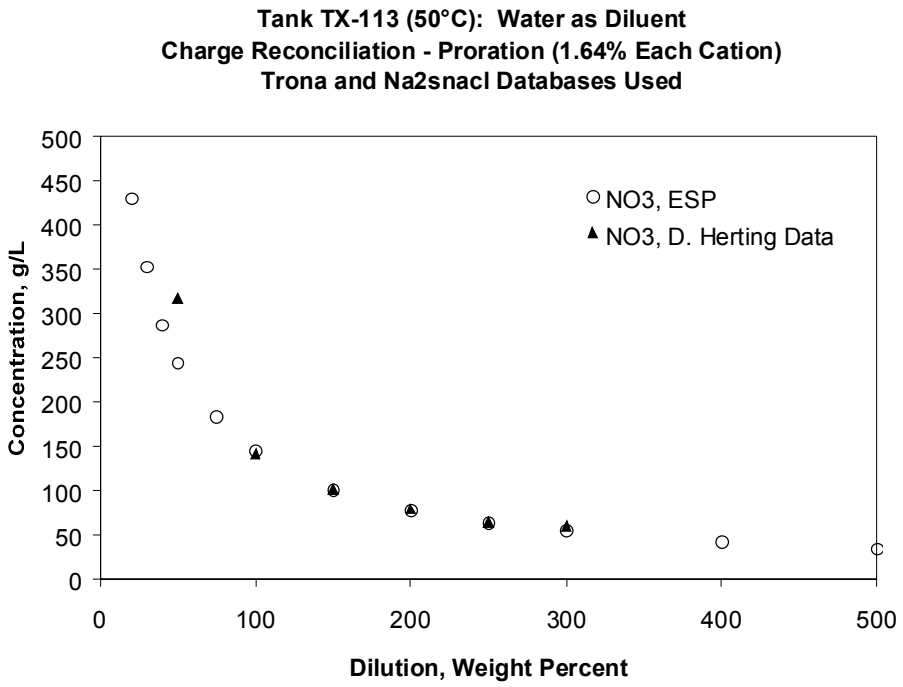

Figure 5. **ESP Predictions and Experimental Nitrate Concentrations for TX-113 Saltcake at 50° C**

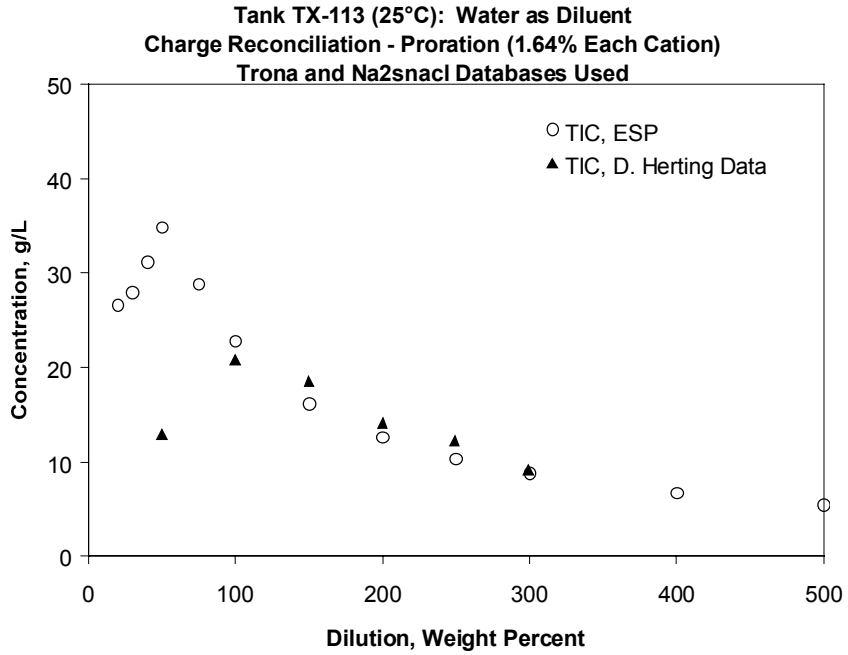

Figure 6. **ESP Predictions and Experimental TIC Concentrations for TX-113 Saltcake at 25° C**

dilution levels of less than 100% by weight. ESP predicts a maximum in the TIC concentration at approximately a 50% by weight dilution, with a magnitude of ~ 36 g/L, while the experimental value is ~ 12 g/L. ESP predicts a significant fraction (~ 1/3) of the solid phase will be the sodium carbonate monohydrate salt and that the remainder of the TIC is partitioned into the liquid phase. In contrast to the predictions at 25° C, the carbonate concentrations demonstrate better agreement with the experimental data as shown in Figure 7. At 50° C, the carbonate is partitioned into the solid phase as the sodium-sulfate-carbonate double salt, $Na_6(SO_4)_2CO_3$, rather than as sodium carbonate monohydrate. In the solid phase, the sodium-sulfate-carbonate double salt is predicted to contribute ~ 53% of the solids at the lowest level of dilution (20% by weight), increasing to ~91% of the solids before finally going into solution at dilutions greater than 200% by weight.

As demonstrated in Figure 2, use of the PUBLIC database alone will not provide for adequate representation of the behavior of sodium sulfate under high ionic strength conditions. Model predictions for sulfate concentration, obtained using the Na2snacl database in combination with the PUBLIC and Trona databases, were previously shown in Figure 3. While the predictions at dilution levels of greater than 200% are in agreement with the experimental measurements, ESP predictions for the lower region of dilution (up to 150% diluent addition by weight) are lower than the experimentally measured concentrations. This implies that ESP is predicting more sulfate to partition into the solid phase than is present experimentally. At 20 % diluent addition, the major constituents of the solid phase predicted by ESP include: anhydrous sodium sulfate (~32% by weight), sodium carbonate monohydrate (~30% by weight), the sodium fluoride-phosphate double salt and sodium nitrate; with these species accounting for over 95% of the solid phase by weight. Only a small fraction of the solid phase is in the form of the sodium-fluoride-sulfate double salt (~3% by weight of the solids at 20% diluent addition). The combination of overestimation of carbonate concentrations with underestimation of sulfate concentrations in the region of lower diluent addition prompts one to consider the sodium-sulfate-carbonate system and whether the formation of the sodium-carbonate-sulfate double salt is impacted by the high ionic strength conditions present in the saltcake at these lower levels of dilution. Due to the thermodynamic data present in the Public database, this double salt is not predicted to form at 25° C, but can form in the temperature range 30° C to 150° C. A preliminary attempt to identify the source of the combined differences in sulfate and carbonate concentrations at 25° C was made by exporting the thermodynamic data for the sodium-sulfate-carbonate double salt to a private database. The lower temperature limit of 30° C was modified and replaced with a lower temperature limit of 25° C. Saltcake dissolution at 40% diluent addition was simulated using this modified database for the sodium-sulfate-carbonate double salt and the solids phase distribution changed markedly with respect to carbonate and sulfate partitioning in the solid phase. Table 3 provides the solid phase distribution for the base case simulation of 40% diluent addition, with and without inclusion of the sodium-sulfate-carbonate double salt as a potential species in the solid phase. The solid species distribution changes very little, excepting the speciation of the sulfate and carbonate in the solid phase. The carbonate partitioned into the solid phase for either case can be evaluated using the molecular weight of carbonate per mole of the solid species into which it is partitioned. For the base case, this results in

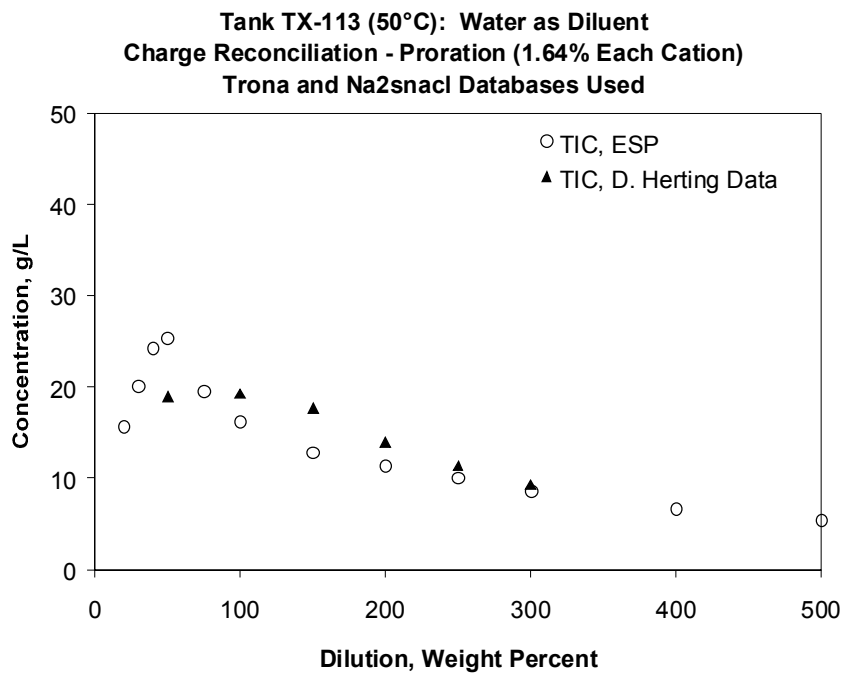

Figure 7. ESP Predictions and Experimental TIC Concentrations for TX-113 Saltcake at 50° C

$$kg(CO_3) = \frac{177.83*(12.011+3*15.9994)}{(2*22.9898+12.011+3*15.9994+2*1.00797+15.9994)} = 86.1kg(CO_3)$$

When the special database including the sodium-sulfate-carbonate double salt is used, the carbonate partitioned into the solid phase is:

$$kg(CO_3) = \frac{335.57*(12.011+3*15.9994)}{(6*22.9898+2*(32.064+4*15.9994)+12.011+3*15.9994)} = 51.6kg(CO_3)$$

For sulfate anion, a similar computation can be performed and for the base case, this leads to:

$$kg(SO_4) = \frac{237.76*(32.064+4*15.9994)}{(2*22.9898+32.064+4*15.9994)} = 160.8kg(SO_4)$$

and when the sodium-sulfate-carbonate double salt is considered, to:

$$kg(SO_4) = \frac{335.57*2*(32.064+4*15.9994)}{(6*22.9898+2*(32.064+4*15.9994)+12.011+3*15.9994)} = 165.3kg(SO_4)$$

These results indicate that an investigation of the sodium-sulfate-carbonate-hydroxide system is warranted to determine the impact of ionic strength on the solubility of the double salt as

well as to determine the effect of ionic strength on the transition temperature for the double salt formation. The impact of ionic strength on the transition temperature in both the sodium carbonate system and the sodium sulfate system are well-documented.

Table 3. Comparison of Solid Phase Speciation – Inclusion of $Na_6(SO_4)_2CO_3$ as Potential Solid Species

Species	Base Case Public + Trona + Na2snacl	Public + Trona + Na2snacl + Special Database
Total Solids (kg)	616.61	546.70
$Al(OH)_3$	6.38	6.18
$Ca_3(PO_4)_2$	0.55	
$CaCO_3$		0.53
$Cr(OH)_3$	0.73	0.74
$Fe(OH)_3$	0.54	0.54
$Na_2C_2O_4$	0.43	0.44
$Na_2CO_3.1H_2O$	177.83	
Na_2SO_4	237.76	
$Na_6(SO_4)_2CO_3$		335.57
Na_3FSO_4	24.05	19.50
$Na_7F(PO_4)_2.19H_2O$	130.46	142.45
$NaNO_3$	37.89	40.75

Figure 8 provides a comparison of the sulfate predictions with the experimental data at 50° C. Again, from the experimental data, it is observed that a large fraction of the sulfate in the original saltcake is partitioned into the liquid phase at lower dilution levels. The ESP calculations indicate complete dissolution of the sulfate salts after approximately 250% dilution by weight, in contrast to the experimental data that indicate that the sulfate is found completely in solution after approximately 150% by weight diluent is added. While the sulfate is primarily found as anhydrous sodium sulfate in the model calculations performed for 25° C, at the higher temperature of 50° C, it is partitioned into the solid phase as the sodium-sulfate-carbonate double salt.

3. Comparison of Model Calculations with Experimental Results For Phosphate and Fluoride Anions for TX-113 Saltcake

The TX-113 saltcake contains considerably more phosphate (3.75% by weight) compared to any of the saltcakes examined during previous years (0.34 to 0.56% by weight). During sequential dissolution experiments performed by Herting, he noted that the sodium- fluoride-phosphate double salt did not completely dissolve even after two sequential washes and thus, the amount of fluoride in this saltcake was estimated [3]. Herting used the ICP results for phosphorus and for sulfur from the centrifuged solids remaining after the two sequential washes and estimated an upper bound for fluoride content of 0.60% by weight. Using only the IC data from the two sequential washes provides a lower bound of 0.28% by weight for

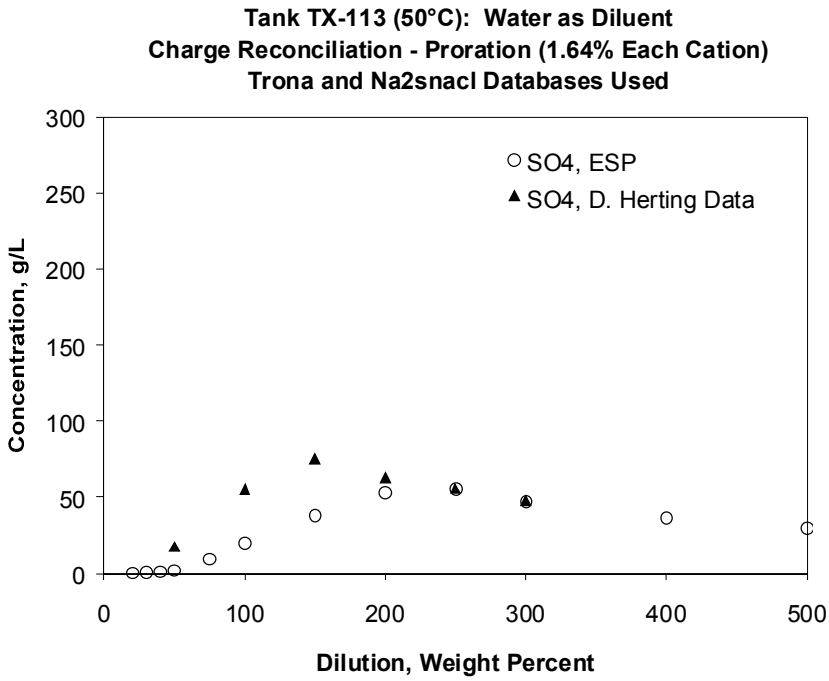

Figure 8. ESP Predictions and Experimental Sulfate Concentrations for TX-113 Saltcake at 50° C

the fluoride. This level of fluoride is in the mid-range for fluoride content of the saltcakes examined during FY98 and FY99 (0.07% to 1.17% by weight). Model results depicted in Figure 9 were obtained using the upper bound as the fluoride input and although the fluoride concentrations are small, the general trend evident in the experimental data is mimicked by the ESP model calculations. The gradual rise in the experimental data is indicative of the presence of fluoride-containing species in the solid phase. ESP predictions indicate that these species, Na_3FSO_4 and $Na_7F(PO_4)_2.19H_2O$, will persist in the solid phase until a 300% by weight dilution is achieved. Experimental dissolution results are limited to the range of 50 to 300% by weight, so experimental verification that complete dissolution of the fluoride containing species is achieved at higher levels of dilution (400 %) is not available.

In contrast to the fluoride-containing solids dissolution observed in the experimental data and predicted by the model at 25° C, the results at 50° C (Figure 10) indicate that the model predicts solids dissolution at much lower diluent addition levels than found in the experiments. In this case, the model finds a maximum fluoride concentration at a dilution of 100% by weight, while the experimental maximum is observed at 250% diluent addition by weight. This behavior is under investigation. Further improvements to the ESP database for $Na_7F(PO_4)_2.19H_2O$ and for Na_3FSO_4 system are in progress. Solid-liquid equilibrium data for the Na-F-PO_4-OH system have been provided to A. Hu at Hanford for data regression to determine parameters for the Bromley model [6]. The Bromley formulation is used in ESP to express activity coefficients. Recent experimental results for the Na-F-SO_4-OH system are reported in Section IV of this report.

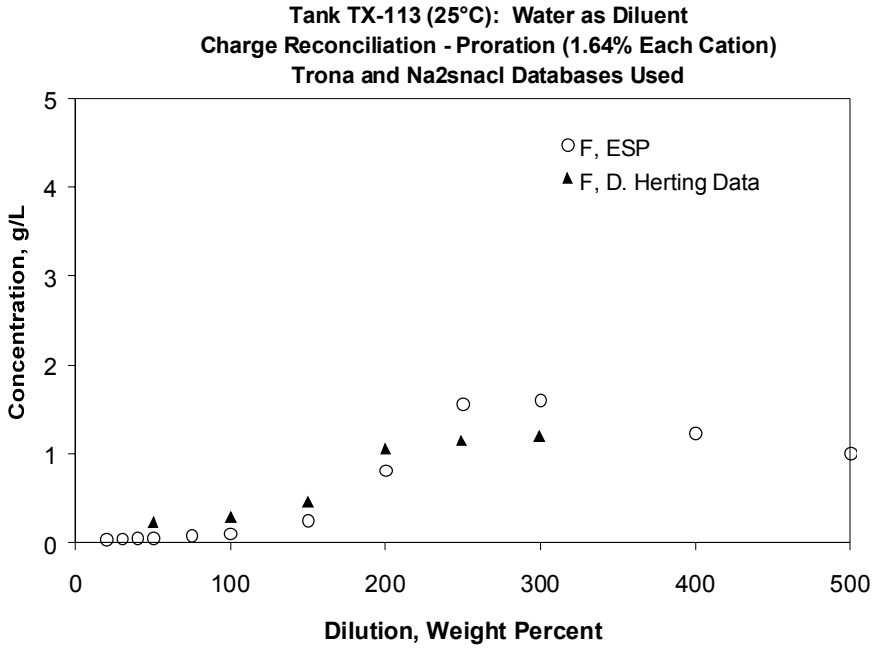

Figure 9. ESP Predictions and Experimental Fluoride Concentrations for TX-113 Saltcake at 25° C

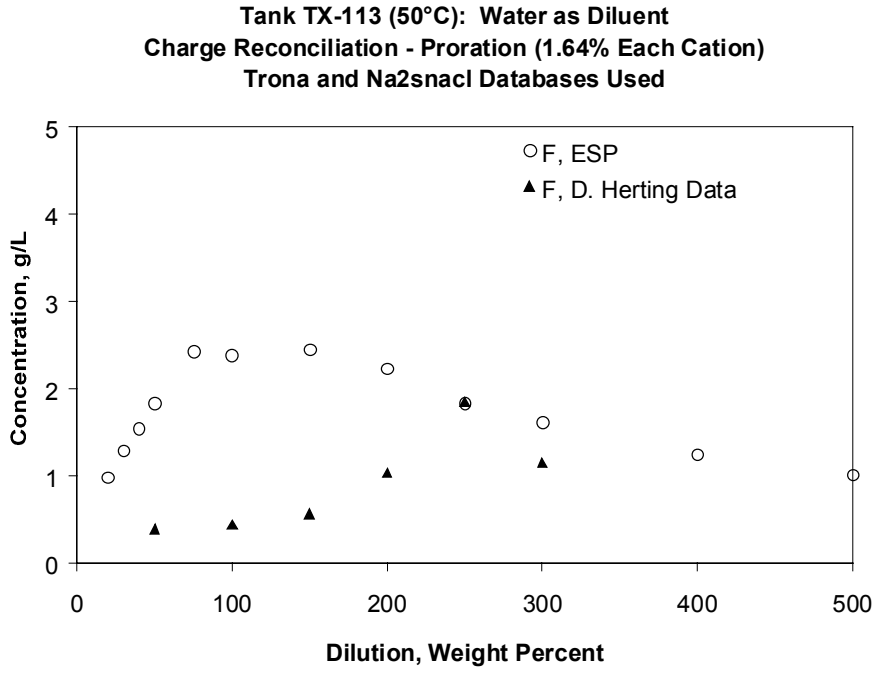

Figure 10. ESP Predictions and Experimental Fluoride Concentrations for TX-113 Saltcake at 50° C.

ESP predictions for phosphate concentrations at 25° C are shown in Figure 11. Again, the model calculations overestimate the phosphate concentration compared to the experimental measurements. The total phosphorus content in the liquid and solid phases predicted by ESP were calculated and compared with the phosphorus weight % in the original TX-113 saltcake and found to be in agreement. For this saltcake, Herting indicated that a considerable amount of the phosphorus present in the sample remained in the centrifuged solids phase after the two-step sequential dissolution [3]. It is possible that the discrepancy between ESP predictions for phosphate concentrations and the experimental measurements may be due to overestimation of the amount of phosphate in the original saltcake. A lower bound for the amount of phosphate in the waste can be estimated from the IC concentrations measured for the two-water wash steps in the sequential dissolution process. If only these contributions to the phosphate are used, the weight percentage of phosphate in the original saltcake decreases from 3.75% by weight to ~1.6% by weight. ESP simulations using this smaller input concentration for phosphate may provide a lower bound on the prediction of phosphate anion in solution as a function of diluent addition.

As shown in Figure 12, the model predictions are seen to continue to underestimate the experimental phosphate ion solubility at the elevated temperature of 50° C. The questions raised in evaluating the 25° C data also apply at the higher temperature.

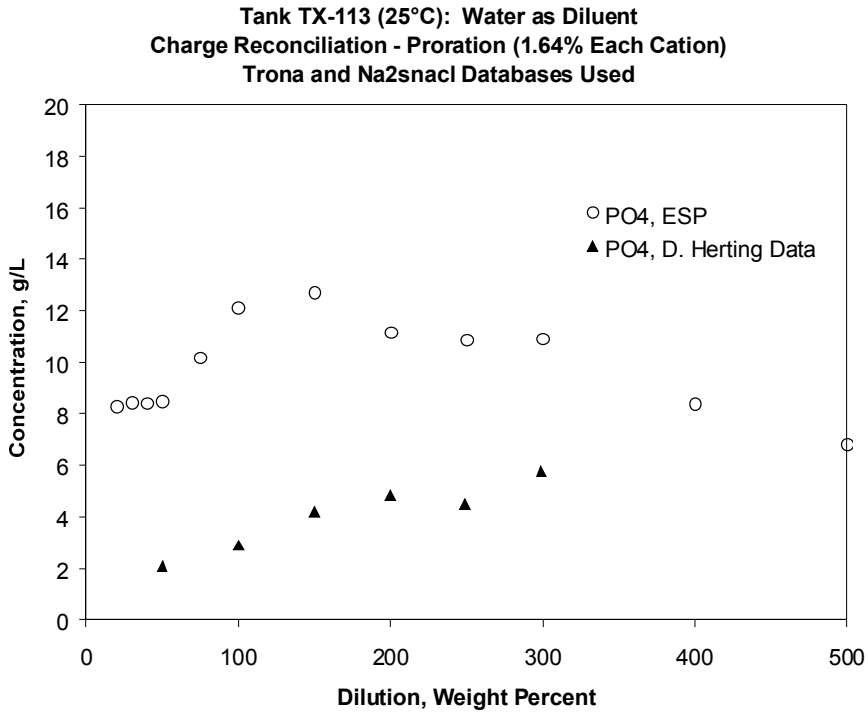

Figure 11. ESP Predictions and Experimental Phosphate Concentrations for TX-113 Saltcake at 25° C

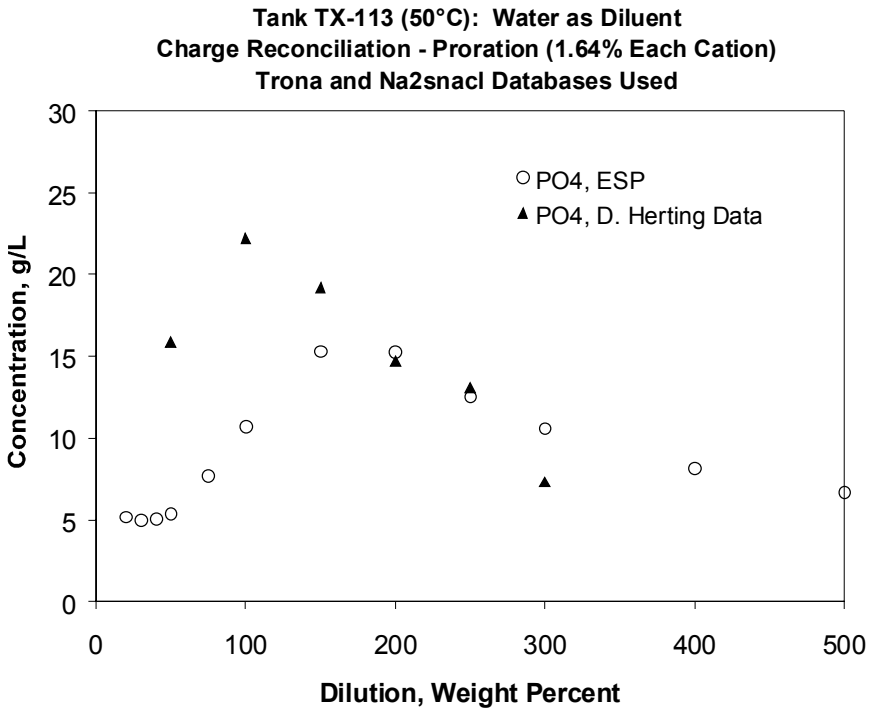

Figure 12. ESP Predictions and Experimental Phosphate Concentrations for TX-113 Saltcake at 50° C

4. Comparison of Model Calculations with Experimental Results For Nitrite, Chloride and Oxalate Anions for TX-113 Saltcake

The amounts of nitrite, chloride and oxalate contained in the TX-113 saltcake are relatively low compared to the other anions present in this saltcake. In addition, compared to the four saltcakes examined in previous work, the weight % for each of these anions is the lowest examined thus far. ESP predicts that both nitrite and chloride will be partitioned only into the liquid supernate and that no solid sodium nitrite or solid sodium chloride is present in the solid phase of the saltcake. Model predictions at 25° C for nitrite concentration agree well with experimental data over the range of diluent addition examined and are shown in Figure 13. Similar behavior is observed in Figure 14 for the dissolution studies at 50° C. For chloride, the low initial content (0.06% by weight in saltcake TX-113) compared to the range examined in earlier studies (0.11 to 0.41% by weight) may be responsible for the discrepancies observed in Figures 15 and 16 between model calculations and experimental dissolution data.

The measured experimental chloride concentrations do not exceed 1 g/L at any level of dilution. Agreement between ESP predictions of chloride concentration and experimental data from dissolution studies on other tanks have indicted that quantitative prediction is realized for chloride present at higher weight fractions.

For oxalate, Figures 17 and 18, approximately one half of the analytical measurements resulted in reported concentration level below the detection limit of the instrument. Thus,

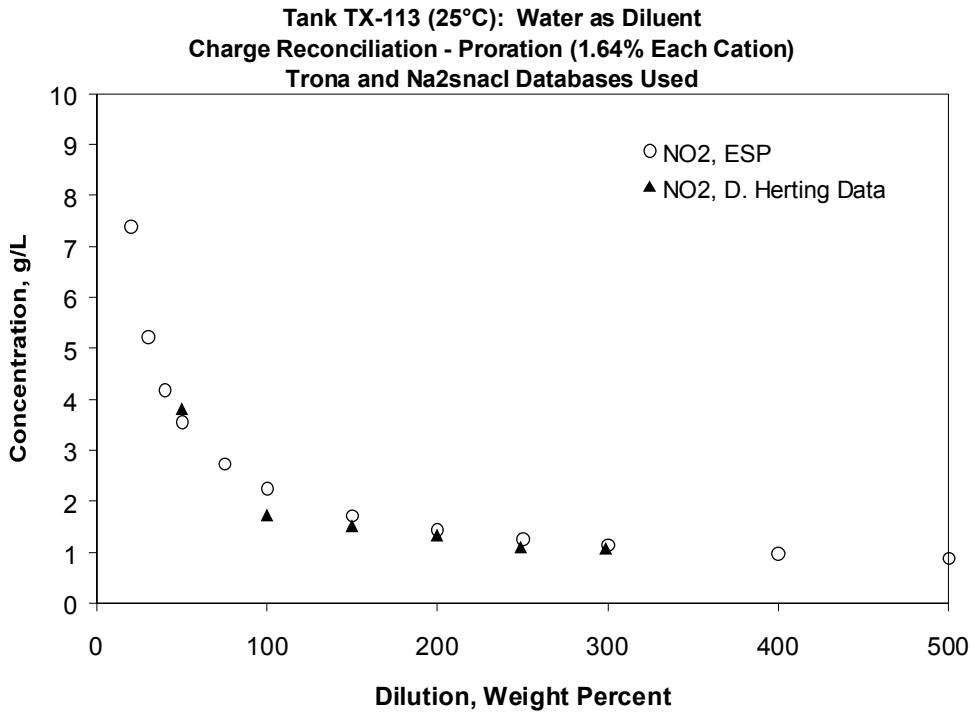

Figure 13. ESP Predictions and Experimental Nitrite Concentrations for TX-113 Saltcake at 25° C

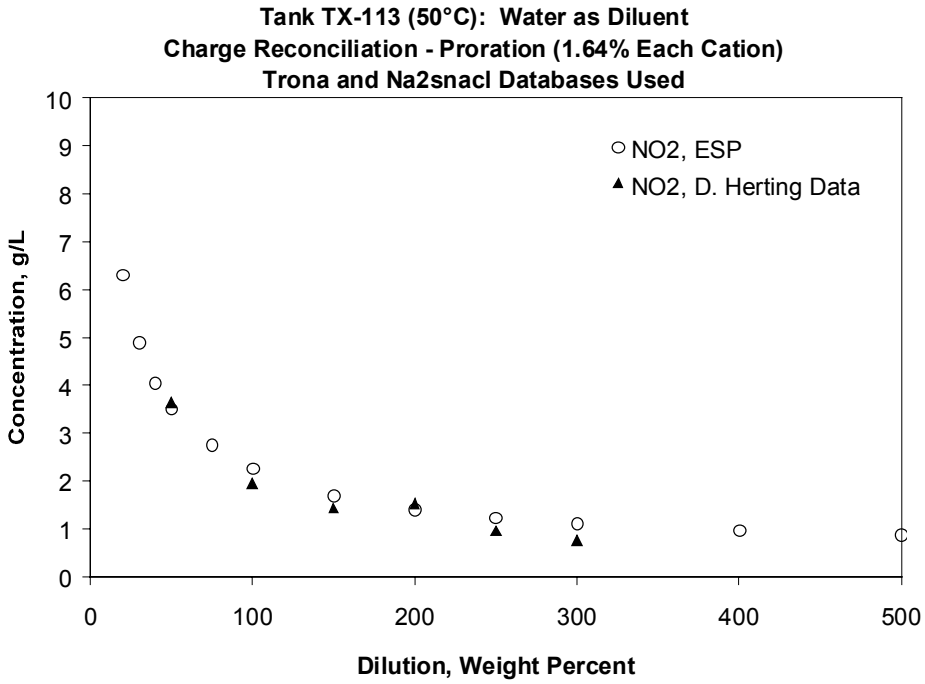

Figure 14. ESP Predictions and Experimental Nitrite Concentrations for TX-113 Saltcake at 50° C

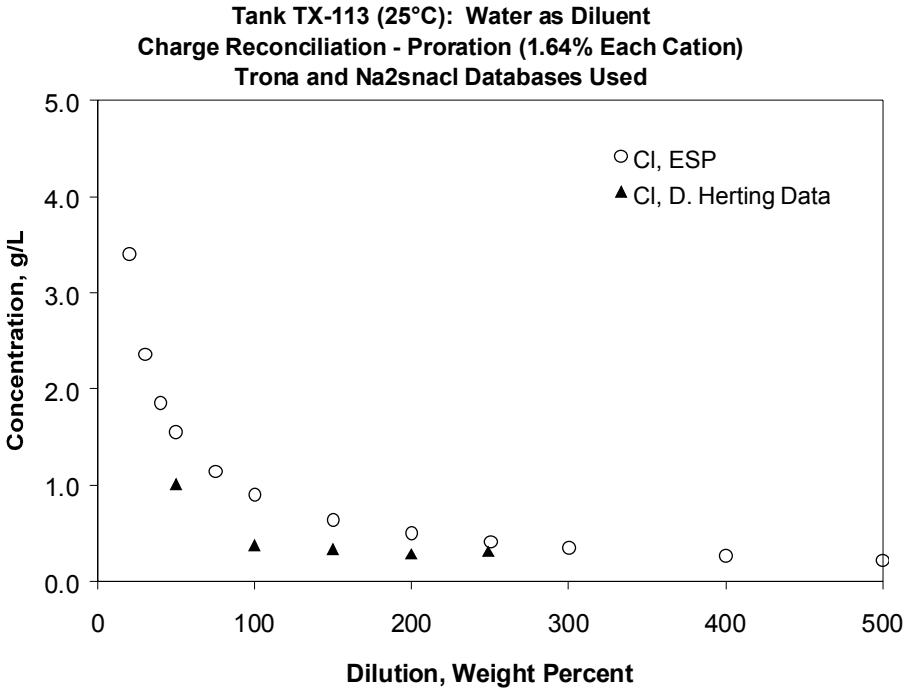

Figure 15. ESP Model Predictions and Experimental Chloride Concentrations for TX-113 Saltcake at 25° C

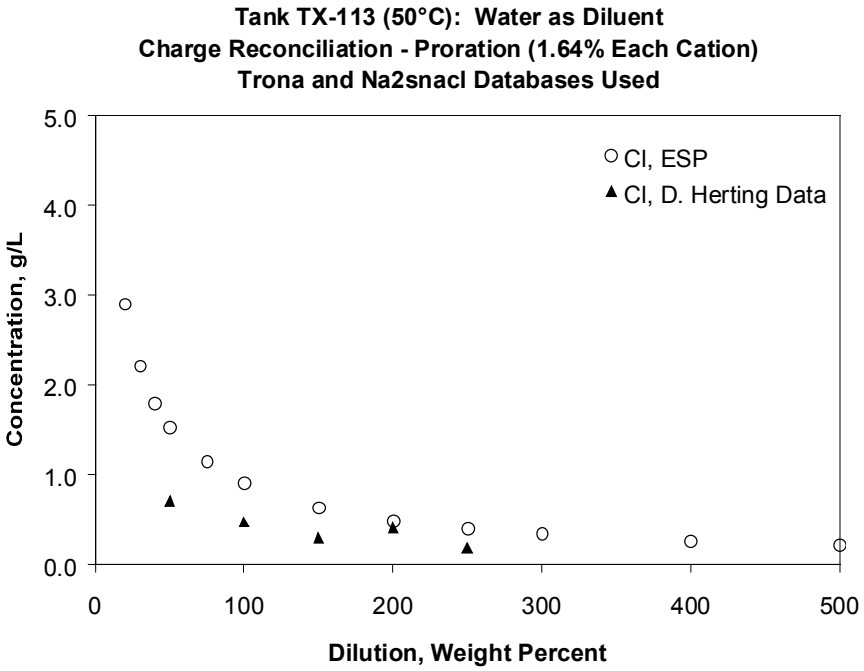

Figure 16. ESP Predictions and Experimental Chloride Concentrations for TX-113 Saltcake at 50° C.

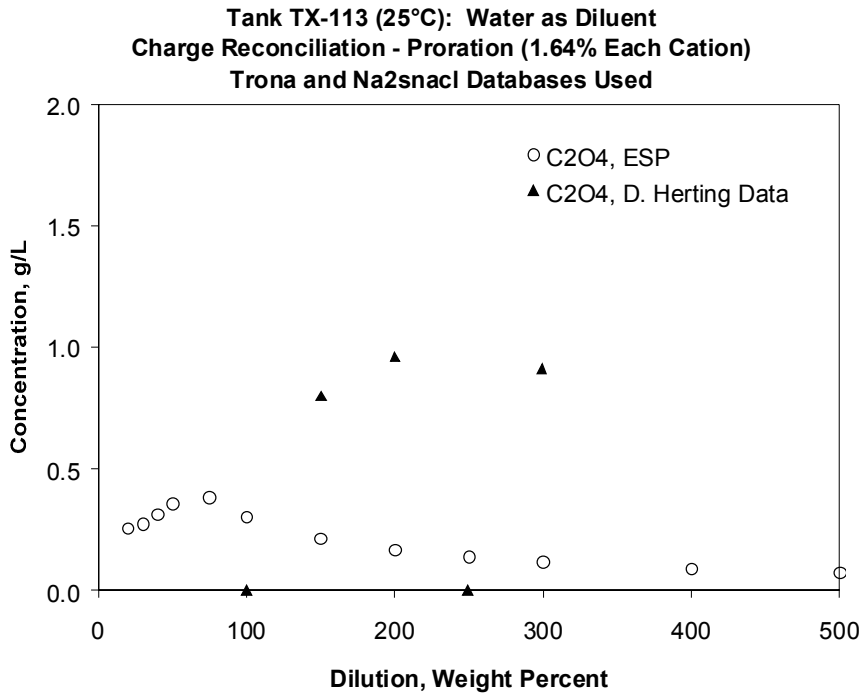

Figure 17. ESP Model Predictions and Experimental Oxalate Concentrations for TX-113 Saltcake at 25° C

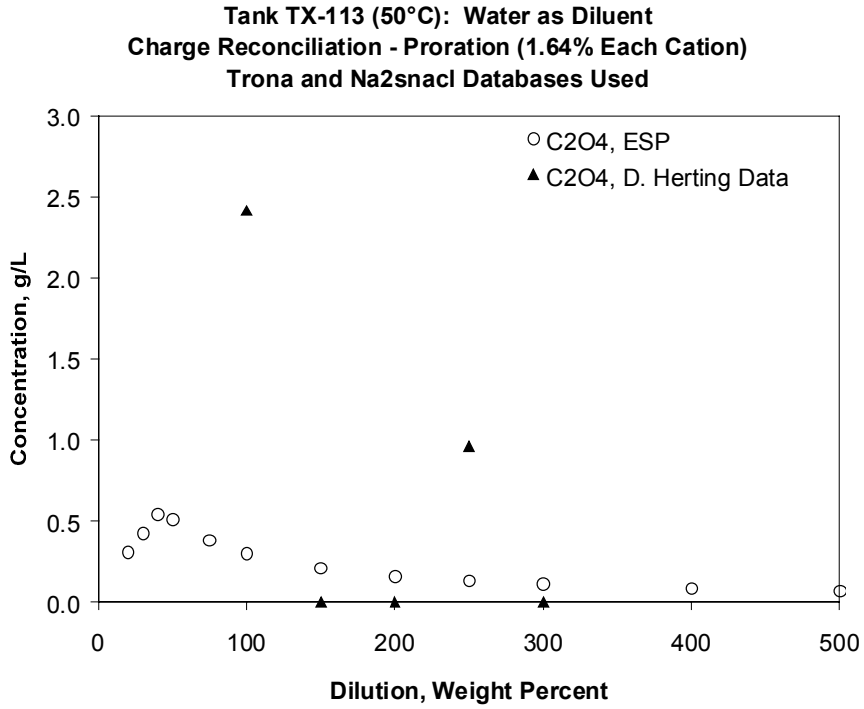

Figure 18. ESP Predictions and Experimental Oxalate Concentrations for TX-113 Saltcake at 50° C

any conclusion regarding reproducibility of experimental results by the model predictions is questionable. The predictive capabilities of ESP with regard to oxalate anion are better assessed through examination of experimental dissolution data from saltcakes with higher initial oxalate levels [4].

5. Summary/Conclusions for TX-113 Saltcake Dissolution Modeling

The choice of TX-113 saltcake for the FY00 dissolution studies was productive in terms of extending the knowledge base for ESP users at the Hanford Site. The high levels of sulfate in the saltcake led to the identification of inadequacies in the PUBLIC database for modeling the behavior of sodium sulfate salts in high ionic strength solutions. As a result, the OLI supplied database, Na2snacl, was incorporated along with the Trona database and used for all modeling reported herein. It is extremely important that these deficiencies be identified through comparison of model results to the experimental data, so that ESP can be used with confidence in staging retrieval operations at the Hanford site. The incorporation of the Na2snacl database significantly impacted the model results for the TX-113 saltcake. In addition, comparisons with experimental data are needed for the sodium-sulfate-carbonate-hydroxide system. Using the PUBLIC database coupled with the two auxiliary databases for carbonate and sulfate does not significantly impact the solid phase predictions for saltcakes that are much lower in sulfate content. This is demonstrated in Section II, where ESP model predictions are compared with experimental data from the Feed Stability Experiments conducted by Herting.

6. Comparison of Model Calculations with Experimental Results For Nitrate, TIC, and Sulfate for S-102 Saltcake

By contrast, saltcake from tank S-102 also had low water content, but nitrate alone accounted for approximately 54% of the original saltcake weight. All other anions contributed less than 5% of the original saltcake weight. Fluoride, if present, is present at less than detectable levels. Preliminary simulations for the dissolution studies of saltcake from S-102 were reported in the FY99 status report [4]. Figure 1 is a reproduction of the nitrate dissolution profile obtained during these preliminary simulations and demonstrates the systematic deviation noted for the nitrate concentrations. These earlier studies were completed using the FY99 recommended approach for charge reconciliation, but this procedure gave rise to difficulties due to the low water content of the original saltcake. Thus, the alternate strategy used for charge reconciliation and density tuning for low water saltcakes employed for saltcake from tank TX-113 was also employed for the saltcake from tank S-102. The nitrate concentration experimentally measured by Herting at a dilution level of 300% by weight was used to adjust the water content in the original saltcake with the added water of dilution. For saltcake from tank S-102, 1000 kg of the original saltcake composition were combined with 300 kg of diluent water and input to the Water Analyzer component to achieve a converged molecular stream.

All simulations for tank S-102 saltcake were performed using the triad of databases: PUBLIC, Trona, and Na2snacl. Figure 19 provides a comparison of the experimental data

for nitrate anion along with the ESP predictions obtained using the charge reconciliation and density approach recommended in Section I, part B of this report. Apart from the noticeable shift in the predicted concentrations to the experimental data and slightly lower predicted ionic strengths, no significant changes in the solid-liquid partitioning of species were noted in the revised simulations.

As indicated above, the composition of this saltcake is dominated by nitrate and sodium. All other anionic species are present at fairly low levels, but the absence of fluoride in this saltcake does provide an indication of the ability of ESP to predict saltcake dissolution in the absence of double salt formation. Of the double salts that have been predicted through ESP during simulations of dissolution for other saltcakes, the only double salt of potential interest in S-102 saltcake is the sodium-sulfate-carbonate double salt (predicted only at 50° C).

Figure 20 provides a comparison of the experimental TIC concentrations measured by Herting and the ESP predictions at 25° C. The weight percentage of TIC in the original saltcake is less than 1 % (~ 0.6% by weight). This is reflected in the low concentrations realized for TIC during the dissolution studies. No carbonate is partitioned into the solid phase at even the lowest level of dilution examined (20% by weight).

Sulfate was also present in this saltcake at fairly low levels (~0.3 % by weight). The general trend exhibited by the experimental data is predicted by ESP as evidenced in Figure 21.

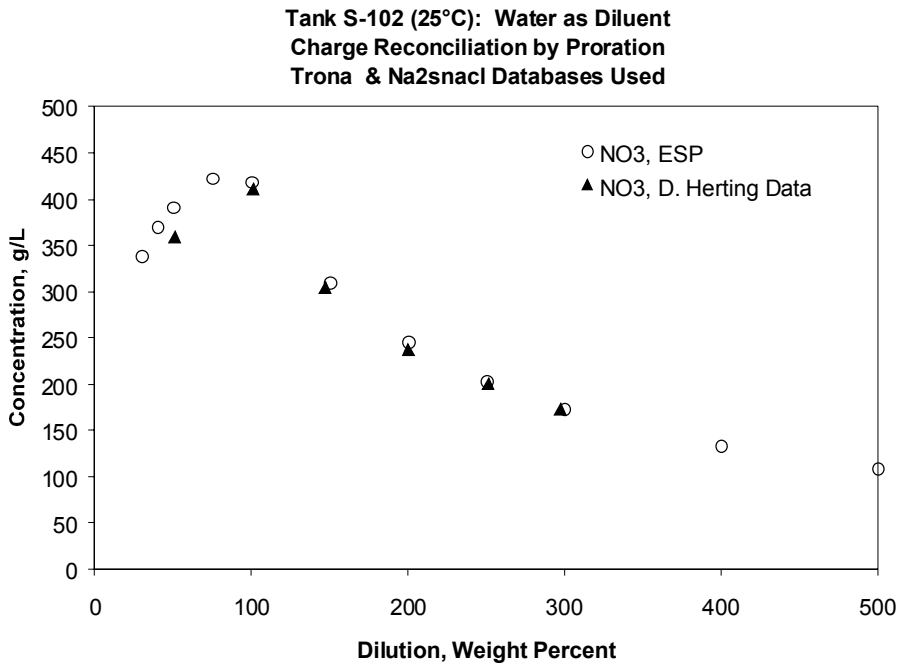

Figure 19. Comparison of Experimental Nitrate Concentrations with Model Predictions for S-102 Saltcake at 25° C.

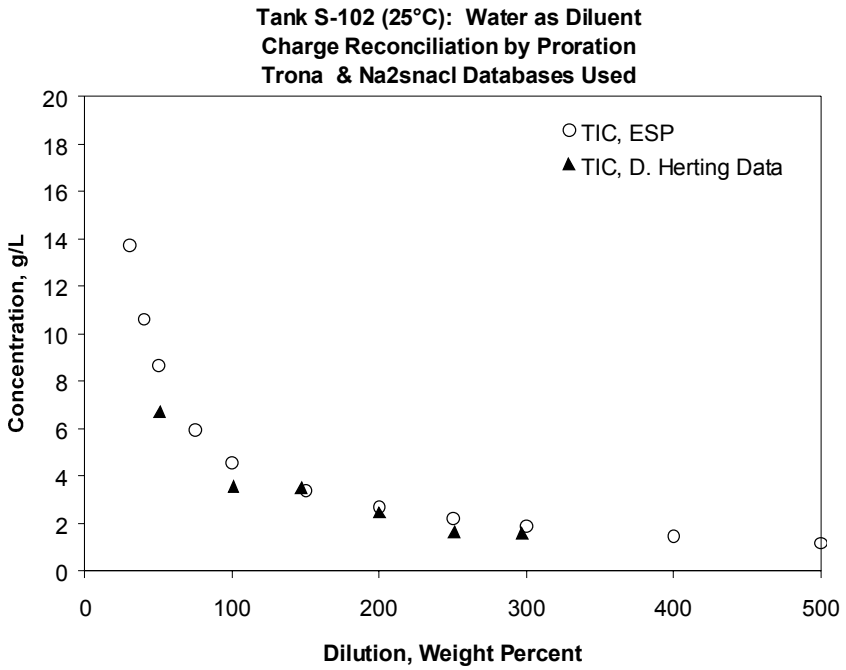

Figure 20. Comparison of Experimental TIC Concentrations with Model Predictions for S-102 Saltcake at 25° C.

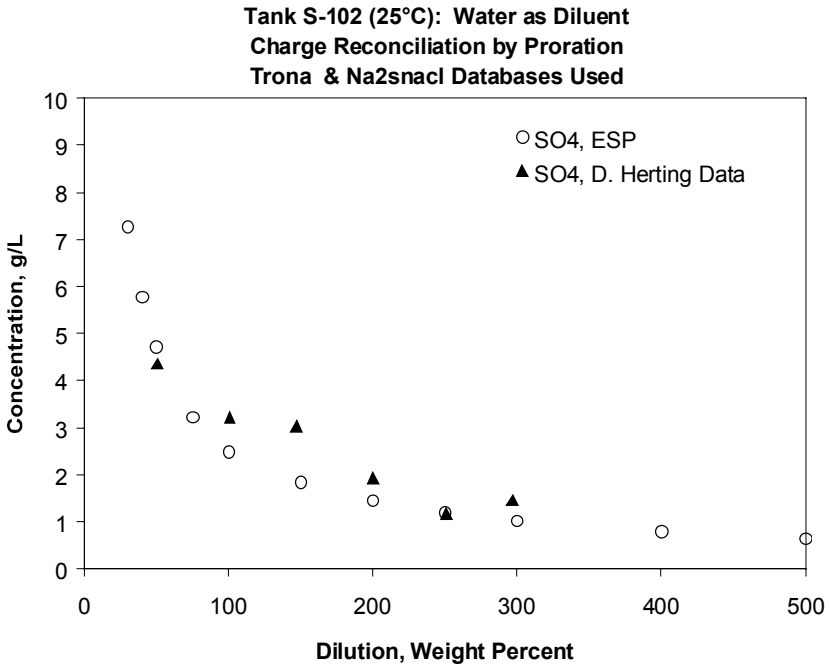

Figure 21. Comparison of Experimental Sulfate Concentrations with Model Predictions for S-102 Saltcake at 25° C.

7. Comparison of Model Calculations with Experimental Results For Phosphate, Nitrite, Chloride, and Oxalate for S-102 Saltcake

In Figure 22, experimental data and ESP predictions of the phosphate anion are compared for the S-102 saltcake. The original saltcake contains ~0.52% by weight phosphate. In the preliminary simulations (reported in FY99), trisodium phosphate, $Na_3PO_4.0.25NaOH.12H_2O$, was predicted to be present in the solid phase at 0% dilution, but quickly undergo dissolution, resulting in complete dissolution by approximately 30% diluent addition. This level of diluent addition was the lowest addition level examined with the revised charge reconciliation and density tuning approach employed during FY00.

Nitrite and chloride are also present at low levels in the S-102 saltcake, 2.0% and 0.16% by weight, respectively. In all saltcakes examined thus far, the levels of nitrite and chloride have been sufficiently low that all of the nitrite and chloride has been predicted to partition into the liquid phase, in accordance with experimental measurements. Figure 23 provides a comparison between the experimental data of Herting and the ESP predictions for nitrite anion, while Figure 24 provides a similar comparison for chloride anion. The agreement between experimental measurements and ESP predictions has been demonstrated for every saltcake examined thus far. Validation of the representation for these species within ESP has been demonstrated for the composition ranges examined thus far (0.06% to 0.41% by weight for chloride; 0.26% to 7.43% by weight for nitrite). It would be beneficial to identify whether these ranges encompass the variability in composition that may be encountered at

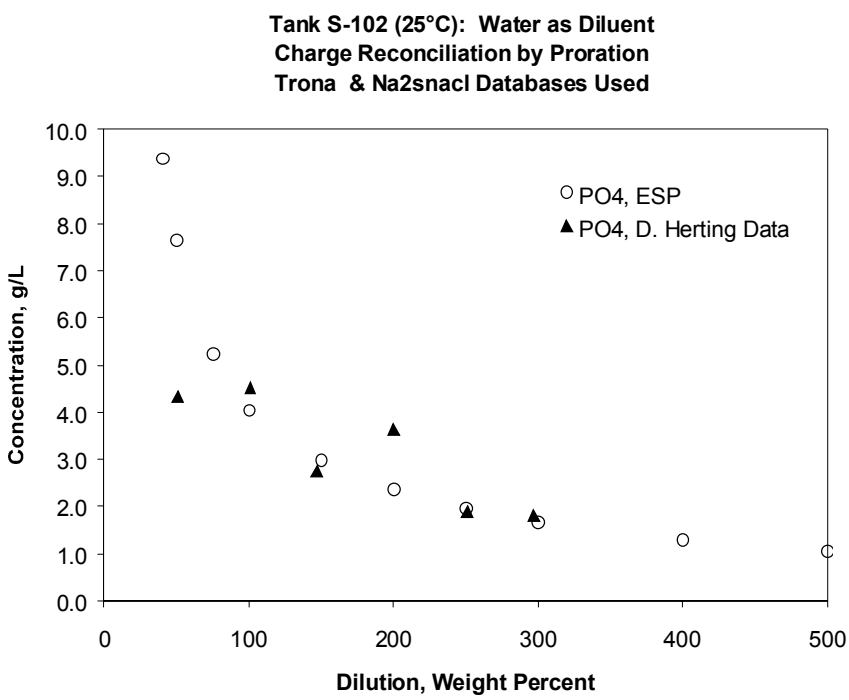

Figure 22. Comparison of Experimental Phosphate Concentrations with Model Predictions for S-102 Saltcake at 25° C.

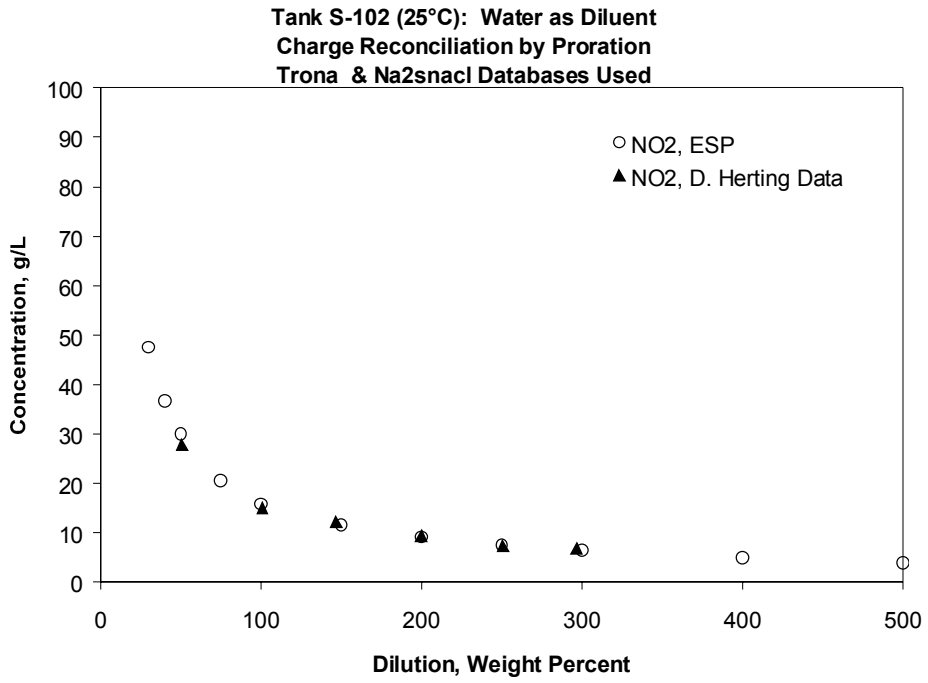

Figure 23. Comparison of Experimental Nitrite Concentrations with Model Predictions for S-102 Saltcake at 25° C.

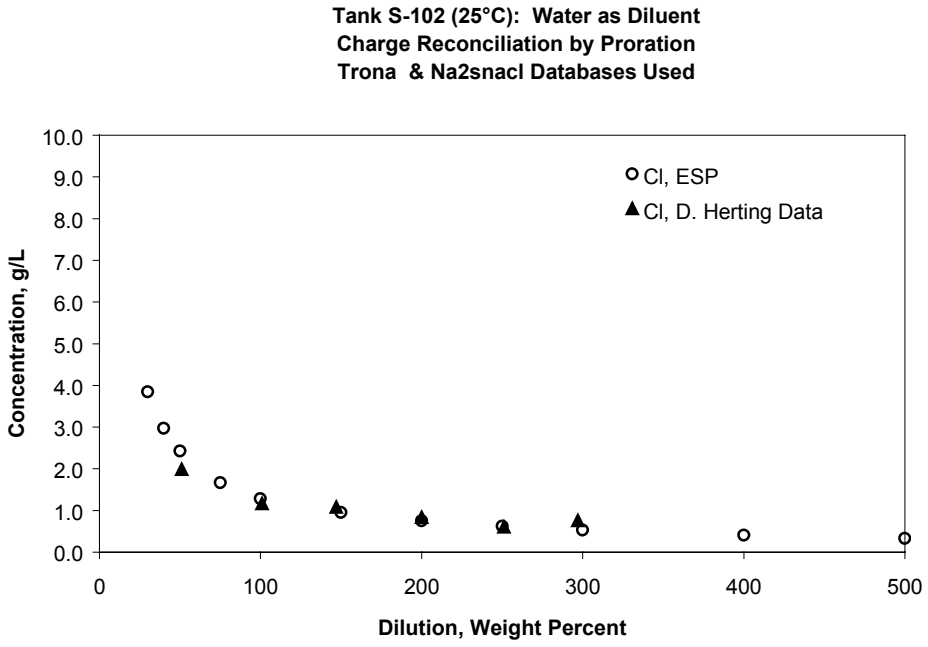

Figure 24. Comparison of Experimental Chloride Concentrations with Model Predictions for S-102 Saltcake at 25° C.

the Hanford Site or if there are saltcakes at the Hanford Site which contain significantly higher levels of either chloride and/or nitrite. If such saltcakes are identified, it would be of interest to examine the dissolution behavior of these saltcakes by comparison of ESP prediction with experimental studies.

Saltcake from tank S-102 contains approximately 0.17% oxalate by weight. Experimental data for the oxalate concentration are not available for two of the six diluent addition levels examined because the oxalate was not present above detectable levels. ESP predictions are compared with the available experimental data in Figure 25. The general trend evidenced in the experimental data is also provided by the ESP predictions. Again, a more thorough examination of the behavior of oxalate with regards to its prediction by ESP could be gained through examination of a saltcake containing significantly more oxalate.

8. Summary/Conclusions for S-102 Saltcake Dissolution Modeling

The revised charge reconciliation and density tuning method reported in Section I, Part B, of this work has been used to provide improved predictions for the S-102 saltcake dissolution studies compared to similar predictions reported during FY99. Tabulations of data used to prepare the comparison plots are contained in Appendix A. Also included in Appendix A are tables containing solid phase speciation and comparison with the experimental measurements of Herting [2,3]. Appendix B contains comparison plots for the S-102 dissolution studies at 50° C.

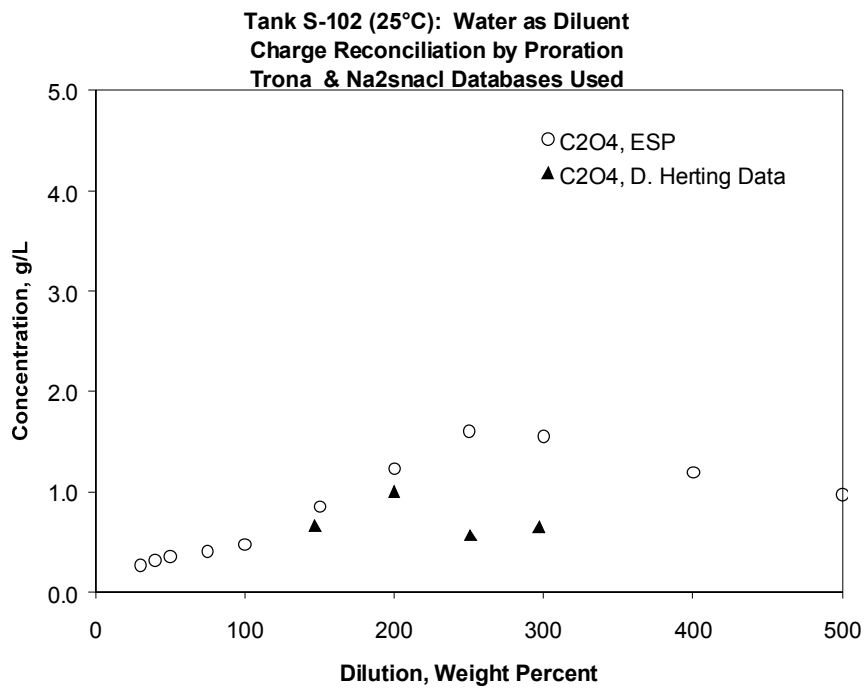

Figure 25. Comparison of Experimental Oxalate Concentrations with Model Predictions for S-102 Saltcake at 25° C.

9. Overall Summary for Saltcake Dissolution Modeling

Major progress in modeling saltcake dissolution experiments was made during FY00. Difficulties encountered during data pre-processing of low-water content saltcakes have been addressed through the revised charge reconciliation and density tuning method reported herein. Additionally, the identification of deficiencies in the representation of sulfate species using the Public database alone resulted in the incorporation of a special database which provides more accurate representation of known behavior for the sodium sulfate species under high ionic strength conditions. Experimental efforts scheduled during FY01 on the behavior of the sodium-sulfate-carbonate double salt under high ionic strength conditions should address the questions that have arisen during analysis of the TX-113 saltcake dissolution comparison.

Deficiencies in ESP's capabilities with respect to carbonate and to sulfate have only been identified through judicious selection of saltcakes containing sufficient levels of these anions. It would be beneficial to identify other saltcakes containing the maximum levels of phosphate, fluoride, nitrite and oxalate. If these maximum levels are significantly greater than the ranges that have already been examined through the saltcake dissolution studies thus far, it may be worthwhile to conduct similar saltcake dissolution studies with these select samples.

II. ESP Simulation of Feed Stability Studies

As part of the FY00 workscope, Herting performed a series of experiments, Feed Stability Studies, which were designed to examine the possible formation of solids when liquid supernates from different stages in the retrieval process are remixed. It was evident from the series dissolution testing performed by Herting [1,2] that the composition of the liquid supernate will vary with time as diluent is added to the tank because the various salts present in the solid phase will dissolve at different times. The feed stability experiments were conducted using the five saltcakes (from Tanks BY-102, BY-106, A-101, S-102, and TX-113) examined in the series dissolution tests. Thus, saltcake input streams for ESP modeling of the feed stability experiments were the molecular streams generated for the series dissolution tests. These streams are compiled in Appendix C.

In the feed stability study, a known amount of saltcake (30 g) was contacted with a known amount of inhibited water. The weight of added diluent was either 15 g (contacts 1 through 6) or 30 g (contacts 7 through 10). The saltcake/diluent sample was thoroughly mixed, then centrifuged to separate the liquid supernate from the undissolved solids. The liquid supernate was decanted and stored in a cumulative receiving tank. The undissolved solids were then contacted with another 15 g (or 30 g) of diluent, and the mixing, centrifugation, and decantation process repeated. The liquid supernate from this second contact was added to the cumulative receiving tank where it mixed with the liquid supernate from earlier contacts. The cumulative receiving tank was monitored for precipitated solids for a period of approximately 24 hours. If solids precipitated, then the mixture in the cumulative receiving tank was decanted and the solids recovered for identification. All experiments were conducted at ambient conditions. Identification of solids using PLM provided qualitative information as to the species present in these solids as well as identification of the major species present. More detail regarding experimental procedures is given by Herting [3].

Herting also conducted 'Radionuclide Distribution' studies during FY00 [3]. In these studies, a known amount of saltcake (30 g) was contacted initially with 10 grams of inhibited water. The sample was then mixed, and centrifuged to separate the liquid supernate from the undissolved solids. The undissolved solids were then contacted with another 10 grams of inhibited water and the mixing/centrifugation process repeated. The liquid supernates obtained from each contact stage were analyzed by IC, ICP and radionuclide analysis. From the analysis, it is possible to determine the fraction of each particular analyte that had been dissolved at each stage. These results can then be presented to demonstrate that the various analytes are recovered at different stages of retrieval. Herting reported these results in his FY00 report for studies using saltcakes from tanks A-101, S-102 and BY-106. Similar experiments were conducted during FY99 for saltcake from tank BY-102 and are reported in his FY99 report [1]. These experiments were not conducted on saltcake from tank TX-113.

These two experiments, 'Feed Stability' and 'Radionuclide Distribution' provide experimental data that can be compared to ESP model calculations designed to mimic the experiments. The simulation of these staged contact experiments using ESP requires a sequence of processes to model each contact (with mixing) and the subsequent partitioning into supernate and solid fractions using centrifugation. Each staged contact is modeled using

a MIX block, where the original saltcake (or undissolved solids) is combined with the desired amount of diluent. Equilibration is carried out at 25° C and 1 atm. The effluent from the MIX block passes to a SEPARATE block where the liquid and solid fractions are partitioned into two streams, one representing the liquid supernate and the other the solid fraction. The liquid stream flows into a MIX block (representing the cumulative receiver tank) and the solid stream is passed to another MIX block representing the next contact. Version 6.3 of ESP was used along with the PUBLIC, Trona and Na2snacl databases.

A. Data Post-Processing of Simulation Output

Post-processing of the simulation output requires the examination of the solid phase and of the liquid phase leaving a given contact stage to determine what fraction of a particular anion has been dissolved from the original saltcake during a given contact. The solid phase speciation predicted by ESP is compared with the results of the 'Feed Stability' experiments, while the liquid phase predictions are compared with the results of the 'Radionuclide Distribution' experiments. Appendix D contains summary tables that show the dissolution of various anions as a function of contact stage and can be used to track the degree of dissolution of one anion with respect to another. These summary tables have been used to generate comparison plots that show the various anions dissolving at different stages of contact. The supernate obtained from each stage of contact will differ not only in ionic strength, but also in the relative concentrations present for various anions. Recombination of these liquid fractions in the cumulative receiver can give rise to precipitation of solids. The solids formed in the cumulative supernate are tracked as a function of contact number (or cumulative diluent addition by weight). The variations, both in the amount of solids formed as well as the composition of the solid, are depicted in bar plots.

B. Discussion of Results

1. Anion Dissolution Behavior – Model Predictions

As expected, the various anions in the saltcake dissolve to different degrees as the saltcake is contacted with inhibited water. The presence of relatively high amounts of phosphate, sulfate, and fluoride in saltcakes from TX-113, BY-102, and BY-106 caused a considerable fraction of the original solids in the saltcake to be present as the sodium double salts of these anions, $Na_7F(PO_4)_2.19H_2O$ and Na_3FSO_4. These double salts along with sodium oxalate tended to remain in the solid phase, dissolving only to a small extent, while sodium carbonate monohydrate (if present in the solid phase) and sodium nitrate dissolved during the initial contact with inhibited water. These behaviors are demonstrated for the most part in all of the saltcakes examined, with the exception of the saltcake from tank S-102, which contained primarily sodium nitrate.

Dissolution profiles for the various anions present in TX-113 saltcake are shown in Figure 26. This saltcake, high in nitrate, sulfate and carbonate, demonstrates that the various anions in the saltcake are dissolved at different diluent addition levels. The carbonate, initially present as the sodium carbonate monohydrate, is dissolved along with a significant portion of the sodium nitrate during the first contact stage where 30 grams of TX-113 saltcake is

contacted with 15 grams of inhibited water. Slower to dissolve are the sodium fluoride sulfate double salt and the sodium fluoride phosphate double salt. Thus, the liquid supernate from the first contact will be rich in nitrate and carbonate, while the liquid supernate from the second contact will be rich in sulfate with small amounts of nitrate and phosphate. These streams, when remixed in the cumulative receiving tank, will combine to give rise to precipitates (discussed in the following section). This behavior was mirrored by all of the saltcakes examined. The liquid supernate obtained at each stage of contact was not uniform in composition, but was rich in the particular anion(s) that were dissolving.

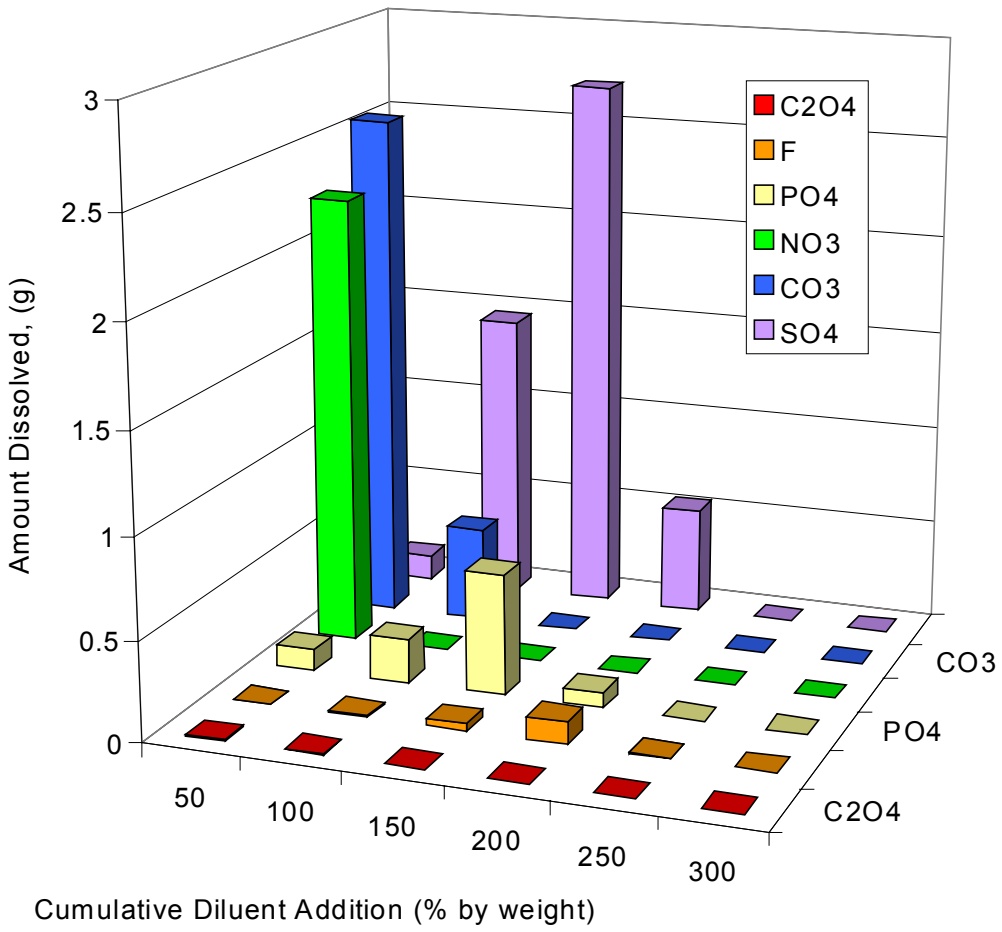

Figure 26. Dissolution Profiles for TX-113 Saltcake – ESP Predictions for Feed Stability Experiment of Herting [3].

Figure 27 provides fractional dissolution curves for select anions from the BY-102 saltcake. The experimental data of Herting [3] were used to prepare the curves depicted. The open symbols represent the ESP prediction for the fraction of a particular anion which had dissolved at a given level of cumulative diluent addition. Two generalizations can be made regarding the data depicted in this figure. First, ESP overestimates the fraction of each particular anion dissolved at a given level of cumulative diluent addition. This is to be expected as the ESP program establishes the equilibrium composition of the liquid and solid

phases, in essence, providing for a mixing time approaching infinity. For finite mixing times such as those realized during the experiments conducted by Herting, it is expected that a lesser amount of a given anion would dissolve. Second, the general trends depicted by the experimental data are demonstrated by the ESP predictions. The predictions indicate that, for the BY-102 saltcake, dissolution of carbonate will precede sulfate, fluoride, and phosphate. This trend is identical to that depicted by the experimental data. Not shown in Figure 27 are the dissolution profiles for nitrate, nitrite, chloride, or oxalate. Nitrate, nitrite and chloride are predicted to be essentially dissolved (100%) at the lowest level of diluent addition examined (50% by weight). This finding was also verified by the experimental data. Oxalate, on the other hand, was predicted to be completely dissolved by a diluent addition level of 100% by weight, yet experimentally, was demonstrated to slowly dissolve, with only 3.5% dissolved at a cumulative diluent addition level of 100% by weight.

The dissolution profiles for BY-106 and A-101 saltcakes are shown in Figures 28 and 29, respectively. Fewer contacts were performed experimentally, thus, the experimental data are limited to the range of 50 to 150 % cumulative diluent addition. The feed stability simulations, however, examine the cumulative diluent addition range of 50% to 300% by weight. For both saltcakes, the same generalizations can be made as were made for BY-102 saltcake. ESP predictions overestimate the fraction of each anion dissolved at a given stage of diluent addition. However, the general trends exhibited in the sequence in which anions are dissolved from the solid and partition into the liquid phase are the same as those demonstrated experimentally.

Simulation of the feed stability experiment was also performed for S-102 saltcake; however, because of the high level of nitrate and the combined low level of all other anions, the dissolution profile for this saltcake does not provide any interesting behavior.

2. Formation of Solids in Cumulative Supernate Receiver

During the feed stability experiment, the supernate collected from each contact was added to a cumulative supernate receiver and monitored for solids formation. ESP predictions of the solids that would form upon mixing of the supernates from the staged contacting are tabulated in Table 4. Since ESP performs an equilibrium calculation when the supernate from a particular contact is combined with the cumulative supernate from all preceding contacts, the solids predicted are those that would form given an infinitely long period of time. In the experiment, Herting waited approximately 24 hours after addition of supernate to the cumulative receiver to visually determine whether solids had formed. Gibbsite was not observed experimentally, but was predicted to form by ESP.

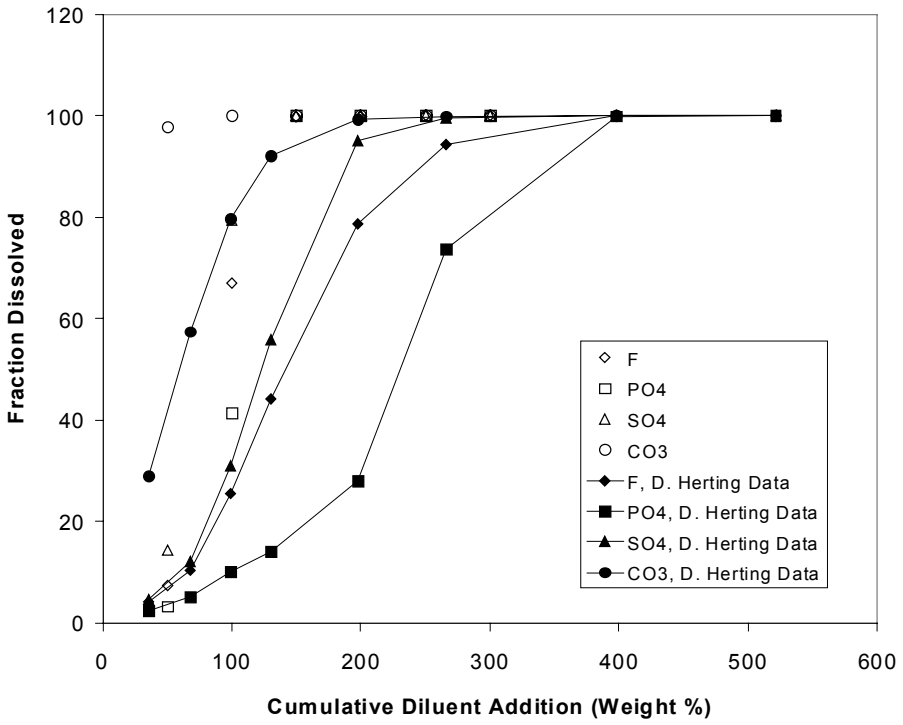

Figure 27. Dissolution Profiles for BY-102 Saltcake

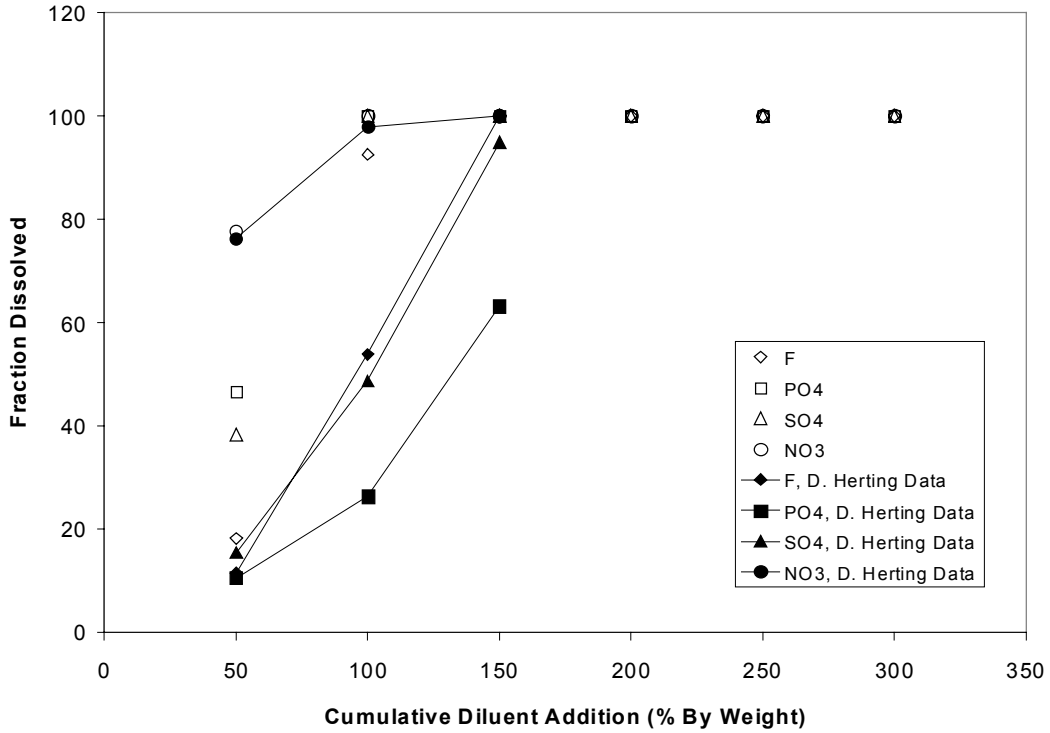

Figure 28. Dissolution Profile for BY-106 Saltcake

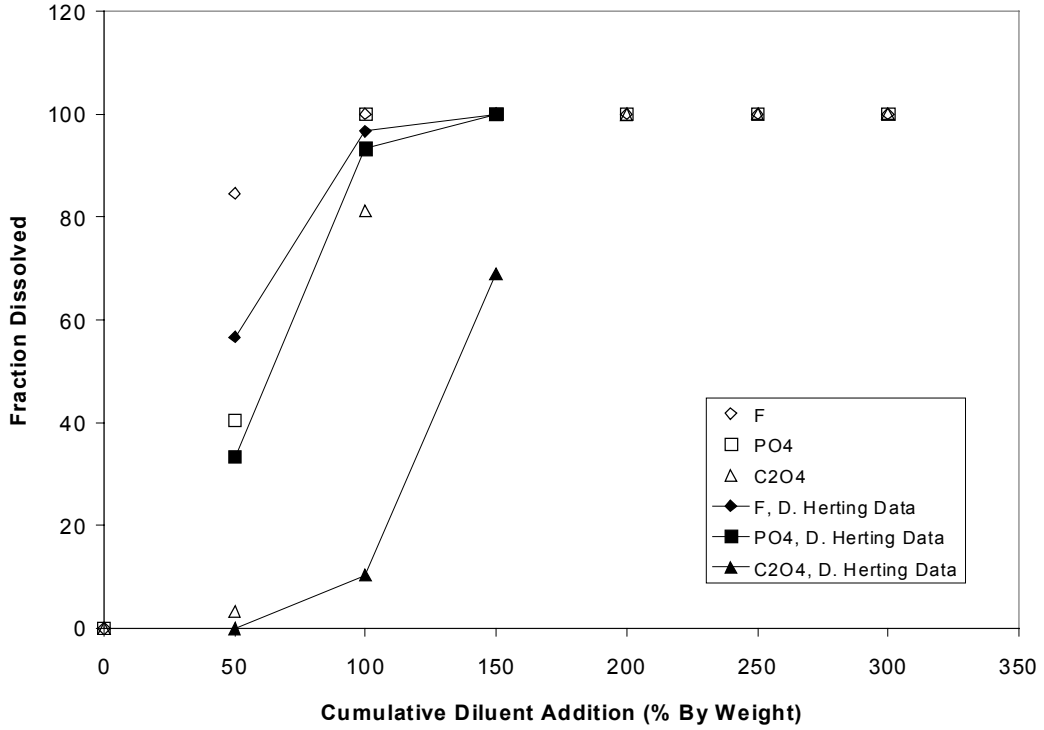

Figure 29. Dissolution Profile for A-101 Saltcake

The kinetics of precipitation of gibbsite are slow and have been documented by earlier Hanford researchers [7,8]. Other hydroxides were also predicted to form including those of chromium and iron, but were not observed experimentally. ESP predicted the majority of sodium salts Herting isolated from the cumulative receiving tank and identified through PLM. In many cases, the species identified as the major crystalline species by Herting, was also predicted by ESP to form the bulk of the reprecipitated solids.

Figures 30 through 34 provide a more detailed picture of the re-precipitation of solids in the cumulative receiver tank. These are presented in descending order of the amount of solids formed during the mixing of liquid supernates in the cumulative receiving tank. Figure 30 depicts the amounts of the various species predicted to form in the cumulative receiving tank for BY-102 saltcake. The original BY-102 saltcake contained the highest weight percentage of fluoride of all five tanks examined (1.17% by weight) and the second highest weight percentage of sulfate (5.12% by weight), as well as a significant amount of phosphate (0.6% by weight). Not surprisingly, the solids precipitation in the cumulative receiving tank was dominated by the formation of the sodium double salts involving fluoride: $Na_7F(PO_4)_2.19H_2O$ and Na_3FSO_4. It is evident from Figure 30 that both of these double salts begin to precipitate out of solution when the liquid supernate from the first contact (high in nitrate and carbonate) is mixed with the supernate from the second contact (rich in sulfate, phosphate, fluoride). As the liquid supernate from the third contact is added to the cumulative receiving tank, the levels of sulfate, phosphate and fluoride increase, and larger amounts of the double salts precipitate in the cumulative receiving tank. By the third contact with inhibited water (cumulative diluent addition of 150% by weight with respect to the

original BY-102 saltcake), all of the nitrate, carbonate, sulfate, phosphate and fluoride in the original saltcake have been dissolved and further contacting with inhibited water results in partial dissolution of the sodium oxalate from the residual saltcake solids. The liquid supernate retrieved from the fourth and subsequent contacts has lower ionic strength and serves to dilute the mixture in the cumulative receiving tank, thereby causing the solids that have reprecipitated in this tank to undergo dissolution. ESP predictions indicate that after the fifth contact, the solids in the cumulative receiving tank would be predominantly gibbsite and other metal hydroxides.

Figure 31 provides a depiction of the solids speciation in the cumulative receiving tank for saltcake from tank A-101. This saltcake contains approximately half as much sulfate (2.41% by weight) as does BY-102 saltcake, significantly more phosphate (0.44 % by weight), and fairly low levels of fluoride (0.069% by weight). The same trends shown by BY-102 saltcake are found for A-101 saltcake. The solids which could be expected to reprecipitate in the cumulative receiving tank are again the sodium double salts containing fluoride. However, approximately equal amounts of the two double salts are predicted to form during the mixing of liquid supernate from the first and second contacts. The amount of solids reprecipitated from the clear solutions again passes through a maximum at a cumulative diluent addition level of approximately 150% (equivalent to the third contact stage).

The solids speciation predicted for the TX-113 saltcake is impacted by the high level of sulfate (16.67% by weight) in the original saltcake. Figure 32 provides an examination of the solids speciation in the cumulative receiving tank for saltcake from tank TX-113. For this saltcake, examination of Figure 26 indicates that the bulk of the sulfate is predicted to undergo dissolution during the third contact with inhibited water. Not surprisingly, the solids formation in the cumulative receiving tank is impacted by this behavior also. The high levels of various anions in the original saltcake serve to provide liquid supernates which have higher concentrations of the various anions at each stage of contact compared to those obtained for other saltcake samples. As a result, the solids formed as the liquid supernate from the second and then the third contact are mixed into the cumulative receiving tank are dominated by the sodium-fluoride-phosphate double salt. As the liquid supernate from the fourth contact with inhibited water, which is rich in sulfate, is added to the cumulative receiving tank, a substantial amount of the sodium-fluoride-sulfate double salt is predicted to precipitate out of solution. The solids loading in the cumulative receiving tank goes through a maximum at a cumulative diluent addition level of ~200% by weight (equivalent to the fourth contact stage). As further liquid supernate is added to the receiving tank, the ionic strength decreases since the majority of the anions have been leached from the original saltcake, and the double salts formed in the receiving tank are predicted to redissolve, leaving only gibbsite in the solid phase once the sixth and final contact has been completed.

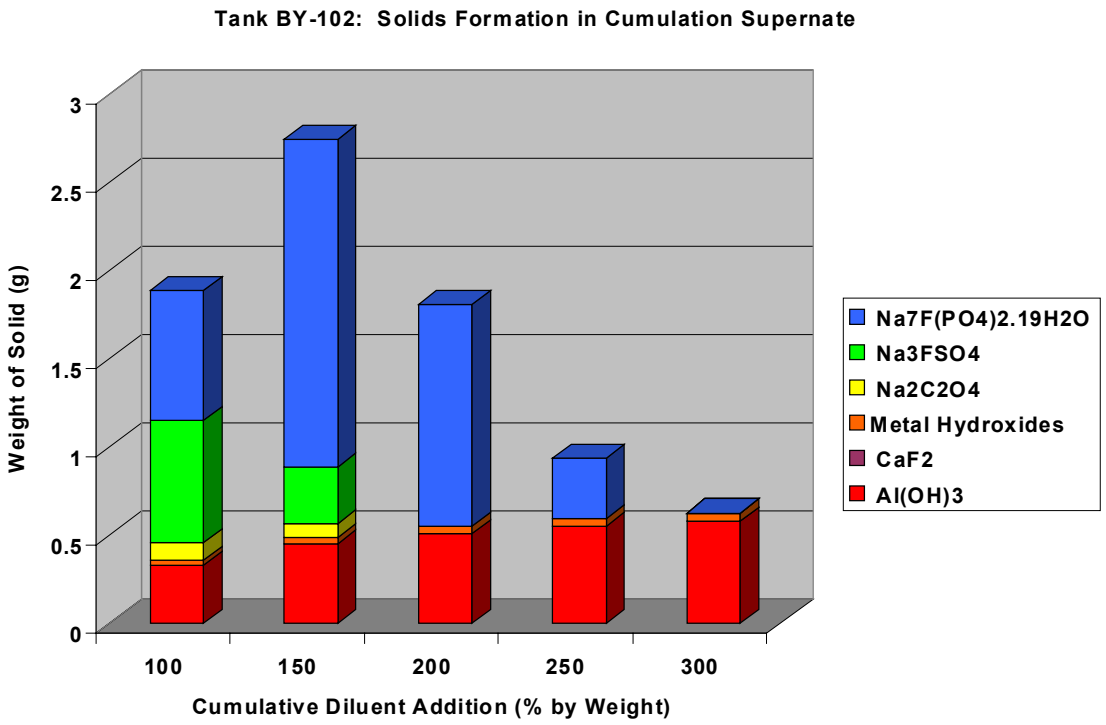

Figure 30. Solids Speciation – Cumulative Receiver Tank – BY-102 Saltcake

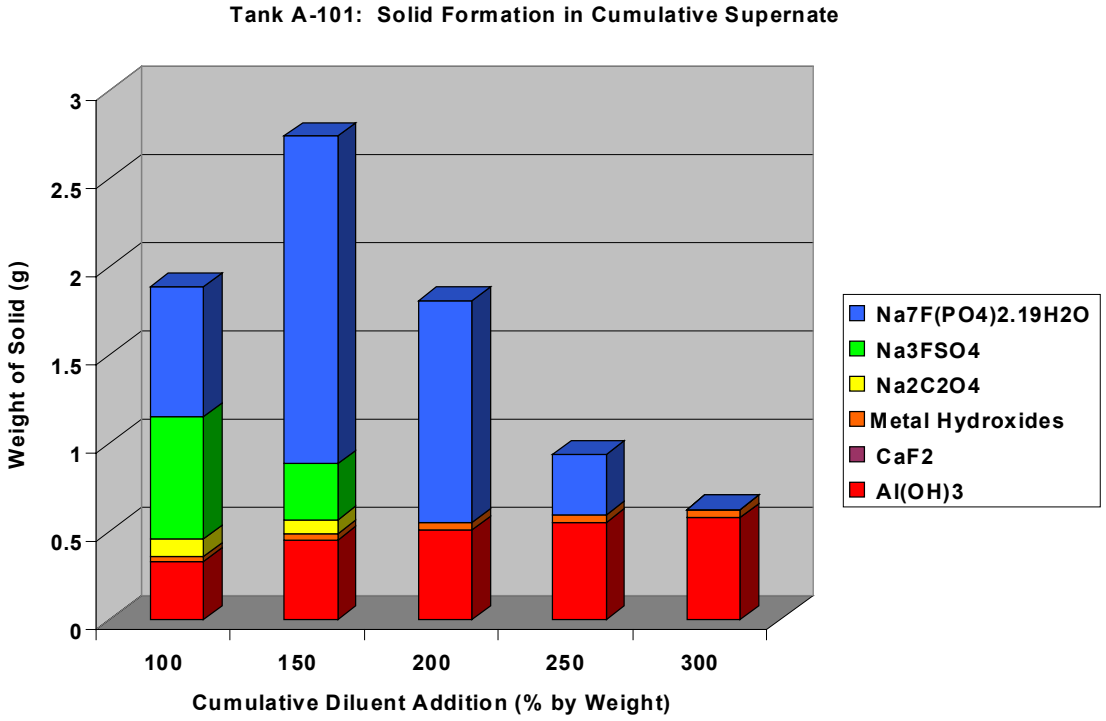

Figure 31. Solids Speciation – Cumulative Receiver Tank – A-101 Saltcake

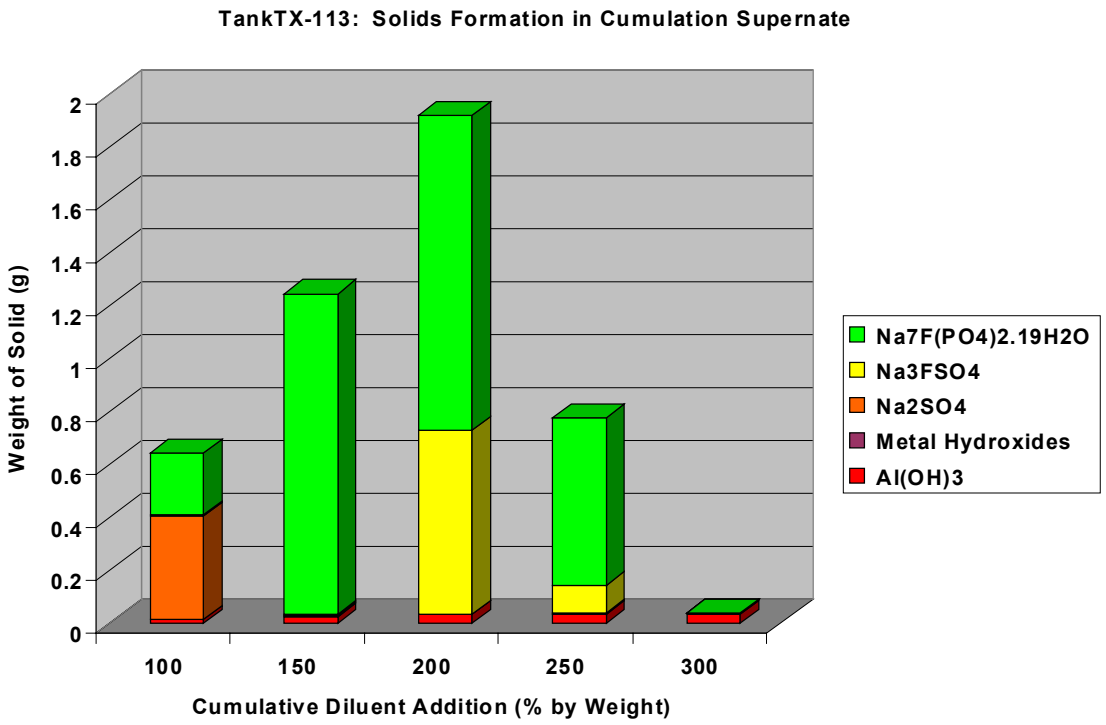

Figure 32. Solids Speciation – Cumulative Receiver Tank – TX-113 Saltcake

Saltcake from tank BY-106 is rich in nitrate and has only moderate levels of other anions present. Figure 33 provides solids phase speciation in the cumulative receiving tank for BY-106 saltcake. The majority of anions are in the mid-range of the range examined through the five saltcakes. Sulfate, present at 1.16% by weight, is approximately half the level realized in saltcake A-101; phosphate, present at 0.34 % by weight, is comparable to the level in saltcake A-101; while fluoride, at 0.62% by weight, is approximately half the level realized in saltcake BY-102. The lower levels of sulfate and phosphate give rise to lesser amounts of the double salts forming in the cumulative receiving tank. Only the sodium-fluoride-phosphate double salt is predicted to form, but in much smaller amount compared to that formed in BY-102 or A-101. The sodium-fluoride-sulfate double salt is not predicted to reprecipitate at all. The solids predicted to form in the cumulative receiving tank for BY-106 are dominated by sodium oxalate and gibbsite.

For saltcake from tank S-102, rich in nitrate (~54% by weight), the near absence of any appreciable amounts of other anions gives rise to very dissimilar behavior in the cumulative receiving tank with respect to the other saltcakes studied. Examination of Figure 34 indicates that the only species that will reprecipitate in the cumulative receiving tank is gibbsite.

Table 4 provides the comparison of solids observed experimentally by Herting [3] with those predicted by ESP to form in the cumulative receiving tank. ESP predictions are listed in order of decreasing amount. Agreement between the experimental observations

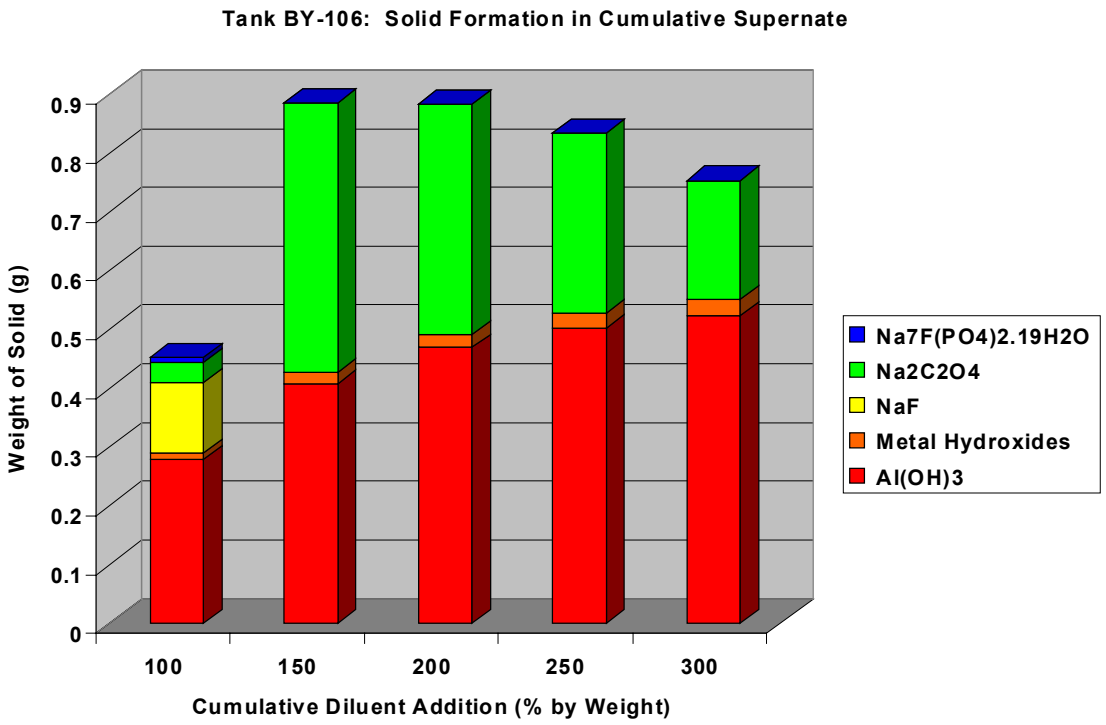

Figure 33. Solids Speciation – Cumulative Receiver Tank – BY-106 Saltcake

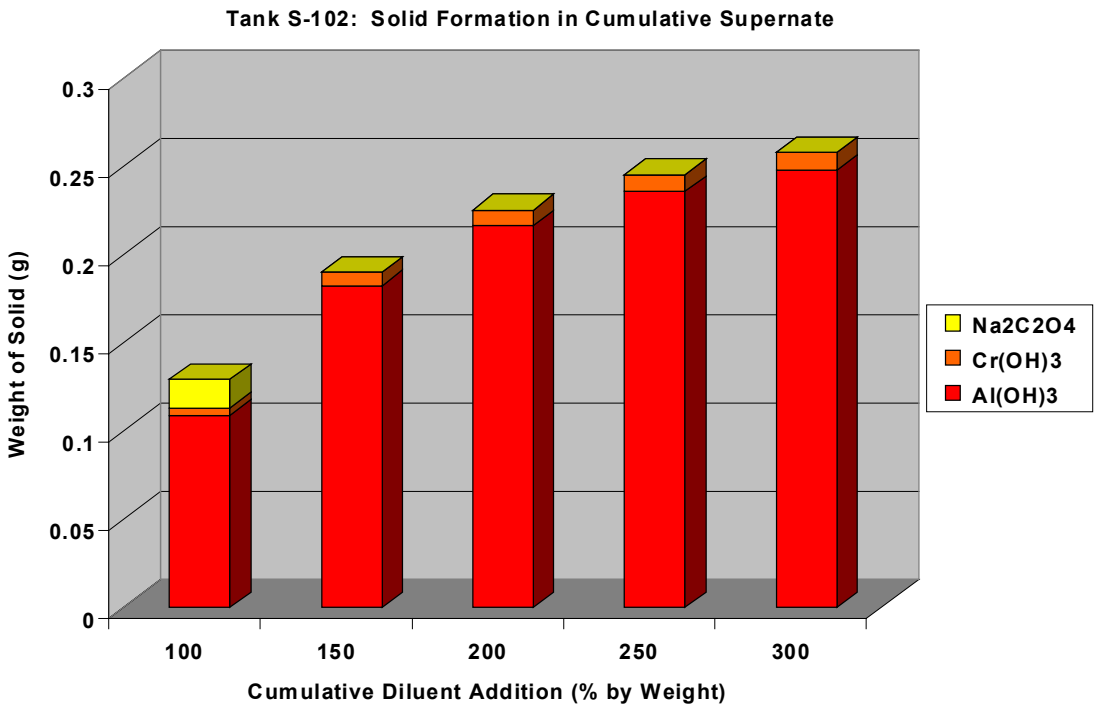

Figure 34. Solids Speciation – Cumulative Receiver Tank – S-102 Saltcake

and ESP predictions is observed for the majority of species for saltcakes TX-113 and BY-102. For both of these tanks, the levels of sulfate, phosphate and fluoride are such that significant amounts of the sodium double salts are predicted to form. For A-101 and BY-106 saltcakes, the amount of sodium double salts predicted to form are much less even in the initial contact stages. No solids were isolated experimentally from the combined liquid supernate of the first and second contact stage for either of these saltcakes.

C. Summary of Feed Stability Studies

The Feed Stability studies were conceived as a means to examine the potential for reprecipitation of solids as liquid supernates from a staged retrieval process were recombined. Herting's experiments demonstrated that reprecipitation may occur for select saltcakes. The potential for solids formation appears to be most closely linked to the levels of sulfate, phosphate and fluoride in the original saltcake. The initial supernate will be rich in nitrate and carbonate while subsequent liquid supernate will be rich in sulfate, phosphate, and fluoride. Recombination of these supernates will give rise to the formation of the sodium double salts. The variety among the saltcakes examined through this study may provide guidance to operations at Hanford in identifying which saltcake compositions are more likely to give rise to reprecipitation of solids as supernates from different stages of retrieval are mixed.

Table 4. Solids Present in Cumulative Supernate

Contact		TX-113	BY-102	BY-106	A-101	S-102
2	ESP	Na_2SO_4 Na_3FSO_4 $Na_7F(PO_4)_2.19H_2O$ [Al, Cr, Fe]$(OH)_3$	$Na_7F(PO_4)_2.19H_2O$ Na_3FSO_4 $Na_2C_2O_4$ [Al, Cr, Fe]$(OH)_3$ [Mg, Mn] $(OH)_2$	NaF $Na_2C_2O_4$ $Na_7F(PO_4)_2.19H_2O$ [Al, Cr]$(OH)_3$	$Na_7F(PO_4)_2.19H_2O$ Na_3FSO_4 $Na_2C_2O_4$ [Al, Cr, Fe]$(OH)_3$ $Mn(OH)_2$	$Na_2C_2O_4$ [Al, Cr, Fe]$(OH)_3$
	LAB	Na_2SO_4 Na_3FSO_4	Na_3FSO_4 Na_2SO_4 $Na_7F(PO_4)_2.19H_2O$	No solids	No solids	No solids
3	ESP	$Na_7F(PO_4)_2.19H_2O$ Na_3FSO_4 [Al, Cr, Fe]$(OH)_3$	$Na_7F(PO_4)_2.19H_2O$ Na_3FSO_4 $Na_2C_2O_4$ [Al, Cr, Fe]$(OH)_3$ [Mg, Mn] $(OH)_2$	$Na_2C_2O_4$ [Al, Cr, Fe]$(OH)_3$	$Na_7F(PO_4)_2.19H_2O$ Na_3FSO_4 $Na_2C_2O_4$ [Al, Cr, Fe]$(OH)_3$ $Mn(OH)_2$	[Al, Cr, Fe]$(OH)_3$
	LAB	$Na_7F(PO_4)_2.19H_2O$ Na_2SO_4	Na_3FSO_4 Na_2SO_4 $Na_7F(PO_4)_2.19H_2O$	$Na_2C_2O_4$	$Na_2C_2O_4$	No solids
4	ESP	$Na_7F(PO_4)_2.19H_2O$ Na_3FSO_4 [Al, Cr, Fe]$(OH)_3$	$Na_7F(PO_4)_2.19H_2O$ [Al, Cr, Fe]$(OH)_3$ [Mg, Mn] $(OH)_2$	$Na_2C_2O_4$ [Al, Cr, Fe]$(OH)_3$	$Na_7F(PO_4)_2.19H_2O$ [Al, Cr, Fe]$(OH)_3$ $Mn(OH)_2$	[Al, Cr, Fe]$(OH)_3$
	LAB	$Na_7F(PO_4)_2.19H_2O$	No solids	$Na_2C_2O_4$	No solids	No solids
5	ESP	$Na_7F(PO_4)_2.19H_2O$ Na_3FSO_4 [Al, Cr, Fe]$(OH)_3$	$Na_7F(PO_4)_2.19H_2O$ [Al, Cr, Fe]$(OH)_3$ [Mg, Mn] $(OH)_2$	$Na_2C_2O_4$ [Al, Cr, Fe]$(OH)_3$	$Na_7F(PO_4)_2.19H_2O$ [Al, Cr, Fe]$(OH)_3$ $Mn(OH)_2$	[Al, Cr, Fe]$(OH)_3$
	LAB	No solids	$Na_2C_2O_4$	No solids	No solids	No solids
6	ESP	[Al, Cr, Fe]$(OH)_3$	[Al, Cr, Fe]$(OH)_3$ [Mg, Mn] $(OH)_2$	$Na_2C_2O_4$ [Al, Cr, Fe]$(OH)_3$	[Al, Cr, Fe]$(OH)_3$ $Mn(OH)_2$	[Al, Cr, Fe]$(OH)_3$
	LAB	No solids	$Na_2C_2O_4$	No solids	No solids	No solids

III. ESP Comparison Studies

A. Calculations for Sodium Nitrate

Comparison of ESP predictions with saltcake dissolution experiments conducted by Herting during FY98 and FY99 [1,2] identified a major discrepancy between model predictions and experimental measurements at dilutions of less than 100% by weight (a dilution of 100% by weight is defined as 100 g saltcake combined with 100 g of water). It was unclear whether this discrepancy was due to deficiencies in the thermodynamic data for various sodium salts (including the double salts) contained in the ESP databases or whether the discrepancy was due to deficiencies perhaps introduced when the ESP activity coefficient calculation methods were used for prediction of activities under high ionic strength conditions. In order to address this question and identify the primary reason for the observed discrepancy, ESP predictions for the sodium nitrate/water system as a function of temperature and ionic strength were compared with model results obtained by M. Ally using a lattice model to describe the thermodynamics of the sodium nitrate/water system [9]. Also included in the comparison were available literature data from the International Critical Tables [10]. The high solubility of sodium nitrate in water provides for a continuous examination of its behavior over a wide range of ionic strength conditions. Temperatures of 25, 100 and 125°C were examined.

At a given temperature, the bubble point pressure (pressure exerted over a solution which is at the onset of vaporization) over the aqueous sodium nitrate solution was predicted using the MIX block in ESP. Version 6.3 of ESP was used to conduct these simulations with the PUBLIC database providing necessary thermodynamic data. Solvent activity (in this case, water activity) was determined using:

$$a_{H_2O} = \frac{P}{P^0}$$

where a_{H_2O} is the water activity, P is the vapor pressure over the aqueous sodium nitrate solution and P^0 is the vapor pressure of pure water at the solution temperature.

Figures 35 through 37 provide a comparison of ESP predictions of the vapor pressure over the aqueous sodium nitrate solution with the predictions of M. Ally using the lattice model and with the literature data at the three temperatures examined. Tabulated results for vapor pressure over solution and for water activity are provided in Tables E.1 through E.3 of Appendix E. At 25°C, the ESP predictions, shown in Figure 35, coincide with Ally's model results and with the literature data over the range of ionic strengths from 0 to ~6 (< 1% error between model results and literature data). Above this ionic strength, both the ESP predictions and the lattice model predictions show slight underestimation of the bubble point pressures (between 1.5 to 3%) compared to the literature data from the International Critical Tables [10]. Based on the comparison, it is concluded that the discrepancies observed between ESP predictions of the saltcake series dissolution and the experimental data in the region of low dilution (<100%) are not due to deficiencies

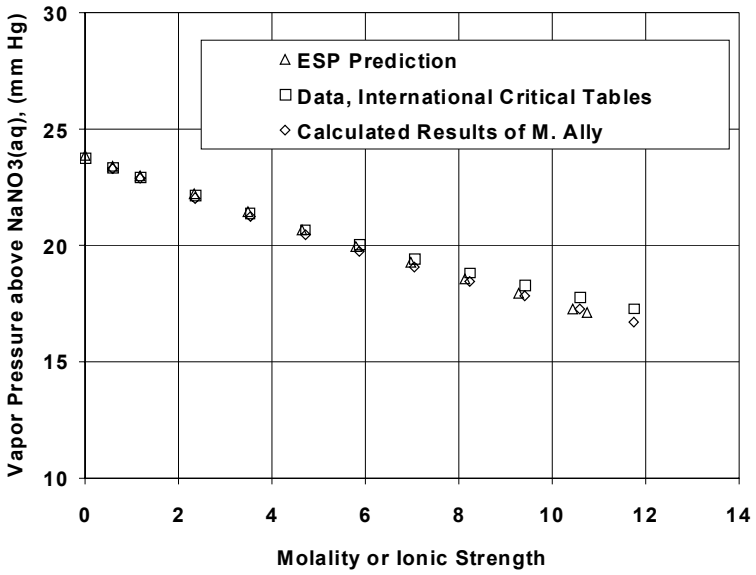

Figure 35. Comparison of ESP Predictions with Lattice Model Results and Literature Data at 25° C.

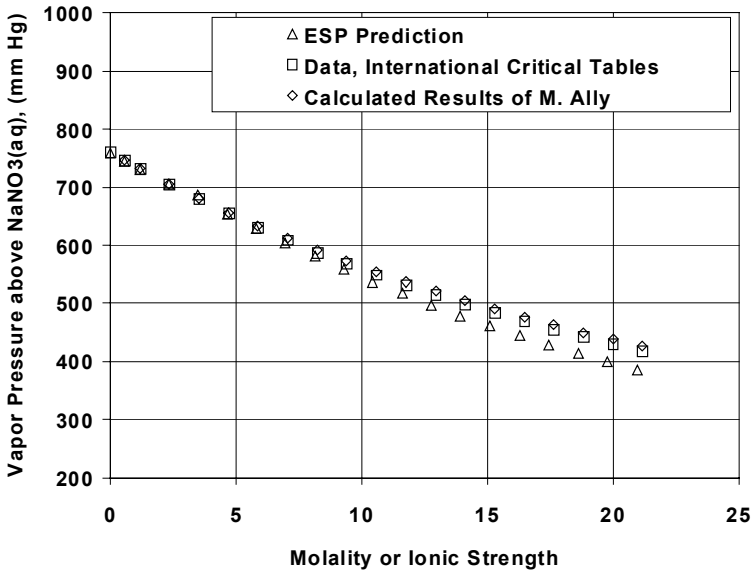

Figure 36. Comparison of ESP Predictions with Lattice Model Results and Literature Data at 100° C.

introduced when the ESP activity coefficient calculation methods are used for prediction of activities under high ionic strength conditions at ambient temperature.

The comparison at 100° C is shown in Figure 36 and at 125° C, in Figure 37. At these higher temperatures, the solubility of sodium nitrate in solution is much higher, allowing an examination of a larger range of ionic strength. As with the comparison at 25° C, both models, ESP and the lattice model, compare well with the literature data, again up to an ionic strength of ~6. However, above this value, deviations from literature data ranged from ~3 to 8% at 100° C and from ~3 to 10% at 125° C. ESP predictions underestimate the vapor pressure over the aqueous sodium nitrate solution, while at 100° C, the lattice model essentially reproduces the literature data over the entire range of ionic strength. At 125° C, the lattice model predictions slightly overestimate the solution vapor pressure, but differences between literature data and the lattice model predictions are < 5% at the highest ionic strength condition. The cause of the systematic deviation exhibited by the ESP predictions at these higher temperatures compared to the literature data is under investigation.

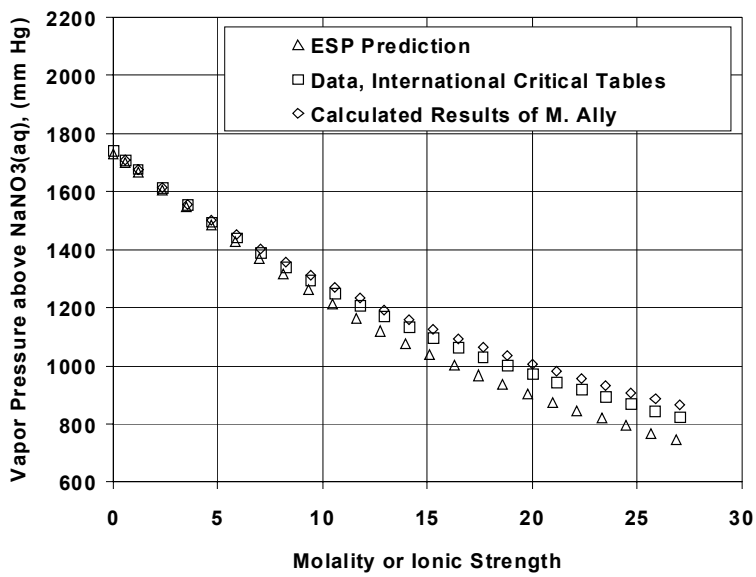

Figure 37. Comparison of ESP Predictions with Lattice Model Results and Literature Data at 125° C.

B. Comparative Calculations for Sodium Double Salts

The variety and concentration of numerous anions in the Hanford Waste enhance the possibility of the formation of double salts in the solid phase of Hanford saltcakes. The ability to adequately predict the formation of these double salts is desirable, in that overestimation or underestimation of the solubility envelope for one double salt may adversely impact the estimation of the solubilities of other species. The impact of ionic strength and temperature on the solubility of double salts must be adequately represented within the ESP framework if the model is to be used with some degree of assurance that the predictions reflect behaviors that are realized in practice. One method of examining the predictive capabilities of the ESP model is through comparison with similar calculations performed with other thermodynamic equilibrium models. The SOLGASMIX model has been used extensively at ORNL to perform these types of predictive computations as well as to regress experimental data to obtain fundamental thermodynamic properties for species. During FY99, comparative calculations for the sodium-fluoride-phosphate-hydroxide-water were completed [11]. Similar comparisons were undertaken during FY00 focusing on the sodium-fluoride-sulfate-hydroxider system and the sodium-nitrate-sulfate-hydroxide system [5].

These two systems are of interest for a number of reasons. Within the ESP Public database, thermodynamic data for the sodium-fluoride-sulfate double salt, Na_3FSO_4, are available, while for the sodium-nitrate-sulfate double salt, $Na_3NO_3SO_4.2H_2O$, these data are not available. For both of these double salts, literature data are available [12] for the solid liquid equilibrium in aqueous solution. For the fluoride-sulfate system, the available data are incorporated into ESP. Due to the limited temperature range of the data, ESP has built-in lower and upper temperature limits that preclude the prediction of this species in the solid phase at temperatures outside of this restricted range. Additionally, these two double salts are representative of two different classes of double salts that can form: congruent and incongruent. The fluoride-sulfate double salt is of the former type while the nitrate-sulfate double salt is of the latter. A congruent double salt will equilibrate with a liquid phase that has the same molar ratio of the anions as are present in the double salt. An incongruent double salt cannot exist in equilibrium with a solution of the same molar constitution as in the solid [13]. As the sodium-nitrate-sulfate double salt undergoes dissolution, sodium sulfate decahydrate will reprecipitate from solution, making it appear that only the sodium nitrate portion of the double salt is actually dissolving.

1. Sodium-Nitrate-Sulfate-Hydroxide System

Model predictions of the solubility envelope for both systems were completed at 25° C and 50° C and in aqueous solution, 1 m hydroxide and 3 m hydroxide. ESP predictions for the sodium-nitrate-sulfate system in aqueous solution are shown in Figure 38. The ESP predictions were obtained using Version 6.3 of ESP and two database combinations (PUBLIC, PUBLIC + Na2snacl) and are presented along with SOLGASMIX predictions and the available literature data. Preliminary predictions for this double salt system were performed using the ESP PUBLIC database alone. As evidenced in Figure 38, use of this database alone did not allow for prediction of the solubility envelope for this system. The

pure component solubilities were predicted and are in agreement with the existing literature data. ESP correctly identifies the solid phase in the absence of nitrate to be sodium sulfate decahydrate [$Na_2SO_4.10H_2O$]. As the level of nitrate in solution increases, however, the experimental data demonstrate a transition from the decahydrate to the anhydrous sodium sulfate. It is this transition that the data available in the PUBLIC database of ESP are unable to reproduce. In the PUBLIC database, the formation of anhydrous sodium sulfate is limited to temperatures in the range of 32.4° C to 210° C. Thus, at 25° C, ESP prohibits this species from being included in the calculations. As the nitrate concentration is increased, the solid phase speciation for sulfate should undergo transition from the sodium sulfate decahydrate to the anhydrous sodium sulfate. Since this transition is prohibited within ESP using the PUBLIC database alone, the sulfate concentration rises steeply as the nitrate concentration is increased in the range of 1 m to 3 m. Convergence problems arise in the region between 3 m nitrate to approximately 10.5 m nitrate. The proper behavior for sulfate in solution and the decahydrate-anhydrous phase transition was obtained when the special database, Na2snacl, supplied by OLI Systems, Inc., was included to provide thermodynamic data for the sodium sulfate system under conditions of higher ionic strength. This database provided the data required to predict the transition between the two sulfate species of interest. Also included in Figure 38 are the predictions for this system using the Na2snacl database coupled with the PUBLIC database. This database combination provides predictions for the solubility envelope that are more consistent with the available experimental data. The only region in which discrepancies between the literature data and the predictions are apparent is in the range of nitrate concentrations between 4 m and 6 m nitrate. In this region, the literature data indicate the transition from sodium sulfate decahydrate to anhydrous sodium sulfate to occur at a nitrate concentration of 4.842 m and the transition from anhydrous sodium sulfate to the sodium-nitrate-sulfate double salt [$Na_3NO_3SO_4.2H_2O$] to occur at a nitrate concentration of 5.264 m. Convergence difficulties were encountered in this region and precluded the identification of the invariant point associated with the sodium sulfate decahydrate-anhydrous sodium sulfate transition. However, for the majority of the nitrate concentration range considered, the reproduction of the solubility envelope for the sodium-nitrate-sulfate system by ESP agrees with the literature data. This agreement is obtained even in the absence of thermodynamic data for the sodium nitrate-sulfate double salt. The solubility envelope evaluated by Weber at ORNL using SOLGASMIX is also included. Details on the SOLGASMIX calculations are provided in a recent report on double salt formation [5]. The parameters used in the SOLGASMIX model are obtained by regression of the literature data. Thus, the reproducibility of the experimental data by the SOLGASMIX model is expected.

The solubility envelopes were also predicted for 1 m hydroxide and 3 m hydroxide using ESP. The model results are presented in Figure 39. In the presence of hydroxide, the shape of the solubility envelope differs. In 1 m hydroxide, the ESP and SOLGASMIX predictions of the pure component solubility of sodium sulfate decahydrate agree with one another. However, as the level of nitrate in solution is increased, ESP predictions display a smooth decline in the amount of sulfate that can be present in the liquid phase. At a nitrate concentration of approximately 2.5 m, convergence problems again preclude

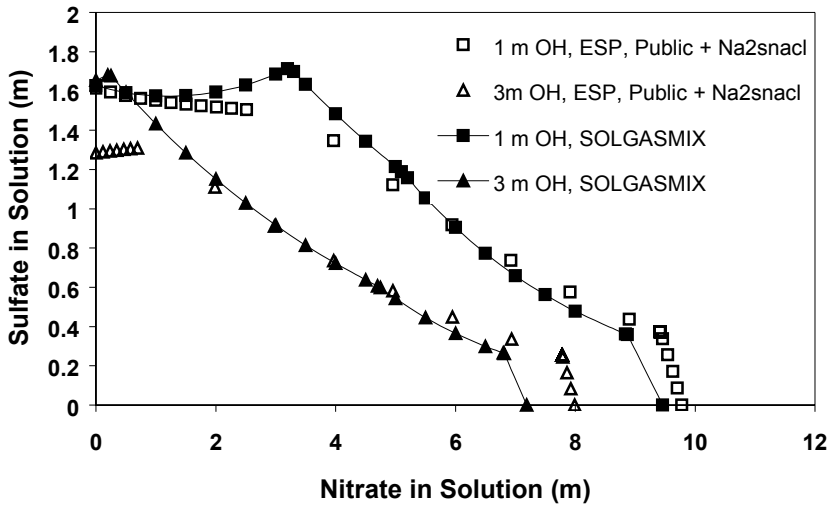

Figure 38. Solubility Envelope for Sodium-Nitrate-Sulfate System at 25°C. Comparison of Model Predictions with Literature Data.

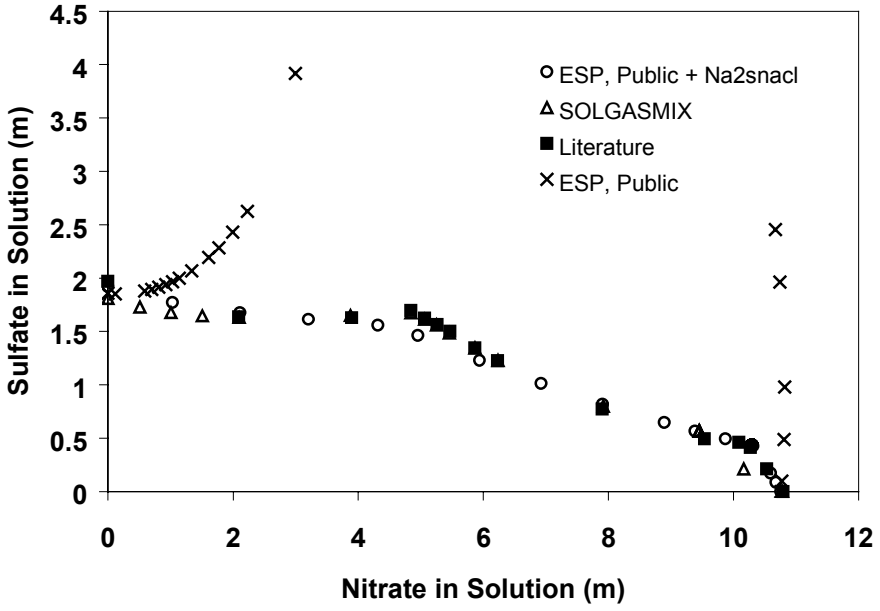

Figure 39. Solubility Envelope for Sodium-Nitrate-Sulfate-Hydroxide System at 25°C. Comparison of Model Calculations.

the prediction of the equilibrium compositions of the liquid and solid phases. These convergence problems persist up to a nitrate concentration of approximately 4 m. In the region of low nitrate concentrations, the solubility envelope predicted by SOLGASMIX coincides with that predicted by ESP up to a nitrate concentration of ~ 1.5 m. For nitrate concentrations between ~ 1.5 m and 3 m, the solubility envelope predicted by SOLGASMIX shows an increase in the sulfate concentration as the nitrate concentration is increased until the invariant point associate with the sodium sulfate decahydrate/anhydrous sodium sulfate phase transition is reached. As observed for the ESP predictions in aqueous solution, ESP is also unable to predict this phase transition in 1 m hydroxide solution. As the nitrate concentration increases, the ESP and SOLGASMIX predictions agree well, but ESP predicts a slightly higher solubility for pure sodium nitrate. In 3 m hydroxide solution, SOLGASMIX predicts that the stable crystalline form for sulfate will be the sodium sulfate decahydrate salt, but the transition to anhydrous sodium sulfate will occur with very little nitrate added to the solution. ESP, in contrast, predicts the stable crystalline form, sodium sulfate decahydrate, to persist until much higher levels of nitrate are realized in solution, ~1 m. Again, ESP cannot predict the phase transition to the anhydrous sodium sulfate salt and predictions in this region of ~ 1m to 2 m nitrate exhibit convergence difficulties. For the region in which SOLGASMIX predicts the formation of the double salt, $Na_3NO_3SO_4.2H_2O$, the ESP predictions lie in close proximity to those of SOLGASMIX, even though ESP does not predict the existence of this species in the solid phase.

Predictions for this system at 50° C are provided in Figure 40. At 50° C, the stable crystalline phase for sulfate is as the anhydrous sodium sulfate. Both models, SOLGASMIX and ESP, in aqueous solution as well as in 1 m hydroxide and 3 m hydroxide solutions, predict this species as the stable crystalline phase. ESP predicts lower pure component solubility for sodium sulfate than does SOLGASMIX while predicting slightly higher pure component solubility for sodium nitrate. SOLGASMIX also does not predict the formation of the sodium-nitrate-sulfate double salt and predictions of the two models agree well with one another through the majority of the nitrate concentration range examined.

2. Sodium-Fluoride-Sulfate-Hydroxide System

Comparative calculations were also completed for the sodium-fluoride-sulfate-hydroxide system at 25° C and 50° C as a function of ionic strength. ESP predictions were conducted using Version 6.3 along with the PUBLIC and Na2snacl databases. In order to perform predictions at 50° C, the thermodynamic data for the sodium-fluoride-sulfate double salt, Na_3FSO_4, was exported to a private databank. In this private databank, the upper temperature limit on the solubility curve fit was edited and increased to 50° C to allow the double salt to be considered as a potential precipitate at 50° C. No other modifications to the thermodynamic data for this double salt were made.

Figure 41 provides a comparison of the ESP and SOLGASMIX predictions at 25° C. Also presented are the literature data for this system at 25° C. SOLGASMIX model parameters are determined through regression of the literature data and details of this procedure,

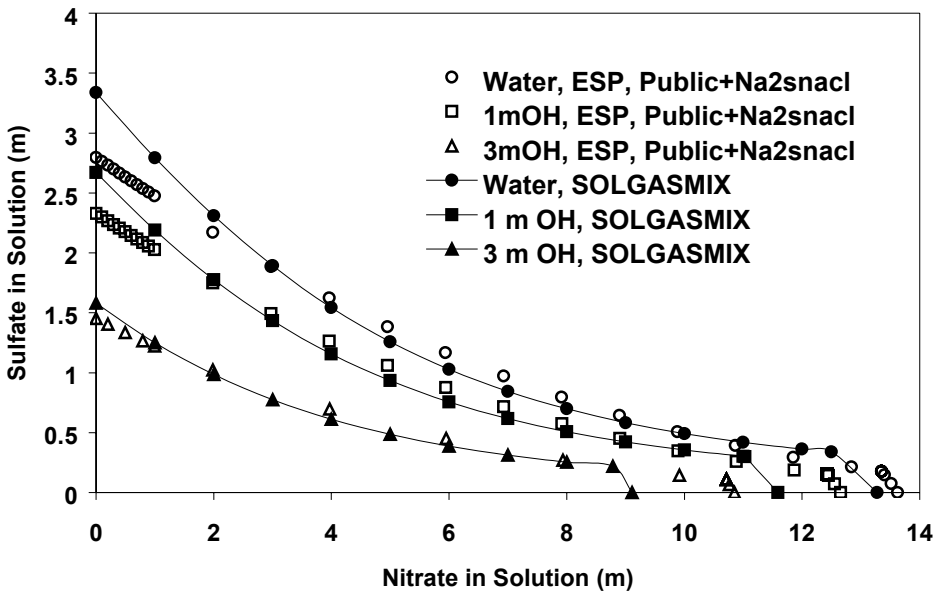

Figure 40. Predicted Solubility Envelopes in the Sodium-Nitrate-Sulfate-Hydroxide System at 50° C.

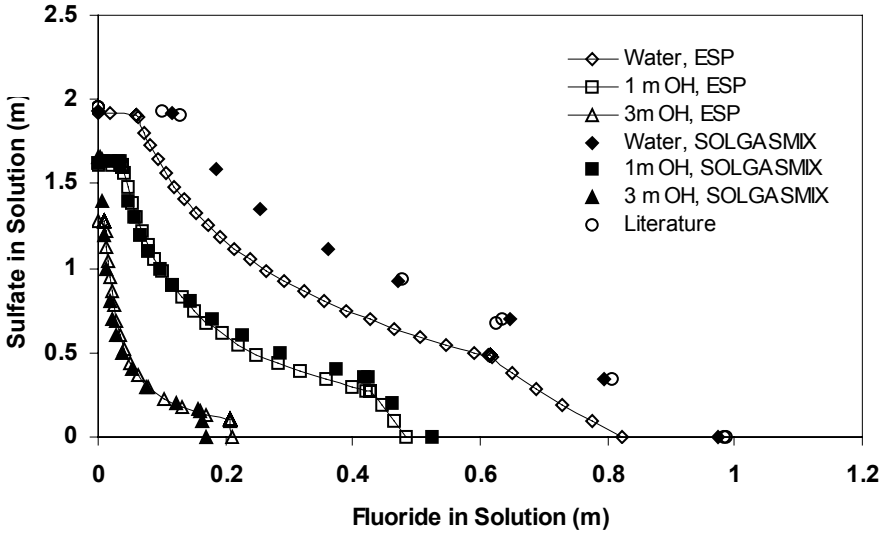

Figure 41. Solubility in the Sodium-Fluoride-Sulfate-Hydroxide System at 25° C.

performed by Weber at ORNL, are given in reference [5]. The solubility envelope predicted by ESP in aqueous solution, is located at concentrations approximately 15% below both the literature data and the SOLGASMIX predictions. The pure component solubilities for sodium sulfate decahydrate in aqueous solution at 25° C is in agreement with the literature data and the SOLGASMIX prediction. The pure component solubility of sodium fluoride in aqueous solution is underestimated by ESP. This underestimation was also observed in prior model calculations for the sodium-fluoride-phosphate system. If the ESP database is modified so as to use the Gibbs Free Energy of Formation, rather than the KFIT expression, for the prediction of the solubility of pure sodium fluoride, the calculated solubility for pure sodium fluoride is in agreement with the literature data and the SOLGASMIX prediction.

In contrast to the obvious differences in the ESP predictions and the SOLGASMIX predictions in aqueous solution, the model calculations for the two models coincide with each other at 25° C in 1 m hydroxide and in 3 m hydroxide solutions, with significant deviations from one another only in the pure component limits.

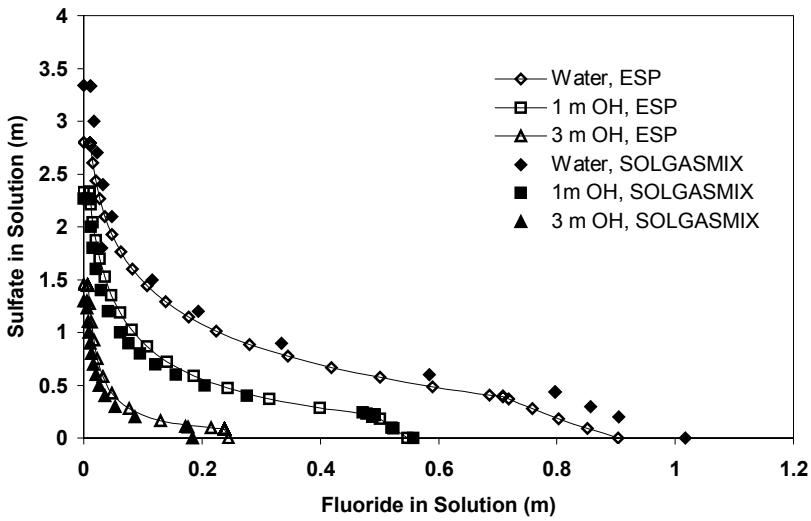

Figure 42. Solubility in the Sodium-Fluoride-Sulfate-Hydroxide System at 50° C.

Figure 42 provides a comparison of the ESP predictions with those of the SOLGASMIX model for the sodium-fluoride-sulfate-hydroxide system at 50° C. At this temperature, the model predictions of ESP and SOLGASMIX again coincide over the majority of the concentration range. However, the pure component solubility predicted by ESP for sodium fluoride is less than the SOLGASMIX prediction in water, approximately the same as the SOLGASMIX prediction in 1 m hydroxide solution and slightly greater than the SOLGASMIX prediction in 3 m hydroxide solution. The behaviors observed in these comparative calculations substantiate the need for conducting the companion experimental effort of measuring the solubility for this system as a function of both temperature and ionic strength.

IV. Experimental Studies of Double Salt Systems

Experimental measurements for the solid-liquid equilibria of the sodium-fluoride-sulfate-hydroxide system were undertaken during the past year. Literature data for the sodium-fluoride-sulfate system is limited, over a restricted temperature range of 18° C to 35° C [12]. No experimental data are available in the literature for the quaternary system, sodium-fluoride-sulfate-hydroxide. ESP contains the sodium-fluoride-sulfate double salt as a species [Na_3FSO_4]; however, due to the limited experimental data, the expression used in ESP to evaluate the solubility does not include any temperature dependence. While this species may appear to be of minor concern with respect to the disposition of saltcakes at the Hanford site, it is important because deficiencies in predicting the solubility of the fluoride-sulfate double salt will impact the prediction of the solubility of natrophosphate [$Na_7F(PO_4)_2.19H_2O$]. This, in turn, will affect the predicted behavior of trisodium phosphate [$Na_3PO_4.1/4NaOH.12H_2O$], which has been implicated in plug formation at the Hanford site.

In previous work, we evaluated the solubility behavior of the Na-F-PO4-OH system [11]. The corresponding double salt, natrophosphate ($Na_7F(PO_4)_2 \cdot 19H_2O$) has been observed in the analysis of the tank wastes at Hanford and was predicted by ESP. Another double salt that has been observed is Na_3FSO_4 [3]. As compared to the previous work on natrophosphate, however, only limited experimental data is available for this system. An exhaustive search of the literature revealed only 1 publication from 1930 [13]. In this earlier work measurements were performed in water at various temperatures between 10 and 35° C. These results were insufficient in establishing the interaction parameters necessary for describing the waste at Hanford. Consequently new studies were initiated

Work on the Na-F-SO4-OH system was begun by performing theoretical calculations (as described above) using both the ESP model and SOLGASMIX. The later model was fit to the data of Foote and Schairer [13]. ESP calculations were performed using version 6.3 with the PUBLIC and Na2sdnacl databases as described above.

Experimental results are provided for work at 25°C in the three media: water, 1m and 3m hydroxide. A major problem in the work to date has been the initial concentration targets. Starting solution concentrations for the water experiments were prepared at concentrations 10% above the SOLGASMIX predictions by first dissolving the sodium fluoride at elevated temperature and then cooling the solutions and adding the anhydrous sodium sulfate. The isotropic solutions were then allowed to equilibrate while shaken for a period of two weeks after which the samples were filtered. Solids obtained during the filtration process were analyzed by Polarized Light Microscopy (PLM). Sulfate and fluoride concentrations in the liquid solution were determined using ion chromatography (IC).

The 1m OH solutions were initially prepared at concentrations 10% larger than the solubility enveloped predicted by ESP. However, following the standard two-week equilibration period, no solids were observed in the prepared solutions. Thus, solutions were prepared at 20% above the ESP model predictions. Again solids were not observed. Test points were then established for the samples in 1m hydroxide based on the ESP solubility estimates in water. Solids were observed in these solutions after the equilibration period. In a similar

manner, the target concentrations of samples for the 3m hydroxide experiments were based upon the ESP predictions for 1 m hydroxide.

Liquid phase concentrations for sulfate and fluoride anions are plotted along with the SOLGASMIX and ESP predictions in Figure 43. All experimental data cited in this section is tabulated in Appendix F. The experimental results are in agreement with the previous study of Foote and Schairer and also with the predictions of the SOLGASMIX model, which was based on the older experimental results. Liquid phase concentration predictions from ESP are considerably less than the experimental results. Comparisons between the ESP results and those from SOLGASMIX have been discussed in greater detail in reference [5].

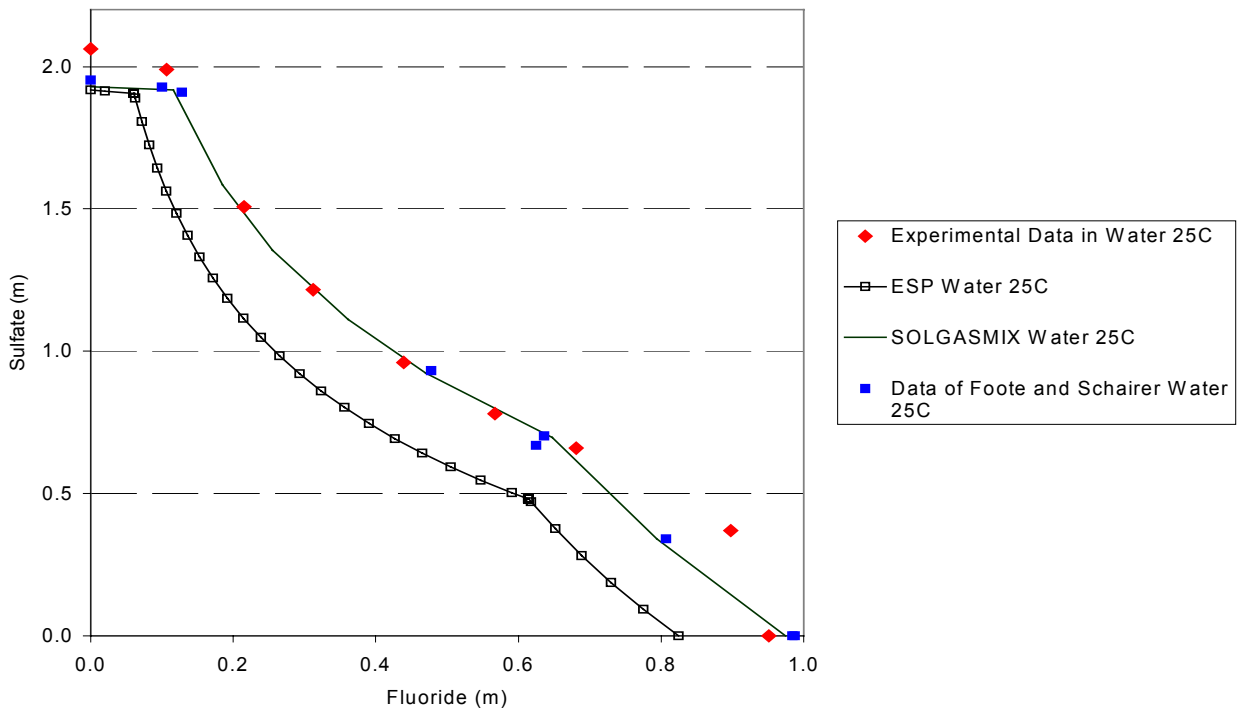

Figure 43. Experimental Solubilities and Model Predictions for the Na-F-SO4-OH System at 25° C in Water.

As with the Na-F-PO_4-OH system, regions near the axis represent the solubilities of the pure components, in this case, NaF and $Na_2SO_4 \cdot 10H_2O$. The curved region of the plot corresponds to the formation of the Na_3FSO_4 double salt. Its existence in these samples was confirmed by PLM. An example of an image for the double salt is given in Figure-44.

Experimental data obtained in the 1m hydroxide solution are plotted along with the model predictions in Figure 45. Agreement between the experimental results and the model predictions is less satisfying and this particular series of experiments may need to be re-examined. Nonetheless, the solubilites in 1m OH are reduced, as expected, when compared to the experimental data in water (Figure 43).

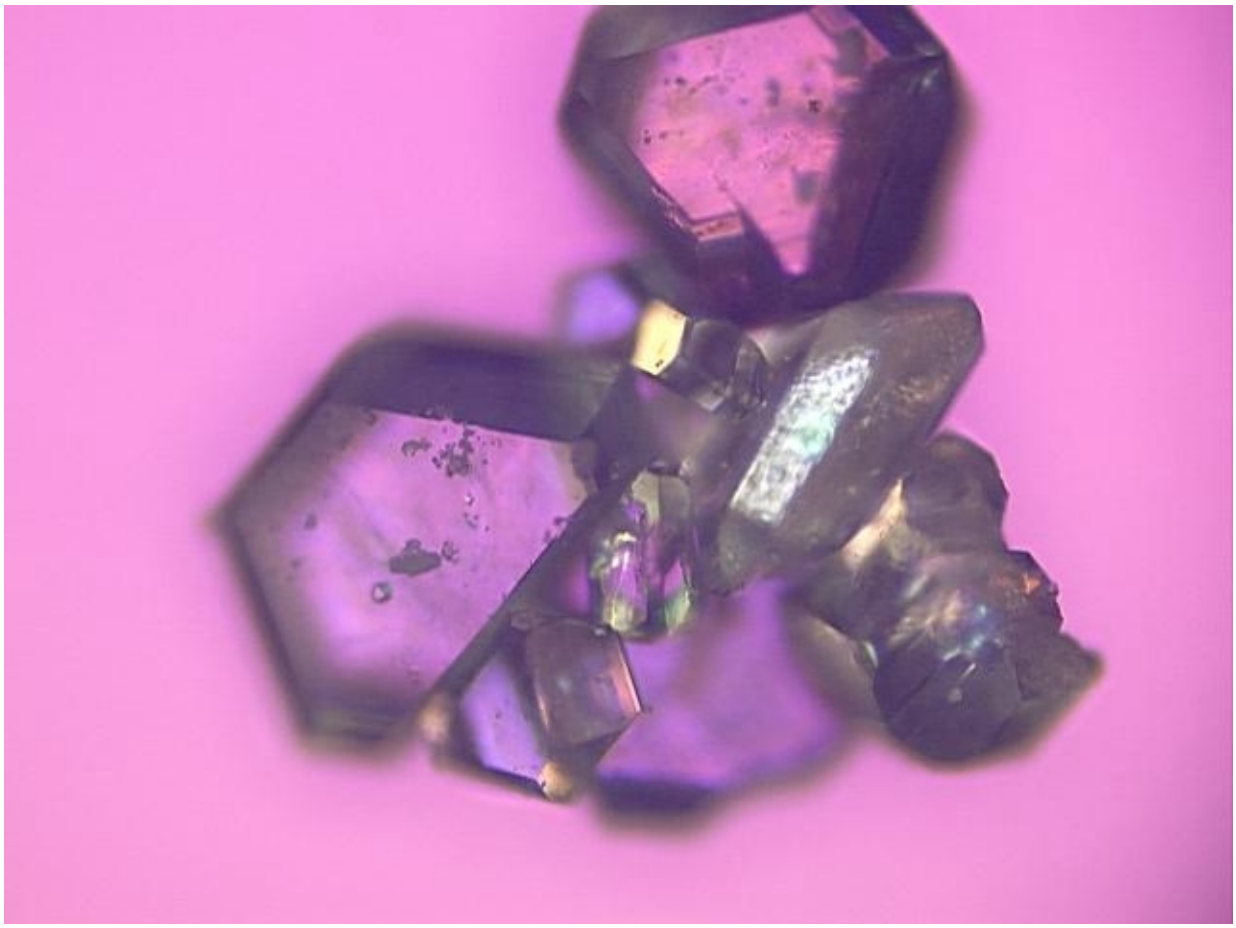

Figure 44. PLM Image of the Na_3FSO_4 Double Salt.

Somewhat better agreement was observed in the 3m hydroxide solutions, Figure 46. The data in 3m are in close agreement with the predictions of the models but tend to larger values. Additional data are being obtained at 50°C and these data along with the results given here will be analyzed for future incorporation into an OLI database.

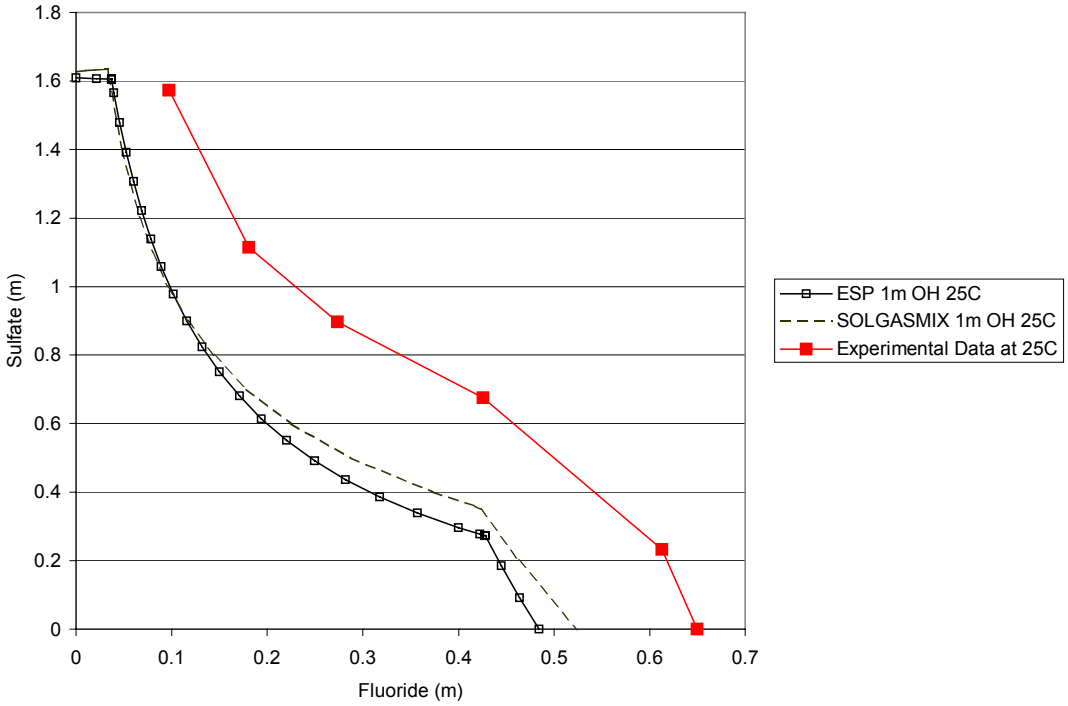

Figure 45. Comparison of the Experimentally Determined Solubilities with the Model Predictions for 1m Hydroxide at 25°C.

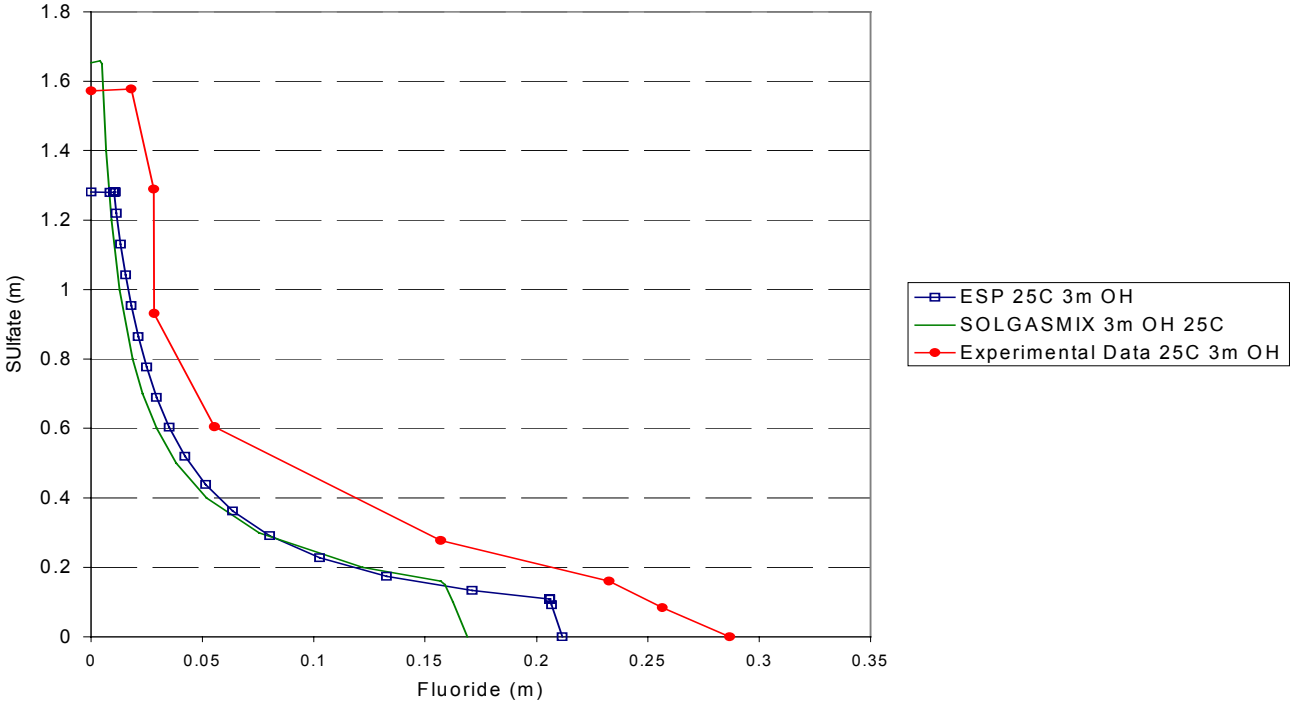

Figure 46. Experimental Measurements and Model Predictions in 3m Hydroxide at 25°C.

References

1. Herting, D.L., Edmonson, D.W., Smith, J.R., Hill, T.A., Delegard, C.H., "Saltcake Dissolution FY 1999 Status Report", HNF-5193, Rev. 0, Numatec Hanford Corp., Richland, WA, (1999).
2. Herting, D.L., Edmonson, D.W., "Saltcake Dissolution FY 1998 Status Report", HNF-3437, Rev. 0., Numatec Hanford Corp., Richland, WA, (1998).
3. Herting, D.L., "Saltcake Dissolution 2000 Status Report", HNF-7031, Rev. 0, Fluor-Hanford, Richland, WA, September 2000.
4. Toghiani, R. K., Lindner, J. S., "Saltcake Dissolution Modeling, FY 1999 Status Report" DIAL-40395-TR99-1, Diagnostic Instrumentation and Analysis Laboratory, Mississippi State University, Mississippi State MS (1999).
5. Toghiani, B, Lindner, J. S., Weber, C. F., Hunt, R. D., "Modeling of Sulfate Double-salts in Nuclear Wastes," ORNL/TM-2000/…, Oak Ridge national Laboratory, Oak Ridge, TN, (2000).
6. Lindner, J.S., personal communication to A. Hu, CH2Group Hanford, July 2000.
7. Reynolds, D.A., "Practical Modeling of Aluminum Species in High pH Wastes", WHC-EP-0872, Westinghouse Hanford Company, Richland, WA, (1995).
8. Barney, G.S., "Vapor-Liquid-Solid Phase Equilibria of Radioactive Sodium Salt Wastes at Hanford", ARH-ST-133, Atlantic Richfield Co., Richland, WA, (1976).
9. Ally, M., Braunstein, J., "Activity Coefficients in Concentrated Electrolytes: A Comparison of the Brunauer-Emmett-Teller (BET) Model with Experimental Values", *Fluid Phase Equilibria*, 120, 131, (1996).
10. International Critical Tables
11. Beahm, E.C., Toghiani, R.K., Weber, C.F., "Comparative Calculations of Solubility Equilibria", ORNL/TM-1999/127, Oak Ridge National Laboratory, Oak Ridge, TN, (2000).
12. Linke, W.F., Solubilities, 4th ed., American Chemical Society, Washington, DC, (1965).
13. Foote, H.W., Schairer, J.F., "The System Na_2SO_4-NaF-NaCl-H_2O, I. The Ternary System with Water and Two Salts", *J. American Chemical Society*, 52, 4202, (1930).
14. Mason, Clyde.W., Handbook of Chemical Microscopy, Vol. 1, (4th ed., John Wiley & Sons, New York: 1983).

Appendix A.

Tabulated Results

ESP Model Calculations
For
TX-113 and S-102 Saltcakes

Table 1A. Solids Distribution for TX-113 Saltcake at 25° C (Basis: 1000 kg TX-113 Saltcake)

Dilution Ratio	**20**	**30**	**40**	**50**	**75**	**100**	**150**	**200**	**250**	**300**	**400**	**500**
Aqueous (kg)	512.25	740.31	934.17	1109.64	1439.61	1775.20	2405.17	2927.78	3465.84	3990.56	4990.56	5990.56
PH	14.32	14.15	14.02	13.90	13.67	13.51	13.29	13.12	13.00	12.91	12.77	12.68
Ionic Strength	17.74	17.93	17.35	16.69	13.29	11.62	9.55	7.51	6.33	5.45	4.13	3.33
Density, (g/mL)	1.50	1.50	1.49	1.48	1.42	1.38	1.33	1.26	1.22	1.19	1.15	1.12
Solids												
% Solids	57.31	43.05	33.27	26.02	17.74	11.24	3.79	2.41	0.98	0.24	0.19	0.16
Total (kg)	687.75	559.70	465.83	390.36	310.39	224.81	94.84	72.25	34.23	9.52	9.56	9.55
Species (kg)												
$Al(OH)_3$	6.77	6.76	6.86	6.97	7.32	7.48	7.65	7.80	7.86	7.90	7.94	7.94
CaF_2								0.37	0.38	0.38	0.37	0.36
$CaCO_3$			0.49	0.49	0.48	0.49						
$Ca_3(PO_4)_2$	0.51	0.50					0.49					
$Ca(OH)_2$												
$Cr(OH)_3$	0.68	0.68	0.68	0.68	0.69	0.70	0.70	0.71	0.72	0.72	0.72	0.72
$Fe(OH)_3$	0.50	0.50	0.50	0.50	0.51	0.51	0.52	0.52	0.52	0.52	0.53	0.53
$Na_2C_2O_4$	0.46	0.39	0.29	0.18								
$Na_2CO_3.1H_2O$	208.83	160.26	100.47	31.98								
Na_2SO_4	221.11	219.16	216.66	212.82	176.10	106.24						
Na_3FSO_4	21.07	22.27	22.97	23.93	27.37	32.24	36.34	23.18	3.53			
$Na_7F(PO4)_2.19H_2O$	124.88	119.95	116.91	112.82	97.93	77.14	49.14	39.67	21.22			
$NaNO_3$	102.97	29.22										

Table 2A. Solids Distribution for TX-113 Saltcake at 50° C (Basis: 1000 kg TX-113 Saltcake)

Dilution Ratio	**20**	**30**	**40**	**50**	**75**	**100**	**150**	**200**	**250**	**300**	**400**	**500**
Aqueous (kg)	582.20	747.53	903.67	1045.39	1326.97	1630.42	2275.25	2923.61	3493.34	3993.34	4993.06	5993.34
PH	13.45	13.27	13.13	13.02	12.81	12.66	12.47	12.34	12.24	12.16	12.03	11.94
Ionic Strength	18.60	16.55	15.34	14.06	10.45	8.93	7.83	7.39	6.57	5.52	4.19	3.38
Density, (g/mL)	1.45	1.42	1.40	1.37	1.31	1.27	1.24	1.22	1.20	1.17	1.13	1.11
Solids												
% Solids	51.48	42.50	35.45	30.31	24.17	18.48	8.99	2.55	0.19	0.17	0.14	0.11
Total (kg)	617.81	552.47	496.33	454.61	423.03	369.58	224.75	76.54	6.54	6.75	6.82	6.80
Species (kg)												
$Al(OH)_3$	3.68	4.01	4.23	4.41	4.82	5.02	5.10	5.06	5.10	5.19	5.26	5.25
CaF_2	0.38	0.38	0.38	0.38	0.38	0.38	0.38	0.38	0.37			
$CaCO_3$												
$Ca_3(PO_4)_2$										0.48	0.48	0.47
$Ca(OH)_2$												
$Cr(OH)_3$	0.77	0.77	0.77	0.77	0.77	0.77	0.77	0.77	0.77	0.77	0.77	0.77
$Fe(OH)_3$	0.24	0.24	0.24	0.25	0.27	0.29	0.30	0.29	0.30	0.31	0.31	0.32
$Na_2C_2O_4$	0.40	0.25	0.07									
$Na_2CO_3.1H_2O$	133.37	88.92	36.52									
Na_2SO_4												
$Na_6(SO_4)_2CO_3$	328.73	328.28	327.49	325.88	309.31	277.83	186.98	70.04				
NaF	3.32	2.81	2.24	1.54								
$Na_7F(PO4)_2.19H_2O$	128.86	126.82	124.40	121.37	107.48	85.28	31.23					
$NaNO_3$	18.06											

Table 3A. ESP Model Predictions for Anion Concentrations for TX-113 Saltcake at 25° C (all concentrations in g/L)

%Dilution by Weight	F	Cl	NO2	NO3	PO4	SO4	C2O4	CO3	TIC
20	0.04	3.41	7.40	324.29	8.30	4.41	0.26	133.03	26.61
30	0.04	2.36	5.23	334.13	8.42	4.45	0.27	139.98	28.00
40	0.05	1.86	4.18	296.90	8.42	5.63	0.31	155.88	31.18
50	0.05	1.55	3.55	247.80	8.48	7.49	0.36	174.29	34.86
75	0.08	1.15	2.74	183.19	10.18	28.25	0.38	144.10	28.82
100	0.10	0.91	2.25	144.72	12.12	57.13	0.30	114.07	22.81
150	0.25	0.64	1.72	102.41	12.70	78.84	0.21	80.72	16.14
200	0.82	0.50	1.45	80.18	11.16	64.68	0.17	63.19	12.64
250	1.56	0.41	1.27	65.67	10.88	56.61	0.14	51.76	10.35
300	1.60	0.35	1.14	55.64	10.91	48.51	0.12	43.86	8.77
400	1.23	0.27	0.99	42.84	8.40	37.35	0.09	33.77	6.75
500	1.00	0.22	0.89	34.83	6.83	30.37	0.07	27.45	5.49

Table 4A. ESP Model Predictions for Anion Concentrations for TX-113 Saltcake at 50° C (all concentrations in g/L)

%Dilution by Weight	F	Cl	NO2	NO3	PO4	SO4	C2O4	CO3	TIC
20	0.99	2.90	6.30	430.63	5.19	0.31	0.31	78.23	15.65
30	1.29	2.21	4.89	353.02	4.99	0.66	0.43	100.57	20.11
40	1.55	1.80	4.05	287.27	5.06	1.14	0.54	121.23	24.25
50	1.84	1.53	3.51	244.42	5.36	2.01	0.51	126.71	25.34
75	2.43	1.15	2.74	183.30	7.67	9.56	0.38	97.54	19.51
100	2.39	0.91	2.26	145.00	10.69	19.66	0.30	80.94	16.19
150	2.45	0.63	1.70	101.22	15.31	38.09	0.21	64.11	12.82
200	2.24	0.49	1.40	77.84	15.26	53.42	0.16	56.84	11.37
250	1.84	0.40	1.23	63.88	12.52	55.70	0.13	50.35	10.07
300	1.62	0.34	1.12	54.49	10.59	47.51	0.11	42.95	8.59
400	1.25	0.26	0.97	42.10	8.18	36.71	0.09	33.19	6.64
500	1.02	0.21	0.87	34.30	6.67	29.90	0.07	27.03	5.41

Table 5A. Comparison of ESP Model Predictions and Experimental Data (LAB) for TX-113 Saltcake at 25° C

	LAB	ESP	LAB	ESP	LAB	ESP	LAB	ESP	LAB	ESP	LAB	ESP
% Dilution	50	50	100	100	150	150	200	200	250	250	300	300
SpG (g/ml)		1.4796		1.3824		1.3254		1.263		1.2247		1.1947
pH		13.9		13.5		13.3		13.1		13.0		12.9
Ionic Strength		16.7		11.6		9.5		7.5		6.3		5.4
Concentrations in g/L												
TIC	12.9	34.86	20.8	22.81	18.5	16.144	14.1	12.64	12.2	10.352	9.17	8.77
F	0.23	0.05	0.29	0.10	0.46	0.25	1.06	0.82	1.15	1.56	1.2	1.60
Cl	1.01	1.55	0.37	0.91	0.33	0.64	0.28	0.50	0.31	0.41	0.2	0.35
NO_2	3.81	3.55	1.72	2.25	1.51	1.72	1.33	1.45	1.09	1.27	1.07	1.14
NO_3	294	247.80	132	144.72	105	102.41	84.5	80.18	66.9	65.67	55.2	55.64
PO_4	2.07	8.48	2.88	12.12	4.2	12.70	4.83	11.16	4.47	10.88	5.75	10.91
SO_4	33.9	7.49	79.6	57.13	86.4	78.84	69.7	64.68	57.8	56.61	47.4	48.51
C_2O_4	<.054	0.36	<.054	0.30	0.8	0.21	0.96	0.17	<.054	0.14	0.91	0.12

Experimental data from Reference [8].

Table 6A. Comparison of ESP Model Predictions and Experimental Data (LAB) for TX-113 Saltcake at 50° C

	LAB	ESP	LAB	ESP	LAB	ESP	LAB	ESP	LAB	ESP	LAB	ESP
% Dilution	50	50	100	100	150	150	200	200	250	250	300	300
SpG (g/ml)		1.37		1.27		1.24		1.22		1.2		1.17
pH		13.0		12.7		12.5		12.3		12.2		12.2
Ionic Strength		14.1		8.9		7.8		7.4		6.6		5.5
Concentrations in g/L												
TIC	18.91	25.343	19.271	16.188	17.699	12.823	13.958	11.37	11.386	10.071	9.31	8.5893
F	0.394	1.84	0.448	2.39	0.568	2.45	1.042	2.24	1.857	1.84	1.16	1.62
Cl	0.702	1.53	0.47	0.91	0.298	0.63	0.409	0.49	0.181	0.40	0.176	0.34
NO_2	3.644	3.51	1.942	2.26	1.432	1.70	1.529	1.40	0.95	1.23	0.761	1.12
NO_3	317.631	244.42	142.04	145.00	101.41	101.22	79.761	77.84	64.281	63.88	60.5	54.49
PO_4	15.857	5.36	22.193	10.69	19.202	15.31	14.693	15.26	13.082	12.52	7.32	10.59
SO_4	17.531	2.01	55.113	19.66	75.117	38.09	62.969	53.42	55.721	55.70	47.9	47.51
C_2O_4	<1.3	0.51	2.415	0.30	<.5	0.21	<.8	0.16	0.964	0.13	<.2	0.11

Table 7A. Solids Distribution for S-102 Saltcake at 25° C
(Basis: 1000 kg S-102 Saltcake)

Dilution Ratio	**30**	**40**	**50**	**75**	**100**	**150**	**200**	**250**	**300**	**400**	**500**
Aqueous (kg)	682.39	875.417	1065.7	1544.3	1970.7	2471.6	2973.3	3475.8	3976.67	4976.39	5976.4
pH	14.265	14.1398	14.043	13.867	13.722	13.418	13.223	13.085	12.9787	12.8236	12.712
Ionic Strength	15.426	14.3796	13.68	12.73	11.645	7.8832	5.9555	4.8037	4.02002	3.02573	2.4266
Density, (g/mL)	1.4657	1.4538	1.4456	1.4341	1.4132	1.3113	1.2492	1.2078	1.1779	1.1378	1.1123
Solids											
% Solids	47.51	37.47	28.95	11.75	1.46	1.14	0.89	0.61	0.58	0.47	0.39
Total (kg)	617.61	524.584	434.28	205.69	29.295	28.406	26.648	24.228	23.3928	23.5064	23.571
% Undissolved											
Species (kg)											
$Al(OH)_3$	19.212	19.2984	19.364	19.451	19.588	20.119	20.364	20.504	20.5936	20.702	20.764
$Cr(OH)_3$	2.740	2.74069	2.742	2.744	2.749	2.774	2.787	2.794	2.79909	2.80454	2.8076
$Na_2C_2O_4$	7.775	7.67536	7.570	7.299	6.958	5.513	3.497	0.930			
Na_2SO_4	0.137										
$NaNO_3$	583.84	494.858	404.61	175.19							
$Na_3PO_4.1/4NaOH.12H_2O$	3.89										

Table 8A. Solids Distribution for S-102 Saltcake at 50° C

Dilution Ratio	30	40	50	75	100	150	200	250	300	400	500
Aqueous (kg)	770.25	983.945	1199.1	1720.8	1974.6	2475.9	2978.3	3479.5	3979.45	4979.17	5978.9
pH	13.417	13.3143	13.23	13.067	12.89	12.626	12.447	12.317	12.2157	12.0661	11.958
Ionic Strength	18.353	17.203	16.509	15.309	11.704	7.9267	6.0156	4.8439	4.04793	3.04741	2.444
Density, (g/mL)	1.4476	1.4411	1.4371	1.4275	1.3651	1.2775	1.2226	1.1849	1.1204	1.1204	1.0967
Solids											
% Solids	40.75	29.72	20.06	1.67	1.27	0.96	0.72	0.58	0.52	0.42	0.35
Total (kg)	529.75	416.056	300.89	29.156	25.425	24.116	21.547	20.464	20.6859	20.9681	21.135
% Undissolved											
Species (kg)											
$Al(OH)_3$	15.301	15.3449	15.365	15.426	16.021	16.811	17.292	17.609	17.8303	18.1117	18.279
$Cr(OH)_3$	2.850	2.84896	2.849	2.848	2.849	2.852	2.854	2.855	2.85549	2.85636	2.8568
$Na_2C_2O_4$	7.736	7.63211	7.525	7.235	6.555	4.453	1.401				
$Na_2CO_3.1H_2O$											
$Na_6(SO4)_2CO_3$	6.6932	6.31385	5.7951	3.6465							
$NaNO_3$	497.17	383.92	269.37								

Table 9A. ESP Model Predictions for Anion Concentrations for S-102 Saltcake at 25° C (all concentrations in g/L)

% Dilution by Weight	F	Cl	NO2	NO3	PO4	SO4	C2O4	CO3	TIC
30	0.00	3.84	47.66	338.50	10.09	7.28	0.27	68.74	13.75
40	0.00	2.97	36.85	369.52	9.38	5.78	0.32	53.15	10.63
50	0.00	2.43	30.10	391.13	7.66	4.72	0.35	43.41	8.68
75	0.00	1.66	20.61	422.50	5.24	3.23	0.41	29.72	5.94
100	0.00	1.28	15.91	418.45	4.05	2.50	0.48	22.95	4.59
150	0.00	0.95	11.77	309.57	3.00	1.85	0.86	16.98	3.40
200	0.00	0.75	9.32	245.15	2.37	1.46	1.23	13.45	2.69
250	0.00	0.62	7.71	202.77	1.96	1.21	1.61	11.12	2.22
300	0.00	0.53	6.57	172.85	1.67	1.03	1.55	9.48	1.90
400	0.00	0.41	5.07	133.41	1.29	0.80	1.20	7.32	1.46
500	0.00	0.33	4.13	108.60	1.05	0.65	0.97	5.96	1.19

Table 10A. ESP Model Predictions for Anion Concentrations for S-102 Saltcake at 50° C (all concentrations in g/L)

% Dilution by Weight	Cl	NO2	NO3	PO4	SO4	C2O4	CO3	TIC
30	3.36	41.70	415.00	10.61	0.35	0.29	58.21	11.64
40	2.62	32.50	444.42	8.27	0.54	0.32	45.45	9.09
50	2.15	26.60	463.84	6.77	0.75	0.35	37.29	7.46
75	1.49	18.41	484.06	4.68	1.40	0.40	26.08	5.22
100	1.24	15.34	403.42	3.90	2.41	0.64	22.13	4.43
150	0.92	11.45	301.08	2.91	1.80	1.19	16.51	3.30
200	0.73	9.11	239.52	2.32	1.43	1.77	13.14	2.63
250	0.61	7.56	198.70	1.92	1.19	1.78	10.90	2.18
300	0.52	6.45	169.71	1.64	1.01	1.52	9.31	1.86
400	0.40	4.99	131.30	1.27	0.78	1.18	7.20	1.44
500	0.33	4.07	107.03	1.03	0.64	0.96	5.87	1.17

Table 11A. Comparison of ESP Model Predictions and Experimental Data (LAB) for S-102 Saltcake at 25° C

	LAB	ESP	LAB	ESP	LAB	ESP	LAB	ESP	LAB	ESP
% Dilution	51	50	101	100	150	150	200	200	300	300
SpG (g/ml)	1.392	1.446	1.377	1.413	1.273	1.311	1.231	1.249	1.165	1.178
pH		14.0		13.7		13.4		13.2		13.0
Ionic Strength		13.7		11.6		7.9		6.0		4.0
Concentrations in g/L										
TIC	6.71	8.68	4.17	4.59	3.51	3.40	2.47	2.69	1.59	1.90
Cl	1.99	2.43	1.17	1.28	1.08	0.95	0.84	0.75	0.76	0.53
NO_2	27.90	30.10	14.70	15.91	12.30	11.77	9.46	9.32	6.87	6.57
NO_3	359.00	391.13	410.50	418.45	304.00	309.57	237.00	245.15	173.00	172.85
PO_4	4.32	7.66	4.51	4.05	2.75	3.00	3.63	2.37	1.80	1.67
SO_4	4.36	4.72	3.23	2.50	3.04	1.85	1.94	1.46	1.46	1.03
C_2O_4		0.35		0.48	0.66	0.86	1.00	1.23	0.65	1.55

Table 12A. Comparison of ESP Model Predictions and Experimental Data (LAB) for S-102 Saltcake at 50° C

	LAB	ESP	LAB	ESP	LAB	ESP	LAB	ESP	LAB	ESP
% Dilution	51	50	101	100	150	150	200	200	300	300
SpG (g/ml)	1.493	1.437	1.381	1.365	1.285	1.278	1.232	1.223	1.154	1.120
pH		13.2		12.9		12.6		12.4		12.2
Ionic Strength		16.5		15.3		7.9		6.0		4.0
Concentrations in g/L										
TIC	7.29	7.46	3.11	4.43	2.97	3.30	1.67	2.63	1.75	1.86
Cl	2.71	2.15	1.52	1.24	1.15	0.92	0.74	0.73	0.55	0.52
NO_2	30.40	26.60	17.60	15.34	12.20	11.45	8.90	9.11	5.90	6.45
NO_3	385.00	463.84	431.00	403.42	283.00	301.08	260.00	239.52	168.00	169.71
PO_4	7.47	6.77	4.84	3.90	2.70	2.91	2.42	2.32	1.79	1.64
SO_4	3.06	0.75	2.52	2.41	1.94	1.80	1.41	1.43	1.64	1.01
C_2O_4		0.35	0.76	0.64	1.12	1.19	1.03	1.77	0.89	1.52

Appendix B.

Comparative Plots
Dissolution Studies
For
Saltcake S-102 at 50° C

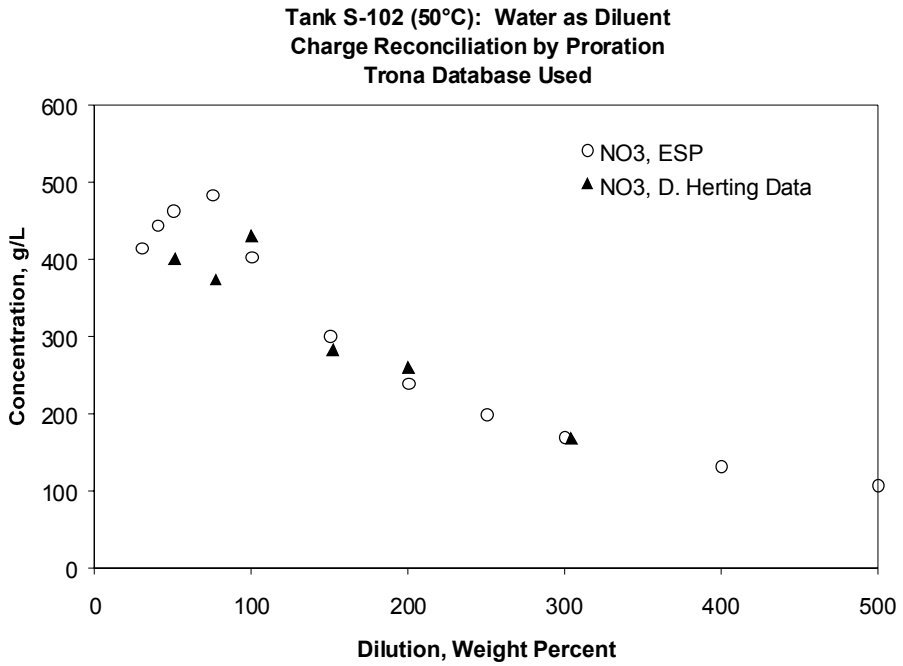

Figure B1. Comparison of ESP Model Predictions and Experimental Nitrate Concentration Data for Tank S-102 Saltcake at 50° C

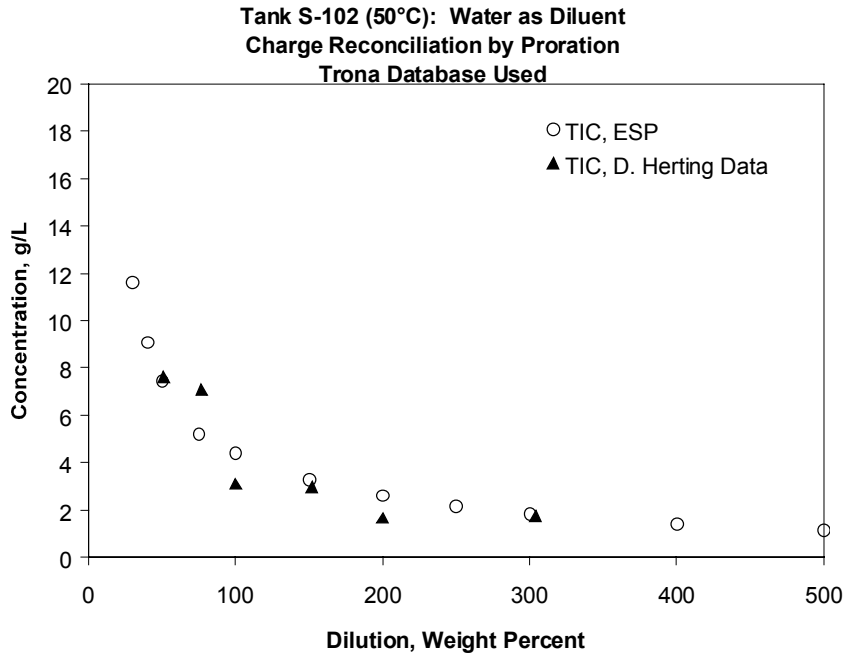

Figure B2. Comparison of ESP Model Predictions and Experimental TIC Concentration Data for Tank S-102 Saltcake at 50° C

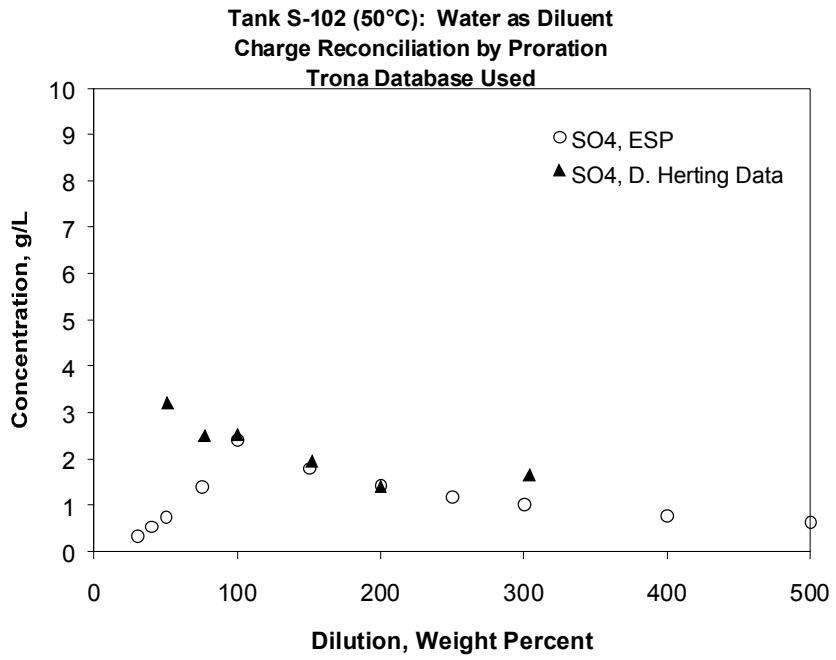

Figure B3. Comparison of ESP Model Predictions and Experimental Sulfate Concentration Data for Tank S-102 Saltcake at 50° C

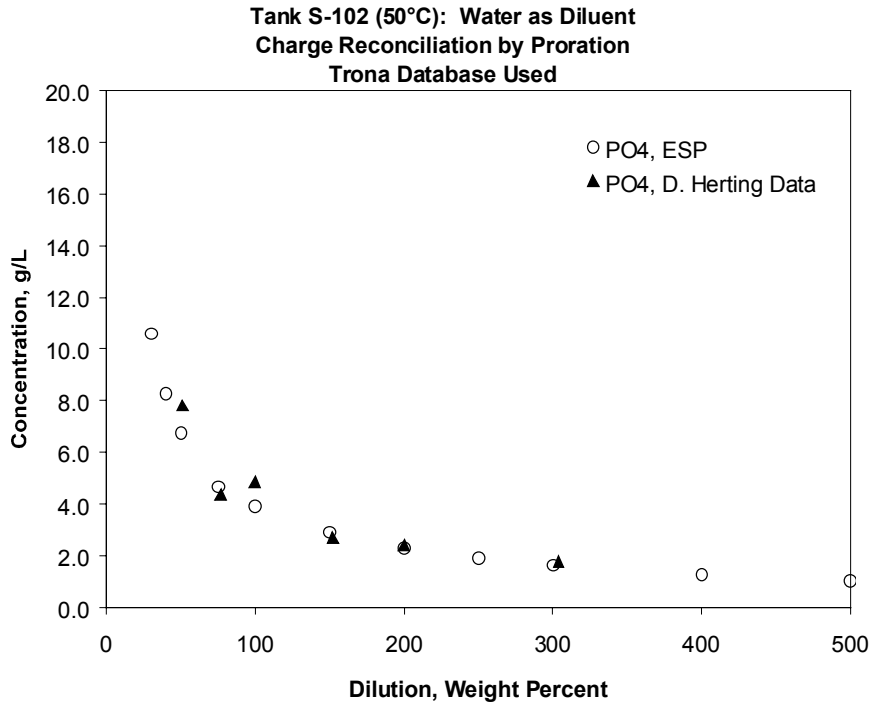

Figure B4. Comparison of ESP Model Predictions and Experimental Phosphate Concentration Data for Tank S-102 Saltcake at 50° C

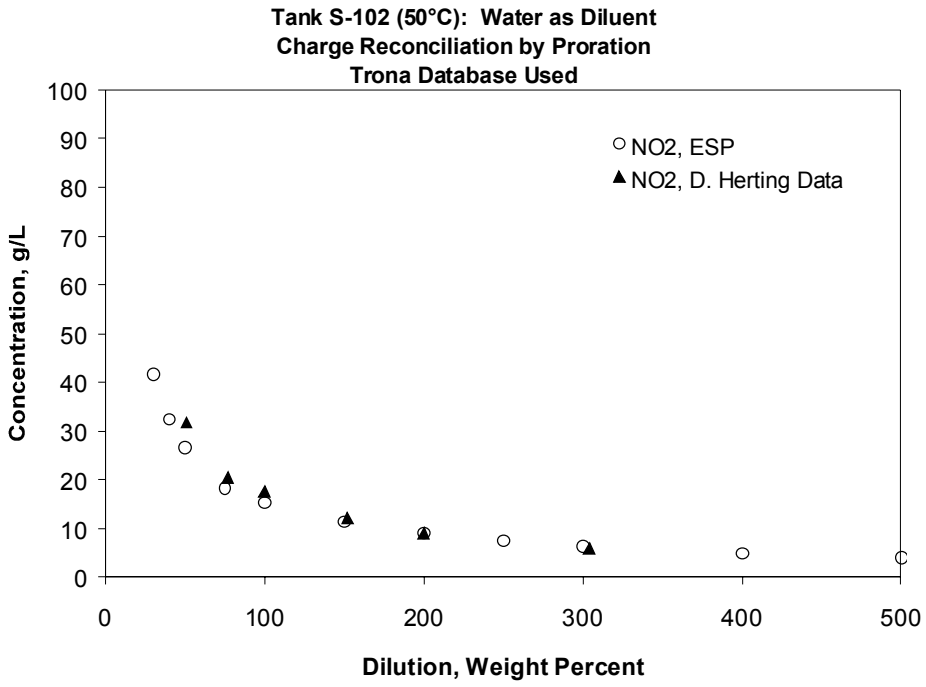

Figure B5. Comparison of ESP Model Predictions and Experimental Nitrite Concentration Data for Tank S-102 Saltcake at 50° C

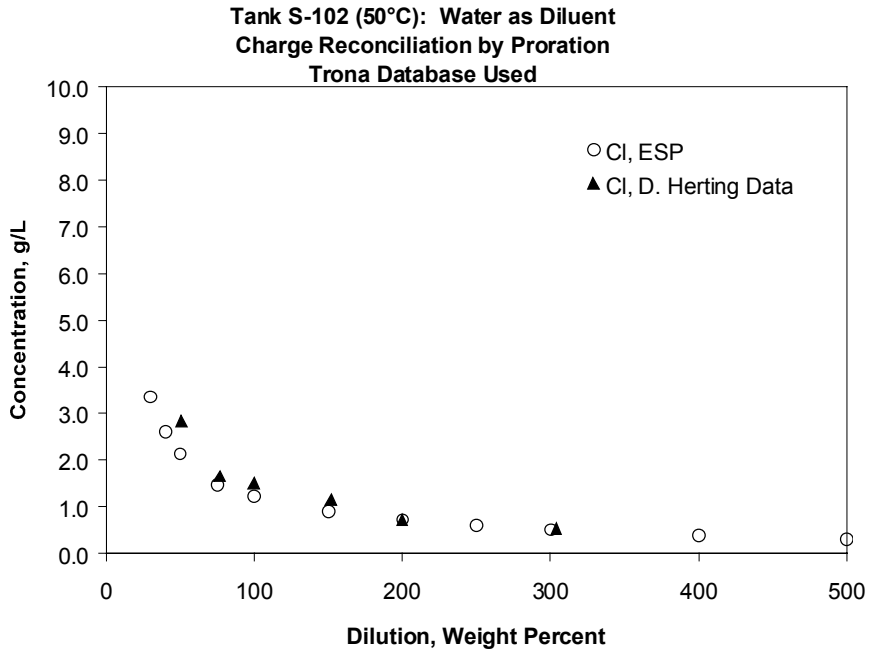

Figure B6. Comparison of ESP Model Predictions and Experimental Chloride Concentration Data for Tank S-102 Saltcake at 50° C

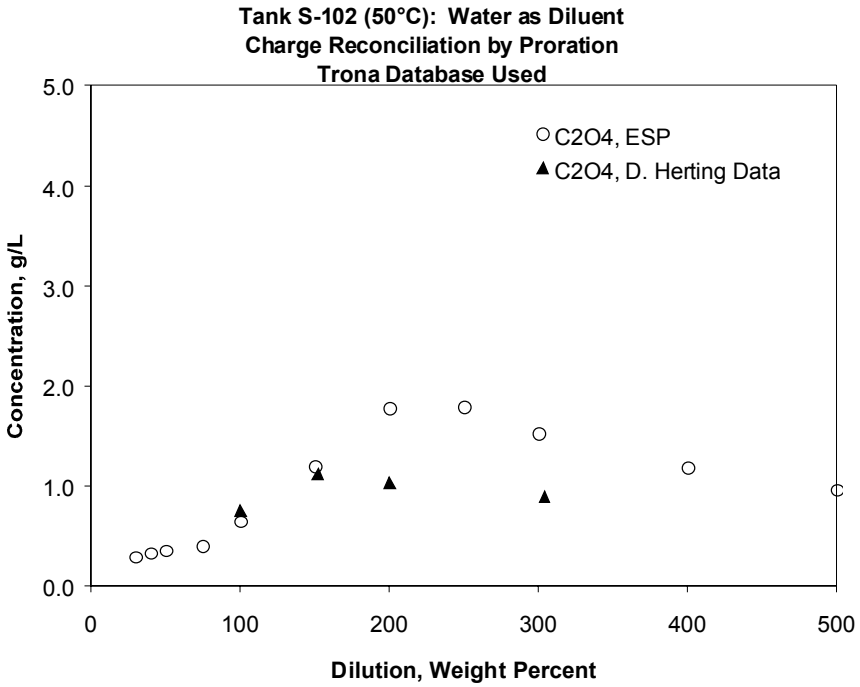

Figure B7. Comparison of ESP Model Predictions and Experimental Oxalate Concentration Data for Tank S-102 Saltcake at 50° C

Appendix C.

Input Molecular Streams
for
ESP Feed Stability Studies

Table 1C. Input Molecular Streams Used for ESP Feed Stability Simulations (all units are molality)

Species	TX-113	BY-102	BY-106	A-101	S-102
H_2O	55.5087	55.5087	55.5087	55.5087	55.5087
$Al(OH)_3$	.571157	2.22938	242.528	5.01234	3.05693
$Ca(OH)_2$	.21929	.0390628		.0113679	
$Cr(OH)_3$	.033805	.139678	8.9739	.186628	.290647
$Fe(OH)_3$	.023605	.0347358	1.41468	.0146489	
H_2CO_3	7.10591	10.8368	436.624	7.43882	
HCl	.145991	.124248	17.7728	.575424	.526999
H_6F_6	.073169	.258308	19.7258	.0148629	
HNO_2	.244337	1.37468	227.728	8.7095	5.03444
HNO_3	13.3315	6.01524	2526.58	10.9648	98.2247
KOH	.033717	.0882075	25.6048	.451894	.216171
$Na_6(SO_4)_2CO_3$	3.75134	.91046	23.4128	.684342	
$Na_7F(PO_4)_2.19H_2O$	.853559	.550394	6.93412	.107006	
NaOH	29.9097	39.2806	4290.86	38.4486	111.969
$H_2C_2O_4$	.019647	.205248	55.2404	.82565	.620668
$Na_3PO_4.0.25NaOH.12H_2O$					.620668
$Na_3H(SO_4)_2$					.189093
$Na_2CO_3.NaHCO_3.2H_2O$					2.78316
$Mg(OH)_2$		.0153049			
$Mn(OH)_2$		.0161979			

Appendix D.

Summary Tables
for
Feed Stability Studies

Table 1D. Liquid Phase Summary for TX-113 (All amounts in grams)

Contact	Cumulative Diluent (% by wt.)	Oxalate $C_2O_4^{2-}$	Fluoride F^-	Phosphate PO_4^{3-}	Nitrate NO_3^-	Carbonate CO_3^{2-}	Sulfate SO_4^{2-}
1	**50**	0.005441	0.000778	0.105732	2.253559	2.55878	0.123374
2	**100**	0.003594	0.008454	0.218468	0.0	0.473025	1.450432
3	**150**	0.0	0.036984	0.60822	0.0	0.0	2.706604
4	**200**	0.0	0.113525	0.076059	0.0	0.0	0.535547
5	**250**	0.0	0.000141	0.0	0.0	0.0	0.0
6	**300**	0.0	0.000141	0.0	0.0	0.0	0.0

Table 2D. Solids Phase Distribution for TX-113 (Grams Predicted to Form in Cumulative Supernate Receiver

	Cumulative Diluent (% by Weight)				
Species	**100**	**150**	**200**	**250**	**300**
$Al(OH)_3$	0.013487	0.025492	0.031116	0.033703	0.035469
CaF_2	0.0	0.0	0.0	4.56e-04	7.01e-04
$Cr(OH)_3$	3.67e-04	8.53e-04	0.001109	0.001242	0.001337
$Fe(OH)_3$	2.42e-04	5.63e-04	7.33e-04	8.2e-04	8.82e-04
Na_2SO_4	0.388956	0.0	0.0	0.0	0.0
Na_3FSO_4	0.004862	0.008388	0.694844	0.105779	0.0
$Na_7F(PO_4)_2.19H_2O$	0.23575	1.20988	1.19037	0.636673	0.0
TOTAL	**0.643664**	**1.245176**	**1.918172**	**0.778673**	**0.038389**

Table 3D. Liquid Phase Summary for BY-102 (All amounts in grams)

Contact	Cumulative Diluent (% by wt.)	Oxalate $C_2O_4^{2-}$	Fluoride F^-	Phosphate PO_4^{3-}	Nitrate NO_3^-	Carbonate CO_3^{2-}	Sulfate SO_4^{2-}
1	**50**	0.08341	0.01878	0.022074	0.837563	4.149986	0.14562
2	**100**	0.087794	0.152654	0.250801	0.0	0.095561	0.664496
3	**150**	0.023668	0.084091	0.386539	0.0	0.0	0.210198
4	**200**	0.0	0.000141	0.0	0.0	0.0	0.0
5	**250**	0.0	0.000142	0.0	0.0	0.0	0.0
6	**300**	0.0	0.000141	0.0	0.0	0.0	0.0

Table 4D. Solids Phase Distribution for BY-102 (Grams Predicted to Form in Cumulative Supernate Receiver

	Cumulative Diluent (% by Weight)				
Species	**100**	**150**	**200**	**250**	**300**
$Al(OH)_3$	0.327498	0.446645	0.509284	0.549088	0.577749
CaF_2	4.32e-05	5.89e-05	3.37e-04	5.99e-04	8.54E-04
$Cr(OH)_3$	0.0124561	0.0171517	0.019593	0.0211151	0.0221896
$Fe(OH)_3$	0.0082284	0.0113301	0.012943	0.0139479	0.0146575
$Mg(OH)_2$	3.52E-05	2.36E-04	2.36E-04	2.36E-04	2.37E-04
$Mn(OH)_2$	0.00661689	0.00834063	0.008904	0.00915414	0.00928798
$Na_2C_2O_4$	0.0989697	0.07775596	0.0	0.0	0.0
Na_3FSO_4	0.695313	0.320834	0.0	0.0	0.0
$Na_7F(PO_4)_2.19H_2O$	0.7399186	1.85743	1.25487	0.343111	0.0
TOTAL	**1.889079**	**2.73978**	**1.80617**	**0.937251**	**0.624975**

Table 5D. Liquid Phase Summary for BY-106 (All amounts in grams)

Contact	Cumulative Diluent (% by wt.)	Oxalate $C_2O_4^{2-}$	Fluoride F^-	Phosphate PO_4^{3-}	Nitrate NO_3^-	Carbonate CO_3^{2-}	Sulfate SO_4^{2-}
1	**50**	0.006728	0.031049	0.040573	8.209611	1.79392	0.123244
2	**100**	0.041311	0.126908	0.046451	2.352598	0.0	0.198816
3	**150**	0.306816	0.012741	0.0	0.0	0.0	0.0
4	**200**	0.0	0.0	0.0	0.0	0.0	0.0
5	**250**	0.0	0.0	0.0	0.0	0.0	0.0
6	**300**	0.0	0.0	0.0	0.0	0.0	0.0

Table 6D. Solids Phase Distribution for BY-106 (Grams Predicted to Form in Cumulative Supernate Receiver

	Cumulative Diluent (% by Weight)				
Species	**100**	**150**	**200**	**250**	**300**
$Al(OH)_3$	0.27921	0.408145	0.468246	0.502035	0.523492
$Cr(OH)_3$	0.0104597	0.0157816	0.018215	0.0195432	0.0203665
$Fe(OH)_3$	0.0	0.00310012	0.0047	0.00555887	0.00609056
$Na_2C_2O_4$	0.0336871	0.45741	0.391338	0.3065	0.203399
NaF	0.119511	0.0	0.0	0.0	0.0
$Na_7F(PO_4)_2.19H_2O$	0.00891563	0.0	0.0	0.0	0.0
TOTAL	**0.451783**	**0.884537**	**0.882499**	**0.833637**	**0.753348**

Table 7D. Liquid Phase Summary for A-101 (All amounts in grams)

Contact	Cumulative Diluent (% by wt.)	Oxalate $C_2O_4^{2-}$	Fluoride F^-	Phosphate PO_4^{3-}	Nitrate NO_3^-	Carbonate CO_3^{2-}	Sulfate SO_4^{2-}
1	**50**	0.01454	0.018623	0.005608	0.806464	1.791249	0.106467
2	**100**	0.337002	0.003393	0.008249	0.0	0.0	0.0
3	**150**	0.081451	0.0	0.0	0.0	0.0	0.0
4	**200**	0.000118	0.0	0.0	0.0	0.0	0.0
5	**250**	0.000118	0.0	0.0	0.0	0.0	0.0
6	**300**	0.000118	0.0	0.0	0.0	0.0	0.0

Table 8D. Solids Phase Distribution for A-101 (Grams Predicted to Form in Cumulative Supernate Receiver

	Cumulative Diluent (% by Weight)				
Species	**100**	**150**	**200**	**250**	**300**
$Al(OH)_3$	0.327498	0.446645	0.509284	0.549088	0.577749
CaF_2	4.32e-05	5.89e-05	3.37e-04	5.99e-04	8.54e-04
$Cr(OH)_3$	0.0124561	0.0171517	0.019593	0.0211151	0.0221896
$Fe(OH)_3$	0.0082284	0.0113301	0.012943	0.0139479	0.0146575
$Mn(OH)_2$	0.00661689	0.00834063	0.008904	0.00915414	0.00928798
$Na_2C_2O_4$	0.0989697	0.07775596	0.0	0.0	0.0
Na_3FSO_4	0.695313	0.320834	0.0	0.0	0.0
$Na_7F(PO_4)_2.19H_2O$	0.7399186	1.85743	1.25487	0.343111	0.0
TOTAL	**1.889044**	**2.73955**	**1.80593**	**0.937015**	**0.624739**

Table 9D. Liquid Phase Summary for S-102 (All amounts in grams)

Contact	Cumulative Diluent (% by wt.)	Oxalate $C_2O_4^{2-}$	Phosphate PO_4^{3-}	Nitrate NO_3^-	Carbonate CO_3^{2-}
1	**50**	0.008952	0.106859	9.362084	0.33715
2	**100**	0.02831	0.0	4.145906	0.0
3	**150**	0.010564	0.0	0.0	0.0
4	**200**	0.0	0.0	0.0	0.0
5	**250**	0.0	0.0	0.0	0.0
6	**300**	0.0	0.0	0.0	0.0

Table 10D. Solids Phase Distribution for S-101 (Grams Predicted to Form in Cumulative Supernate Receiver

	Cumulative Diluent (% by Weight)				
Species	**100**	**150**	**200**	**250**	**300**
$Al(OH)_3$	0.108464	0.182183	0.216069	0.235179	0.247355
$Cr(OH)_3$	0.00431491	0.00738354	0.008754	0.00950244	0.00996712
$Na_2C_2O_4$	0.0160202	0.0	0.0	0.0	0.0
TOTAL	**0.129**	**0.190**	**0.225**	**0.245**	**0.257**

Appendix E.

Comparative Calculations for Sodium Nitrate

Tabulations of Data

Table 1E. Tabulated Data for Sodium Nitrate Comparison Studies - 25° C

	ESP Prediction				Ally Calculated Results				International Critical Tables		
g NaNO3/100 g H2O	Vapor Pressure Over Solution	Ionic Strength	Solvent Activity	% Abs. Error	Vapor Pressure Over Solution	Ionic Strength	Solvent Activity	% Abs. Error	Vapor Pressure Over Solution	Ionic Strength	Solvent Activity
0	23.8509	1.0071E-07	1			0.0000			23.763	0.0000	1.000
5	23.4114	0.586009	0.981573022	0.31	23.3163	0.5883	0.9812	0.10	23.34	0.5883	0.98
10	22.9971	1.16956	0.964202609	0.29	22.879	1.1765	0.9628	0.22	22.93	1.1765	0.96
20	22.1985	2.33271	0.930719595	0.26	22.0402	2.3531	0.9275	0.45	22.14	2.3531	0.93
30	21.4277	3.49279	0.898402157	0.18	21.2441	3.5296	0.894	0.68	21.39	3.5296	0.90
40	20.681	4.65134	0.867095162	0.04	20.4861	4.7062	0.8621	0.99	20.69	4.7062	0.87
50	19.9571	5.80932	0.836744106	0.41	19.7684	5.8827	0.8319	1.36	20.04	5.8827	0.84
60	19.2552	6.9674	0.807315447	0.85	19.0888	7.0592	0.8033	1.71	19.42	7.0592	0.82
70	18.5744	8.12601	0.778771451	1.36	18.4425	8.2358	0.7761	2.06	18.83	8.2358	0.79
80	17.914	9.28547	0.751082768	2.06	17.8294	9.4123	0.7503	2.52	18.29	9.4123	0.77
90	17.2732	10.446	0.724215858	2.80	17.2472	10.5889	0.7258	2.94	17.77	10.5889	0.75
92.7	17.1035	10.7595	0.717100822	1.08							
100					16.6959	11.7654	0.7026	3.44	17.29	11.7654	0.73

Table 2E. Tabulated Data for Sodium Nitrate Comparison Studies - 100° C

	ESP Prediction				Ally Calculated Results				International Critical Tables		
g NaNO3/100 g H2O	Vapor Pressure Over Solution	Ionic Strength	Solvent Activity	% Abs. Error	Vapor Pressure Over Solution	Ionic Strength	Solvent Activity	% Abs. Error	Vapor Pressure Over Solution	Ionic Strength	Solvent Activity
0	758.016	0.0000	1.0000	0.26	760.00	0	1	0.00	760.0	0	1
5	744.095	0.5865	0.9816	0.30	745.712	0.5883	0.9812	0.08	746.3	0.5883	0.98
10	730.786	1.1711	0.9641	0.23	731.804	1.1765	0.9629	0.10	732.5	1.1765	0.96
20	704.519	2.3368	0.9294	0.15	705.128	2.3531	0.9278	0.07	705.6	2.3531	0.93
30	687.551	3.4991	0.9070	1.17	679.820	3.5296	0.8945	0.03	679.6	3.5296	0.89
40	653.035	4.6592	0.8615	0.27	655.956	4.7062	0.8631	0.18	654.8	4.7062	0.86
50	628.148	5.8178	0.8287	0.50	633.384	5.8827	0.8334	0.33	631.3	5.8827	0.83
60	604.025	6.9759	0.7968	0.82	611.952	7.0592	0.8052	0.48	609.0	7.0592	0.8
70	580.768	8.1339	0.7662	1.25	591.736	8.2358	0.7786	0.62	588.1	8.2358	0.77
80	558.44	9.2926	0.7367	1.72	572.508	9.4123	0.7533	0.76	568.2	9.4123	0.75
90	537.081	10.4522	0.7085	2.24	554.344	10.5889	0.7294	0.90	549.4	10.5889	0.72
100	516.706	11.6133	0.6817	2.80	537.092	11.7654	0.7067	1.03	531.6	11.7654	0.7
110	497.311	12.7759	0.6561	3.40	520.752	12.9419	0.6852	1.16	514.8	12.9419	0.68
120	478.877	13.9403	0.6318	4.01	505.172	14.1185	0.6647	1.26	498.9	14.1185	0.66
130	461.374	15.1067	0.6087	4.62	490.428	15.295	0.6453	1.39	483.7	15.295	0.64
140	444.76	16.2748	0.5867	5.25	476.368	16.4716	0.6268	1.48	469.4	16.4716	0.62
150	428.984	17.4449	0.5659	5.86	463.068	17.6481	0.6093	1.62	455.7	17.6481	0.6
160	413.991	18.6166	0.5462	6.46	450.300	18.8246	0.5925	1.74	442.6	18.8246	0.58
170	399.717	19.7900	0.5273	7.06	438.216	20.0012	0.5766	1.89	430.1	20.0012	0.57
180	386.097	20.9647	0.5094	7.70	426.664	21.1777	0.5614	2.00	418.3	21.1777	0.55

Table 3E. Tabulated Data for Sodium Nitrate Comparison Studies - 125° C

	ESP Prediction				Ally Calculated Results				International Critical Tables		
g NaNO3/100 g H2O	Vapor Pressure Over Solution	Ionic Strength	Solvent Activity	% Abs. Error	Vapor Pressure Over Solution	Ionic Strength	Solvent Activity	% Abs. Error	Vapor Pressure Over Solution	Ionic Strength	Solvent Activity
0	1730.88	0.0000	1.0000			0			1740.5	0	1
5	1699.01	0.5867	0.9816	0.58	1707.7786	0.5883	0.9812	0.07	1709	0.5883	0.98
10	1668.34	1.1716	0.9639	0.52	1675.9275	1.1765	0.9629	0.06	1677	1.1765	0.96
20	1607.16	2.3381	0.9285	0.49	1614.8359	2.3531	0.9278	0.01	1615	2.3531	0.93
30	1546.05	3.5011	0.8932	0.51	1557.2254	3.5296	0.8947	0.21	1554	3.5296	0.89
40	1485.67	4.6616	0.8583	0.69	1502.7477	4.7062	0.8634	0.45	1496	4.7062	0.86
50	1426.65	5.8202	0.8242	1.06	1451.0549	5.8827	0.8337	0.63	1442	5.8827	0.83
60	1369.48	6.9780	0.7912	1.48	1402.3209	7.0592	0.8057	0.89	1390	7.0592	0.8
70	1314.54	8.1355	0.7595	1.97	1356.1976	8.2358	0.7792	1.13	1341	8.2358	0.77
80	1262.06	9.2934	0.7291	2.47	1312.511	9.4123	0.7541	1.43	1294	9.4123	0.74
90	1212.18	10.4523	0.7003	3.03	1271.0872	10.5889	0.7303	1.69	1250	10.5889	0.72
100	1164.96	11.6128	0.6730	3.64	1231.7519	11.7654	0.7077	1.88	1209	11.7654	0.69
110	1120.41	12.7750	0.6473	4.24	1194.5052	12.9419	0.6863	2.09	1170	12.9419	0.67
120	1078.48	13.9392	0.6231	4.98	1159.173	14.1185	0.666	2.13	1135	14.1185	0.65
130	1039.06	15.1056	0.6003	5.28	1125.5814	15.295	0.6467	2.61	1097	15.295	0.63
140	1002.04	16.2741	0.5789	5.82	1093.7302	16.4716	0.6284	2.79	1064	16.4716	0.61
150	967.26	17.4448	0.5588	6.27	1063.2715	17.6481	0.6109	3.03	1032	17.6481	0.59
160	934.526	18.6173	0.5399	6.73	1034.3792	18.8246	0.5943	3.23	1002	18.8246	0.58
170	903.64	19.7917	0.5221	7.13	1006.8793	20.0012	0.5785	3.48	973	20.0012	0.56
180	874.395	20.9676	0.5052	7.47	980.5977	21.1777	0.5634	3.77	945	21.1777	0.54
190	846.549	22.1448	0.4891	7.88	955.5345	22.3543	0.549	3.98	919	22.3543	0.53
200	819.873	23.3231	0.4737	8.19	931.6897	23.5308	0.5353	4.33	893	23.5308	0.51
210	794.116	24.5022	0.4588	8.62	908.7151	24.7073	0.5221	4.57	869	24.7073	0.5
220	769.029	25.6819	0.4443	9.10	886.9588	25.8839	0.5096	4.84	846	25.8839	0.49
230	744.362	26.8619	0.4300	9.66	866.0728	27.0604	0.4976	5.11	824	27.0604	0.47

Appendix F.

Experimental Data
for
Na-F-SO4-OH System
at 25° C

Table 1F. Experimental Data for Na-F-SO4 System at 25° C in Water

Sample	$[F^-]$ (m)	$[SO4^{2-}]$ (m)	Solids Identified via PLM
W25-1	0.000	2.062	Non-regular cry.
W25-3	0.106	1.990	DS
W25-4	0.215	1.508	DS
W25-5	0.312	1.216	DS
W25-6	0.439	0.960	DS
W25-7	0.567	0.780	DS & Rods
W25-8	0.681	0.659	DS & Br. Cry.
W25-9	0.898	0.369	Br. Cry. & Flakes
W25-10	0.951	0.000	Br. Cry. & Flakes

Table 2F. Experimental Data for Na-F-SO4-OH System at 25° C in 1 m [OH^-]

Sample	[F^-] (m)	[$SO4^{2-}$] (m)	Solids Identified via PLM
32-4	0.097	1.573	DS
32-5	0.181	1.114	DS
32-6	0.273	0.897	DS
32-7	0.426	0.676	DS
32-9	0.613	0.232	NaF w/flakes
32-10	0.650	0.000	NaF w/flakes

Table 3F. Experimental Data for Na-F-SO4-OH System at 25° C in 3 m [OH^-]

Sample	[F^-] (m)	[$SO4^{2-}$] (m)	Solids Identified via PLM
33-1	0.000	1.573	Amorphous Solid
33-2	0.018	1.578	Conglomerate Cry.
33-3	0.028	1.290	Sm Conglomerates
33-4	0.028	0.931	DS – sm Cry.
33-5	0.055	0.604	Few DS – Conglom
33-6b	0.157	0.278	DS & conglom.
33-7b	0.233	0.159	NaF and Flakes
33-8b	0.256	0.084	NaF and Flakes
33-9b	0.287	0.000	NaF and Flakes